

**Airways Smooth Muscle Plasticity  
Correlation of Structure and Function**

by

ANA MILENA HERRERA

M.D, Instituto de Ciencias de la Salud CES,  
Medellín, Colombia, 1997

A THESIS SUBMITTED IN PARTIAL FULLILLMENT OF THE  
REQUIREMENTS FOR THE DEGREE OF

DOCTOR OF PHILOSOPHY

in

FACULTY OF GRADUATE STUDIES  
(DEPARTMENT OF PATHOLOGY AND LABORATORY MEDICINE)

We accept this thesis as conforming  
to the required standard

THE UNIVERSITY OF BRITISH COLUMBIA

September 2004

© Ana Milena Herrera, 2004

## ABSTRACT

Smooth muscle is widely distributed in the body and controls different physiological functions in animals primarily by generating force and changing length. In the airways, excessive shortening of airway smooth muscle (ASM) has been implicated in pulmonary diseases like asthma. This dissertation is focused on understanding the subcellular ultra-structure and molecular mechanism conferring the ability of ASM to shorten.

Three related groups of experiments (projects) formed the foundation of this thesis. The first project examined various conditions under which myosin filaments assembled (or disassembled) in intact ASM, under the hypothesis that muscle cell length and intracellular calcium levels regulated the number and length of the myosin filaments *in vivo*. The experiments were designed to investigate the changes in the ASM thick filament content before and after the muscle had been activated and after the muscle had been adapted at a longer length, as well as the effect of resting calcium level on thick filament stability. The results showed that in ASM, muscle activation and muscle adaptation at a longer length favor filament formation, and that the resting calcium level is crucial for partial preservation of the filaments in the relaxed state.

The second project examined the role of actin polymerization as part of the normal ASM response to various stimuli. It was postulated that the same responses observed in myosin thick filaments (first project) could be elicited from actins under the corresponding conditions. ASM bundles were fixed for electron microscopic analysis

in the relaxed and activated states at two lengths; the muscle preparations were also fixed after a period of oscillatory strain, a condition known to cause depolymerization of myosin filaments. The results indicated that contractile activation, increased cell length and oscillatory strain enhanced actin polymerization. It was also shown that contractile activation did not preferentially enhance actin polymerization in areas near dense bodies. It was demonstrated then, that actin thin filaments *in vivo* are dynamic structures whose length and number are regulated by the cell in response to changes in extracellular environment and that polymerization/depolymerization of the thin filaments occurs uniformly across the whole cell cross-section.

The third and final project of this thesis investigated the changes in mechanical properties and ultra-structure of ASM immediately after a quick stretch and after the muscle had been fully adapted at the stretched length, to elucidate the effects of contractile filament overlap, isotonic load, myosin evanescence and other intrinsic factors influencing the amount of shortening. ASM bundles were first adapted at a near-*in-situ* reference length (*Lin situ*). Maximal isotonic shortenings under a load equivalent to 30% maximal isometric force ( $F_{max}$ ) were measured in preparations 1) contracting from the initial length of *Lin situ*, 2) contracting immediately after a 30% stretch from *Lin situ* and 3) contracting after adaptation at the stretched length. The muscle bundles were then fixed for electron microscopic examination at the end of the 3 protocols. The results indicated that under acute conditions (e.g., quick stretch) ASM behaves like striated muscle and that the sliding filament mechanism could adequately explain the observations. Under chronic conditions, i.e., after the muscle had been fully adapted to a length change, contractile filament reorganization that accompanied length adaptation altered the amount of maximal shortening without

changing the contractile force. These results could be explained by a model where the maximally shortened length of the muscle was determined by the extent of contractile filament overlap and that a quick stretch resulted in a reduced overlap; adaptation at the stretched length led to polymerization and reorganization of the contractile filaments, and restoration of optimal overlap.

Findings presented in this thesis suggest that the contractile apparatus of airways smooth muscle is malleable. The malleability likely reflects the cell's ability to alter the number and arrangement of the contractile units within a cell, through myosin and actin polymerization or depolymerization in a length-dependent manner. The new concept that smooth muscle, unlike striated muscle, is structurally plastic is strengthened by the data from this thesis and it likely will have a profound effect on our understanding of the tissue's behaviour in health and disease.

## TABLE OF CONTENTS

	<b>Page</b>
<b>Abstract</b> .....	<b>ii</b>
<b>Table of Contents</b> .....	<b>v</b>
<b>List of Figures</b> .....	<b>x</b>
<b>List of Abbreviations</b> .....	<b>xiii</b>
<b>Acknowledgements</b> .....	<b>xv</b>
<b>CHAPTER 1. Smooth muscle structure and physiology</b>	
1.1 General introduction.....	1
1.2 General features of smooth muscle organization.....	2
1.3 Structure of smooth muscle cells.....	3
1.3.1 Cell membrane and specializations.....	4
1.3.2 Organelles.....	7
1.3.3 Cytoskeleton and contractile apparatus.....	10
1.4 Physiology of smooth muscle.....	14
1.4.1 Calcium homeostasis.....	15
1.4.2 Muscle contraction.....	16
1.5 Airway smooth muscle and its function.....	18
<b>CHAPTER 2. Airway smooth muscle plasticity in health and disease</b>	
2.1 Introduction.....	20

2.2	Mechanics of airways smooth muscle.....	20
2.2.1	Plastic adaptation to large changes in cell length.....	29
2.2.2	Comparison of smooth muscle mechanical properties with those of skeletal muscle.....	34
2.3	Airway smooth muscle in disease.....	35
2.3.1	Deep inspiration and how ASM responds to mechanical strain.....	36

**CHAPTER 3. General hypothesis and specific aims**

3.1	Research focus.....	41
3.2	General and specific hypotheses.....	42
3.3	Specific aims.....	43
3.3.1	Determination of thick filament stability and factors affecting thick filament formation in vivo .....	44
3.3.2	Determination of thin filament stability and factors affecting thin filament formation in vivo.....	44
3.3.3	Determination of contractile unit reorganization in ASM adapted to different lengths.....	44

**CHAPTER 4. General methods and experimental protocol**

4.1	Tissue preparation.....	46
4.2	Mechanical measurements of the muscle.....	47
4.3	Electron microscopy.....	48
4.4	Morphometric analysis.....	49
4.5	Statistical analysis.....	51

## **CHAPTER 5. Myosin thick filament stability**

5.1	Thick filament formation <i>in vitro</i> .....	52
5.2	Smooth muscle myosin thick filament stability <i>in vivo</i> .....	53
5.3	Objectives and specific protocol.....	54
5.3.1	Muscle activation and length adaptation protocol.....	54
5.3.2	Extracellular calcium removal and length oscillation protocol.....	55
5.3.3	Morphometric analysis protocol.....	58
5.4	Effects of muscle activation and length adaptation on thick filament density.....	59
5.4.1	Series-to-parallel transition of thick filament lattice due to muscle activation.....	65
5.4.2	Is there plastic rearrangement of contractile units?.....	67
5.5	Influence of calcium on myosin thick filament formation.....	68
5.5.1	Is myosin RLC phosphorylation directly involved?.....	73
5.5.2	Is there myosin monomer-polymer equilibrium <i>in vivo</i> ?.....	74

## **CHAPTER 6. Actin dynamics in ASM plasticity**

6.1	Actin regulation in smooth muscle.....	76
6.2	Mechanical properties of thin filaments in ASM.....	77
6.3	Objectives and experimental protocol.....	78
6.3.1	Protocol for thin filament quantification during muscle activation and length adaptation.....	79
6.4	Thin filament density changes in response to muscle activation, length adaptation and mechanical strain.....	80
6.5	Thin filament regional distribution in the strained and activated muscles	86

6.6	Thin filament role in ASM plasticity.....	90
6.6.1	Activation-dependent thin filament density and its regional variation.	91
6.6.2	Length-dependent thin filament density.....	93
6.6.3	Thin filament lability versus thick filament lability.....	95
<b>CHAPTER 7. Contractile apparatus organization in the ASM cell</b>		
7.1	Are there sarcomeres in smooth muscle?.....	97
7.2	Objectives and experimental protocol.....	98
7.2.1	Determination of the relationship between isotonic loads and the respective amounts of shortening in muscle cells shortening from different initial resting lengths.....	99
7.2.2	Determination of the load-shortening relationship at $L_{in\ situ}$ and after a 10% quick stretch .....	102
7.2.3	Measurement of isotonic shortening and ultrastructural change after a 30% quick stretch .....	103
7.3	Isotonic shortening from different adapted lengths .....	107
7.3.1	Relationship between maximally shortened length under zero external load and initial (adapted) muscle length.....	108
7.4	Isotonic shortening after a 10% ( $0.1 \cdot L_{in\ situ}$ ) quick stretch .....	112
7.5	Isometric force generation and isotonic shortening after muscle lengthening.....	115
7.5.1	Actin/Myosin filament ratio variations after a quick stretch and after adaptation at the stretched length.....	117
7.6	A proposed model of contractile unit in smooth muscle.....	121
7.6.1	Relationship between load on muscle and the amount of shortening...	124

7.6.2	Muscle shortening after a quick stretch.....	127
7.7	Adaptation of smooth muscle to different lengths.....	128
<b>CHAPTER 8. Conclusions and futures directions.....</b>		<b>136</b>
8.1	Thick filament stability and factors affecting thick filament formation <i>in vivo</i> .....	136
8.2	Thin filament stability and factors affecting thin filament formation <i>in vivo</i> .....	137
8.3	Contractile unit reorganization in ASM adapted to different lengths....	138
8.4.	Future directions.....	139
<b>BIBLIOGRAPHY.....</b>		<b>141</b>

## LIST OF FIGURES

	<b>Page</b>
<b>Figure 1.</b> Cell-to-cell junctions in a transverse section from porcine tracheal smooth muscle.....	6
<b>Figure 2.</b> Organelles present in a smooth muscle cell cross section.....	9
<b>Figure 3.</b> Cytoskeleton and contractile filaments in a smooth muscle cell cross-section.....	13
<b>Figure 4.</b> Electron micrographs of a skeletal and smooth muscle cells	22-24
<b>Figure 5.</b> Schematic representation of a contractile unit of smooth muscle...	25
<b>Figure 6.</b> Schematic representation of the series-to-parallel transition of thick filament lattice of airway smooth muscle.....	28
<b>Figure 7.</b> Schematic representation of plastic length adaptation of ASM by rearrangement of the contractile units.....	31
<b>Figure 8.</b> Length-tension curves of passively shortened and lengthened rabbit trachealis.....	32
<b>Figure 9.</b> Effect of oscillatory amplitude on ASM force generation.....	39
<b>Figure 10.</b> Isometric force and thick filament density recovery after ASM length oscillation.....	40
<b>Figure 11.</b> Example of randomly selected areas for morphometric analysis...	50
<b>Figure 12.</b> Experimental protocol for extracellular calcium removal and length oscillation.....	57
<b>Figure 13.</b> Structural comparison of relaxed and activated ASM cells.....	62-63
<b>Figure 14.</b> Myosin (thick) filament densities in different regions of cross-sectional areas of trachealis cells.....	64
<b>Figure 15.</b> Examples of electron micrographs of muscle cell cross-sections	

for the extracellular calcium removal study.....	70-71
<b>Figure 16.</b> Thick filament density and isometric force associated with the 4 conditions in the extracellular calcium removal study.....	72
<b>Figure 17.</b> Electron micrographs showing longitudinal sections of trachealis cells fixed at <i>in situ</i> length in the relaxed and contracted states....	82-84
<b>Figure 18.</b> Thin filament density associated with different muscle states.....	85
<b>Figure 19.</b> An example of a cytoplasmic area surrounding a dense body of a relaxed trachealis muscle.....	88
<b>Figure 20.</b> Ratios of actin filament densities measured in different regions of cell cross-sectional areas.....	89
<b>Figure 21.</b> Schematic illustration of the experimental protocol for the length step change experiment.....	106
<b>Figure 22-A.</b> Isotonic shortening from different adapted lengths.....	109
<b>Figure 22-B.</b> Isotonic shortening from different adapted lengths.....	110
<b>Figure 23.</b> Maximally shortened length at zero external loads as a function of the initial (adapted) muscle length.....	111
<b>Figure 24-A.</b> Isotonic shortening after a 10% ( $0.1 \cdot L_{in\ situ}$ ) quick stretch.....	113
<b>Figure 24-B.</b> Isotonic shortening after a 10% ( $0.1 \cdot L_{in\ situ}$ ) quick stretch.....	114
<b>Figure 25.</b> Isometric force and isotonic shortening measured according to the experiment protocol outline in Fig. 21.....	116
<b>Figure 26.</b> Myosin (thick), actin (thin) filament densities, and the density ratio in trachealis fixed at the 3 time points (A, B, and C) indicated in Fig. 21.....	118
<b>Figure 27.</b> Frequency polygons depicting the distribution of the distance between a dense body and the closest myosin filament.....	120

<b>Figure 28.</b> Examples illustrating the spatial arrangement of myosin filaments and dense bodies that could be interpreted as a standard design of contractile unit in smooth muscle.....	122
<b>Figure 29.</b> Schematic representation of a contractile unit in smooth muscle under different conditions.....	123
<b>Figure 30.</b> Schematic representation of a trachealis cell and the intracellular arrangement of contractile units at different lengths...	133-134
<b>Figure 31.</b> Predictions by the models regarding the relationship between maximally shortened length and isotonic load.....	135

## LIST OF ABBREVIATIONS

Ach	-	Acetylcholine
ATP	-	Adenosine triphosphate
ASM	-	Airway smooth muscle
Ca <sup>2+</sup>	-	Calcium
[Ca <sup>2+</sup> ] <sub>i</sub>	-	Cytosolic calcium concentration
CaM	-	Calmodulin
CSA	-	Cross sectional area
COPD	-	Chronic Obstructive Pulmonary Disease
DB	-	Dense body (ies)
DI	-	Deep inspiration
ECM	-	Extracellular matrix
EFS	-	Electrical field stimulation
EGTA	-	Ethylene glycol-bis- (β-aminoethyl ether) N, N, N', N' tetra acetic Acid
ELC	-	Essential light chain
EM	-	Electronic microscopy
F <sub>max</sub>	-	Maximal force
F-V	-	Force-velocity
HC	-	Heavy chains
K <sup>+</sup>	-	Potassium
L-T	-	Length-tension
L <sub>ref</sub>	-	Reference length

$L_{in situ}$	-	<i>In situ</i> length
$MgCl_2$	-	Magnesium chloride
MLC	-	Myosin light chain
MLCK	-	Myosin light chain kinase
MLCP	-	Myosin light chain phosphatase
mN	-	Milli Newton
mV	-	Millivolts
n	-	Sample size
P	-	P value
PEC	-	Parallel elastic component
PSS	-	Physiological saline solution
RLC	-	Regulatory light chain
SE	-	Standard error
SMC	-	Smooth muscle cell
SR	-	Sarcoplasmic reticulum
TEM	-	Transmission electron micrographs

## **ACKNOWLEDGEMENTS**

After all these years, I have got quite a list of people who contributed in some way to this thesis, for which I would like to express thanks.

It is difficult to overstate my gratitude to my Ph.D. supervisor, Dr. Chun Seow. With his enthusiasm, his inspiration, his patience and his great efforts to explain things clearly and simply, he made muscle physiology fun for me. During my training he provided encouragement, sound advice, good teaching, good company, and lots of good ideas. During all these years I would have been lost without him.

For their kind assistance with writing letters, helping with various applications, and giving wise advice and encouragement, I wish to thank in addition Dr. Peter Paré, Dr. David Walker and Dr. Victor Viau.

I am indebted to my many colleagues and laboratory co-workers for providing a stimulating and fun environment in which to learn and grow.

I am grateful to all my friends , specially to Hubert Walinski and Faye Siriani, from the James Hogg iCAPTURE Centre for Cardiovascular and Pulmonary Research, Who have made Vancouver a very special place over all these years.

Finally, I am forever indebted to my family, my sister Diana and my nephew Juan Fernando for their encouragement when it was most required.

This thesis is dedicated to my parents Orlando and Bernarda, without whom none of this would have been even possible.

## **CHAPTER 1. Smooth muscle structure and physiology**

### **1.1 General introduction**

It is well known that there is an intimate relationship between muscle structure and function. This is obvious in skeletal muscle, where changes in structure directly reflect changes in the mechanical properties of the muscle. In smooth muscle, the attempt to make a direct correlation of structure and function has encountered big challenges. Smooth muscle does not possess a structurally clear and well-defined contractile apparatus. In skeletal muscle, the contractile filaments are highly organized in repeating structures known as sarcomeres. Changes in the sarcomere length or number result directly in changes in the force and velocity of the muscle. In smooth muscle, the lack of sarcomeres makes it difficult to predict variations in the mechanical properties of the muscle based on structural changes. Therefore, we are often forced to seek structural evidence from functional clues, a reversed strategy from that adopted in skeletal muscle research.

Airway smooth muscle (ASM) is of special interest in this thesis research as dysfunction of this tissue is implicated in many respiratory diseases, including chronic obstructive pulmonary disease (COPD) and asthma. Understanding the normal physiology of airway smooth muscle and how it correlates with its structure will facilitate our understanding of pathophysiology of this muscle associated with specific diseases. The main goal of my research was therefore to understand how airway smooth muscle contracts normally. The present thesis is concerned primarily with the morphological (structure/function) changes of airway smooth muscle

occurring during contraction and after length alterations. Thus, some basic knowledge of the structural elements in the smooth muscle and smooth muscle physiology is crucial to understand the research focus and experimental approaches outlined in this dissertation.

## **1.2 General features of smooth muscle organization**

Smooth muscle is widely distributed in the body and it has different functional specializations. It is responsible for the contractility of hollow organs such as the gastrointestinal tract, the airways, the bladder, the uterus and blood vessels. The walls of these conduit organs are usually composed of several layers of smooth muscle organized in numerous sheets, arrays of bundles or long cords (Gardfield and Somlyo, 1985). The total amount of smooth muscle present in the body is difficult to calculate but is estimated to be ~2% of human body weight (Gabella, 1997).

Smooth muscle structure differs greatly from that of skeletal muscle with the most striking feature being the lack of visible cross striations, hence the name “smooth”. Smooth muscle’s uninucleated cells are much smaller (2-10  $\mu\text{m}$  in diameter) than the multinucleated skeletal muscle fibres (10-100  $\mu\text{m}$ ). Despite these structural differences smooth muscle is capable of producing isometric force per cross-sectional area that is equal to that of skeletal muscle (Gabella, 1997).

Smooth muscle cells (SMC) are embedded in copious extracellular matrix with a large fibrous component. The major constituents of the extracellular matrix (ECM) or stroma, the collagen fibrils, are much more abundant in smooth muscle than in

skeletal muscle. The arrangement of the ECM is believed to play an important role in the mechanical function of the muscle (Gabella, 1997).

Based on how the SMC are organized and innervated, they can be classified as single-unit and multi-unit muscles. The muscle fibres that form the single-unit are grouped into dense sheets or bands. They are connected through gap junctions that act as a low resistance pathway for the rapid spread of electrical signals throughout the tissue. Although poorly innervated, single-unit muscles work as a pacemaker with spontaneous and rhythmic myogenic activity (Stephens, 2001). The multi-unit smooth muscle fibres have no interconnecting bridges and are separately innervated by sympathetic and parasympathetic nerve fibres. They are mingled with connective tissue fibres and respond independently from each other upon nerve stimulation. ASM has been shown to be richly innervated like a multi-unit muscle, but it also possesses abundant gap junctions which provide a more single-unit type of behavior (Kannan et al, 1980). Therefore, airway smooth muscle is considered as an intermediate muscle (between the single- and multi-unit types) by most authors (Stephens, 2001).

### **1.3 Structure of smooth muscle cells**

SMC are elongated and spindle-shaped cells of sizes varying considerably between different tissues and species. The cells range in size from 2-10  $\mu\text{m}$  in diameter near the central segment of the cell and from 100 to 1000  $\mu\text{m}$  in length (Gardfield and Somlyo, 1985). In the case of the airways, the cellular dimensions are as follows: ~3-5  $\mu\text{m}$  wide and ~250  $\mu\text{m}$  long (Stephens, 2001). The average volume of an intestinal SMC is 2,500-3,500  $\mu\text{m}^3$  with a corresponding cell surface of 5,000  $\mu\text{m}^2$  (surface-to-

volume ratio of about  $1.5 \mu\text{m}^{-1}$ ) (Gabella, 1997). A large part of the SMC surface is occupied by caveolae, cell membrane specializations described next.

### **1.3.1 Cell membrane and specializations**

SMC membrane or sarcolemma is a tri-laminar structure of  $\sim 8$  nm thickness that possesses different structural specializations that include caveolae, cell-to-cell junctions and dense plaques. On its entire surface, the sarcolemma is occupied by mutually exclusive areas of caveolae and dense plaques. Caveolae are estimated to occupy  $\sim 30\%$  of the cell surface in many smooth muscle cells, however, no quantitative studies have been performed on ASM.

Caveolae are surface vesicles of 50-80 nm in diameter and  $\sim 120$  nm in length (Fig.1). The function of these vesicle like structures is still obscure. These vesicles do not appear to have any micropinocytotic activity, as they are not seen to separate from the cell surface or to be internalized to the cytoplasm. However, they considerably increase the cell surface area, which facilitates the exchange of fluid, nutrients and ions across the membrane (Stephens, 2001). Immunocytochemistry analysis has shown that the plasmalemma calcium pump (ATPase) is located in the membrane of caveolae in smooth muscle (Gabella, 1997). At the same time, caveolae are found to be intimately associated with the sarcoplasmic reticulum, which appears to provide a conduit for calcium transport within a cell (Kuo et al, 2003).

Dense plaques or bands are membrane-associated dense bodies that link the contractile apparatus and cytoskeleton to the cell membrane. They are areas of increased electron density (osmiophilic) in the sarcolemma with an average of 0.2-0.4

$\mu\text{m}$  in width, 30-40 nm in thickness and 1-2  $\mu\text{m}$  in length (Fig.1). Dense bands provide anchoring points to actin and intermediate filaments in smooth muscle like their analogue Z discs do in skeletal muscle. The dense bands are composed mainly of  $\alpha$ -actinin and vinculin, and it has been suggested that these structures provide mechanical coupling between the myofilaments and the ECM (Stephens, 2001).

Cell-to-cell junctions are membrane specializations that provide mechanical and ionic coupling. The mechanical coupling (i.e., transmission of force between cells) is provided by junctions of the adherens type (intermediate junctions or desmosomes). Desmosomes are formed by paired dense plaques from adjacent cells separated by an intercellular space of 40-60 nm filled with electron dense material composed of glycoproteins (Fig.1). Other dense plaques that are not paired form the so-called cell-to-stroma junctions or hemidesmosomes for being mechanically linked to the extracellular matrix (Gardfield and Somlyo, 1985). On the other hand, ionic or electrical coupling (transmission of excitation from cell to cell) is provided by gap junctions. Gap junctions are formed by the opposition of two symmetrical portions of the sarcolemma from two adjacent cells. The space between the two cells is only 2-3 nm wide and it is filled with pairing transmembrane channels called connexons. The number and frequency of gap junctions varies in different smooth muscles but in ASM it has been reported that their frequency is of  $2.7 \pm 0.3$  (SE) per 100 SMC (Stephens, 2001).

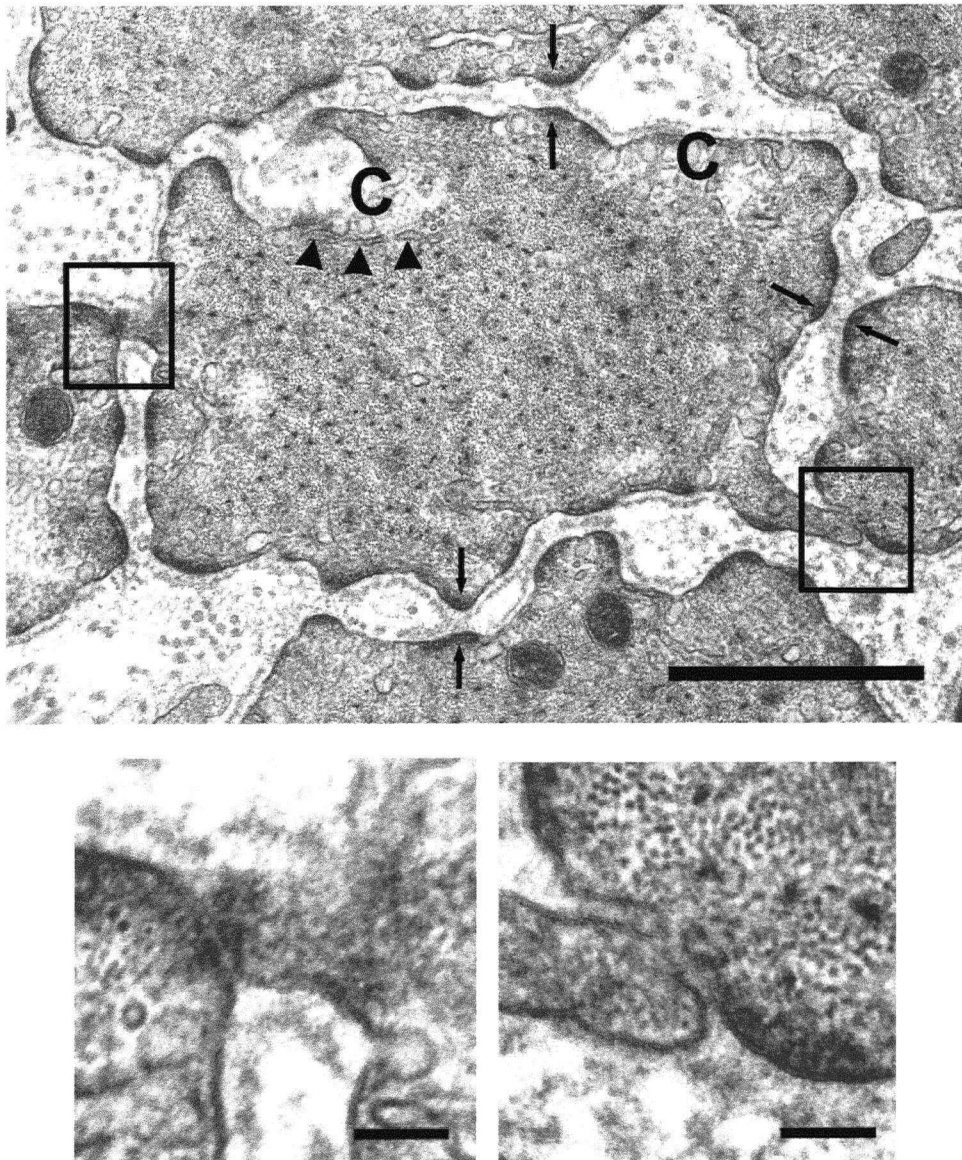


**Figure 1. Cell-to-cell junctions in a transverse section from porcine tracheal smooth muscle.** Areas of the cell membrane occupied by caveolae (C) alternate with areas occupied by dense plaques forming desmosomes with adjacent cells (arrows). Arrowheads show part of the sarcoplasmic reticulum in close association with the cell membrane and caveolae. The gap junctions shown within the squares are magnified in the micrographs above. Note the close proximity of the cell membranes of the adjacent cells. Calibration bars: 1  $\mu\text{m}$  (main picture) and 0.1  $\mu\text{m}$  (magnifications).

### 1.3.2 Organelles

Rough and smooth sarcoplasmic reticulum systems are present in all smooth muscles. They consist of a network of tubules and sacs within the cytoplasm with (rough) or without ribosomes (smooth) that occupies ~ 2 to 7.5% of the cellular volume (Gardfield and Somlyo, 1985). The sarcoplasmic reticulum (SR) is located throughout the cytoplasm, beneath the cell membrane and near the nuclear poles.

The smooth sarcoplasmic reticulum can be divided in 2 general types: superficial and deep SR (Fig.2). The superficial SR lies parallel to the cell membrane where it is believed to serve as a site for maintaining local cytoplasmic calcium gradients, calcium oscillation, and promoting calcium cycling during homeostasis. The deep SR is usually seen positioned perpendicular to the sarcolemma running deep into the cytoplasm where it meets the mitochondria. The deep SR is believed to serve as a compartment for calcium storage as well as a conduit for calcium transport within the cell (Kuo et al, 2003). The rough endoplasmic reticulum is involved in protein and glycoprotein synthesis (Fig.2).

Mitochondria are abundant in the SMC being preferentially located at the nuclear poles of the cell where they form clusters (Fig.2). Mitochondria can also be found near the cell membrane where they are frequently associated with superficial and deep SR. They are usually elongated with a size range of 1-2  $\mu\text{m}$  long and 0.1-0.3  $\mu\text{m}$  wide occupying about 3-10% of the cytoplasm volume (Gabella, 1997). Although smooth muscle mitochondria utilize the same substrates that skeletal muscle mitochondria use, their phosphorylation capacity (amount of adenosine triphosphate

(ATP) synthesised oxidatively per unit weight of muscle) is only one tenth of that of skeletal muscle. Therefore, mitochondrial oxidative phosphorylation provides less energy to smooth muscle than it does to skeletal muscle (Stephens, 2001).

The single nucleus of the SMC is centrally located (Fig.2). In smooth muscle micrographs, the nucleus usually shows well-defined chromatin and a nucleolus. Structural studies have shown direct attachment of the contractile filaments to the nuclear envelope. Hence, the nucleus and the nuclear envelope are speculated to act as force transmitter along the longitudinal axis of the cell (Kuo et al, 2004).

Other organelles found in smooth muscle include Golgi apparatus (Fig.2) located preferentially at the nuclear poles; its function is thought to be that of protein glycosylation, packing and transport, as well as, synthetic and degradative cellular processes. Lysosomes are normally not abundant in normal smooth muscle cells; however, they become abundant in cultured smooth muscle cells (Garfield et al, 1985).

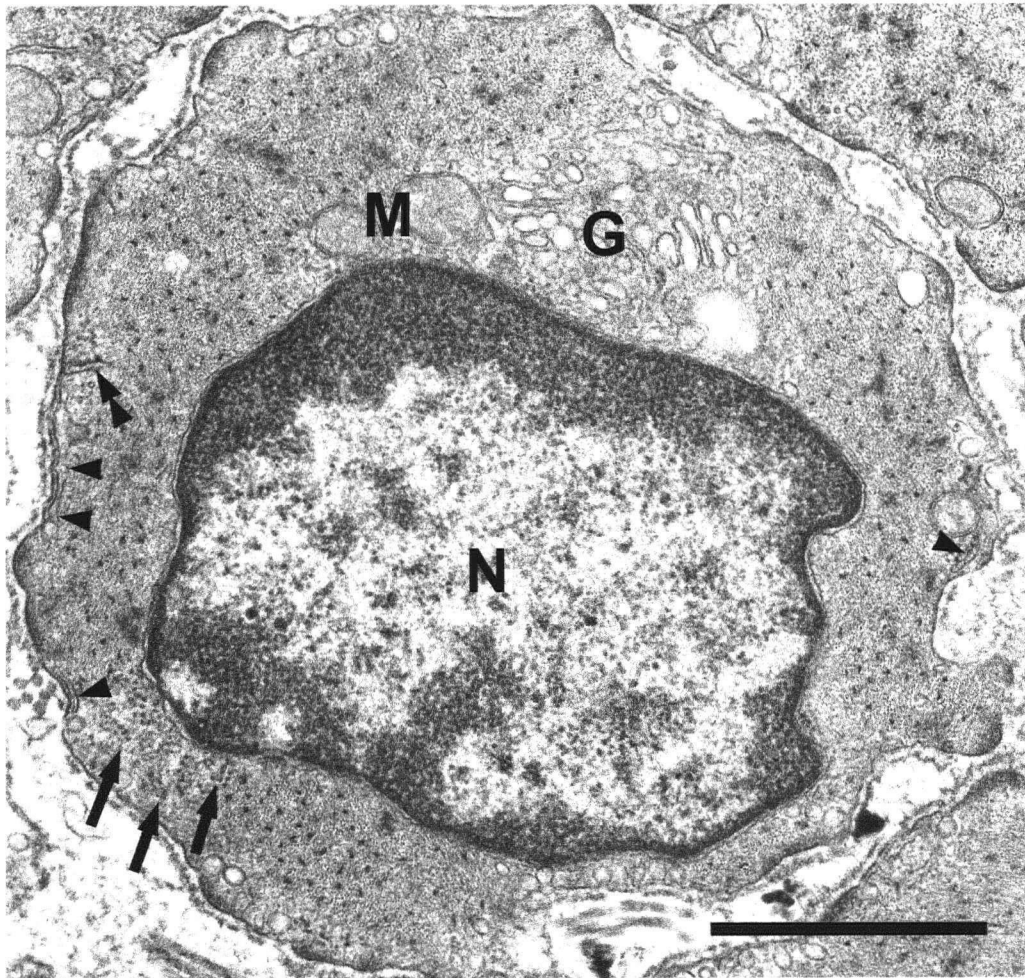


**Figure 2. Organelles present in a smooth muscle cell cross section.** Major organelles observed in this cell cross section include nucleus (N), mitochondria (M) and Golgi apparatus (G). Superficial (arrowheads) and deep (double arrowhead) sarcoplasmic reticulum is present in close proximity with the cell membrane and caveolae. Arrows indicate the presence of rough sarcoplasmic reticulum with multiple ribosomes. Calibration bar: 1 $\mu$ m

### 1.3.3 Cytoskeleton and contractile apparatus

Three different types of filaments have been found in smooth muscle cells: thin, thick and intermediate filaments.

Intermediate filaments are one of the main components of the smooth muscle cellular cytoskeleton and derive their name from their intermediate size (10 nm diameter) between thin and thick filaments (Bagby, 1983). They have a circular cross section and are very uniform in their diameter but their exact length has not been determined (Fig.3). The main component of intermediate filaments in most smooth muscles is desmin, a 55-kDa protein from which the filaments can be reconstituted *in vitro* (Small et al, 1983). However, in vascular smooth muscle intermediate filaments are mostly made of vimentin with little or no desmin (Gabella, 1997). In smooth muscle intermediate filaments make up a substantial proportion (15-25%) of the total structural protein (Small et al, 1983). Intermediate filaments are found to be associated with dense bodies and dense plaques (described earlier) forming the strong network that serves as the cellular cytoskeleton.

Dense bodies are believed to be analogous to the Z-lines in skeletal muscle as they serve as the attachment site for intermediate and cytoplasmic actin filaments. They are mainly composed of  $\alpha$ -actinin and their density comes from the affinity for electron-dense substances used in fixation and staining for electron microscopy (Fig.3). Dense bodies are elongated (in the longitudinal cell axis) and rigid structures found scattered throughout the cytoplasm. They are very variable in size with a range

of up to 1.2  $\mu\text{m}$  long and up to 0.3  $\mu\text{m}$  wide in most of visceral smooth muscle cells; however, no quantitative studies have been carried out on ASM (Gabella, 1997).

Actin filaments, also called thin filaments, have a diameter of 6-8 nm (Fig.3). They are formed by polymerization of monomeric G-actin (MW 42kDa) into two helical strands that run parallel to each other (Small et al, 1983). In smooth muscle, actin can exist in 4 different isoforms: smooth muscle actins ( $\alpha$  and  $\gamma$ ) and nonmuscle cytoplasmic actins ( $\beta$  and  $\delta$ ). The isoform composition of the filaments is believed to determine its intracellular role as either contractile or cytoskeletal actin. Thin filaments are present in greater quantities in smooth muscle cells as the ratio of actin to myosin filaments of 15-18:1 greatly exceeds the 2:1 ratio of skeletal muscle (Stephens, 2001). This actin-to-myosin ratio in smooth muscle was estimated from structural studies on different visceral and vascular muscles; no such estimate is yet available for ASM.

Thick filaments (or myosin filaments) measure 15-20 nm in diameter. They are formed by polymerization of monomeric myosin class II. Myosin II molecules are hexamers composed of 2 heavy chains (HC) of 204 kDa, 2 regulatory light chains (RLC) of 20 kDa and 2 essential light chains (ELC) of 17 kDa. Myosin HC forms the coiled rod and the two globular head portions of the molecule. The RLC and ELC are attached to the head portions where the active site for ATP hydrolysis is also located (Chacko et al, 1995). Myosin II molecules assemble into antiparallel dimers to form “side polar” thick filaments different from the “bipolar” structure displayed by thick filaments in skeletal muscle. In electron micrographs these filaments show an irregular contour in the cross sections due to the projection of the myosin heads also

known as cross bridges (Fig.3). Myosin filaments are scattered throughout the cytoplasm with no evident uniform distribution. The filament length has been estimated at 2.2  $\mu\text{m}$  in vascular smooth muscle, but it remains undetermined in most types of smooth muscle (Gabella 1997).

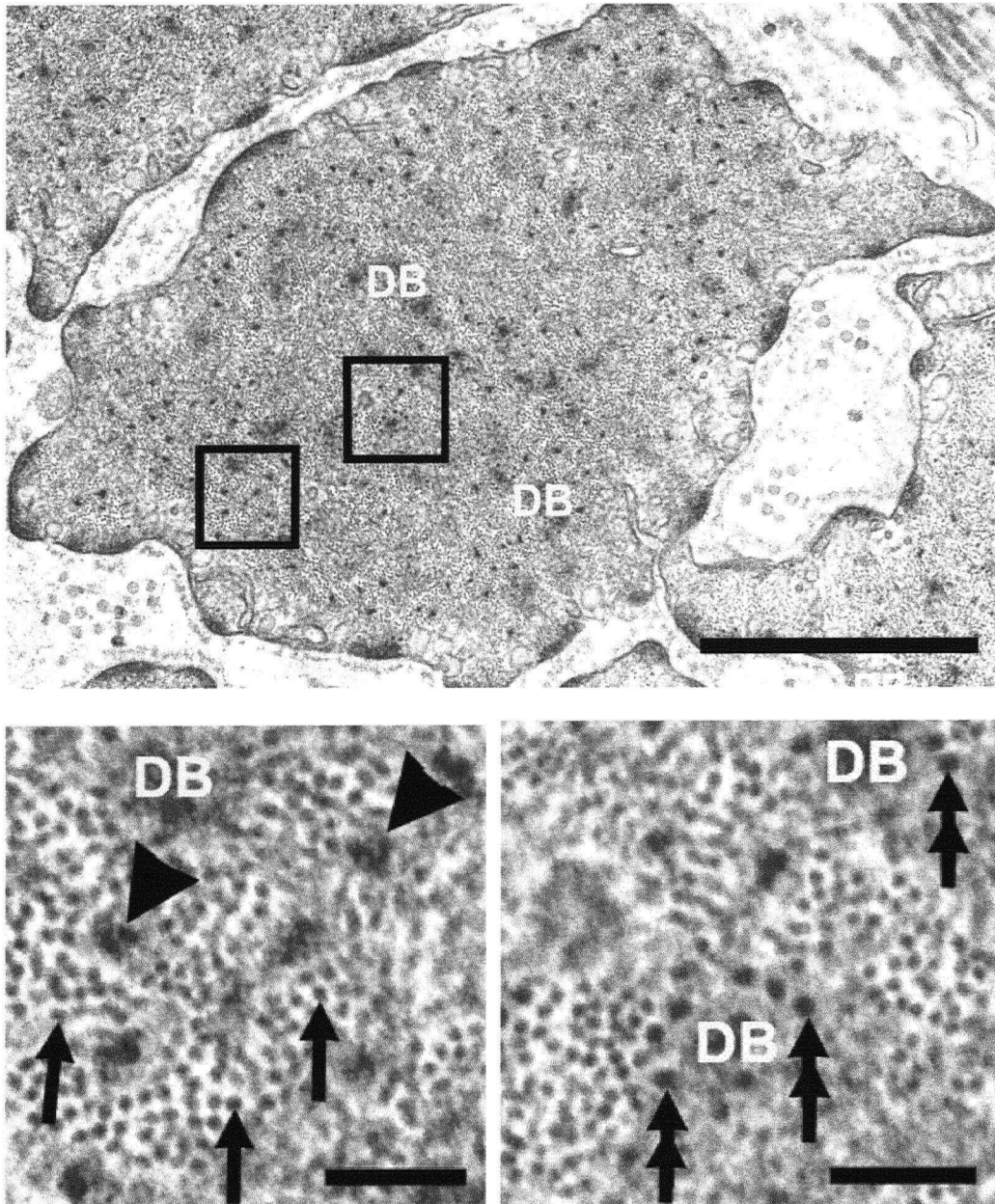


**Figure 3. Cytoskeleton and contractile filaments in a SMC cross-section.** Magnifications show the areas within the squares on the cell cross-section. Left magnification shows thick (arrowheads) and thin (arrows) filaments in more detail. Note the rosette-like structure formed by the thick filaments surrounded by the much smaller thin filaments. Right magnification shows two dense bodies (DB) surrounded by multiple intermediate filaments (double arrows). Calibration bars: 1 $\mu$ m (main micrograph) and 0.1 $\mu$ m (magnifications).

#### 1.4 Physiology of smooth muscle

The quantitative value of the membrane potential of smooth muscle is variable from one type of smooth muscle to another. In the normal resting state, the membrane potential is usually about -50 to -60 millivolts (~30 mV less negative than in skeletal muscle). In canine ASM the steady membrane potential is  $-47 \text{ mV} \pm 2.4$  (SE)(Stephens, 2001). As in skeletal muscle, nerve stimulation causes membrane depolarization of SMC. The excitation occurring at the cell membrane is then followed by a mechanical event, contraction. This excitation-contraction event is called electromechanical coupling. In this kind of coupling, depolarization of the cell membrane opens calcium channels that allow calcium ( $\text{Ca}^{2+}$ ) influx from the extracellular space to activate the SM contractile apparatus (Bárány, 1996).

There are other excitation mechanisms in smooth muscle, one of them is termed pharmacomechanical coupling. In this kind of coupling, membrane depolarization is not a prerequisite for contraction (Stephens, 2001). Instead, receptor operated (voltage independent) calcium channels are activated by drugs or hormones. The resulting  $\text{Ca}^{2+}$  influx stimulates, in turn, the release of internal  $\text{Ca}^{2+}$  from the sarcoplasmic reticulum (Bárány, 1996).

The third type of excitation mechanism in smooth muscle is that of calcium independent activation. Contraction is achieved by activation of protein kinase C that leads to phosphorylation of the thin filament associated proteins caldesmon and calponin. The phosphorylation removes the inhibitory effect of these associated

proteins on actomyosin ATPase activity and causes contraction. Details about calcium regulation and mechanism of contraction in smooth muscle are discussed in the following sections of this thesis.

#### **1.4.1 Calcium homeostasis**

As in skeletal muscle, smooth muscle contraction is regulated by cytosolic  $\text{Ca}^{2+}$  concentration ( $[\text{Ca}^{2+}]_i$ ) and the sensitivity to  $\text{Ca}^{2+}$  of the contractile elements (Karaki et al, 1997). During smooth muscle stimulation,  $\text{Ca}^{2+}$  can be mobilized from both extracellular and intracellular compartments. In the resting muscle, proper functioning of the SMC requires maintenance of low  $[\text{Ca}^{2+}]_i$ ; this is about  $0.1 \mu\text{M} \text{Ca}^{2+}$ . Upon excitation,  $\text{Ca}^{2+}$  channels in the cell membrane open and allow  $\text{Ca}^{2+}$  to move to the cytosol where the  $\text{Ca}^{2+}$  concentration increases about 100-fold (Miller et al, 1997). The rate at which extracellular  $\text{Ca}^{2+}$  enters the SMC increases in response to receptor activation or membrane depolarization (Loutzenhiser et al, 1985). Based on observations by Bolton (1979) and Van Breemen (1979), 2 different pathways for  $\text{Ca}^{2+}$  influx have been proposed: voltage-dependent and receptor-linked  $\text{Ca}^{2+}$  channels. In the former, high potassium ( $\text{K}^+$ ) depolarizes the membrane, opens the voltage-dependent  $\text{Ca}^{2+}$  channels, increases  $\text{Ca}^{2+}$  influx, and elicits sustained contraction. In the receptor-linked pathway, agonist bound to plasma membrane receptor induces the release of  $\text{Ca}^{2+}$  from storage sites (SR) to provoke initial transient contractions and subsequently opens the receptor-linked  $\text{Ca}^{2+}$  channels that are controlled by receptors for contractile agonists (Karaki et al, 1997).

After contraction has occurred, active movement of  $\text{Ca}^{2+}$  out of the cytoplasm across the plasma and SR membranes initiates relaxation. In order to elicit relaxation the  $\text{Ca}^{2+}$  level in the cytosol must be returned to near the resting value (Miller et al, 1997). There are two main mechanisms believed to participate in decreasing the  $\text{Ca}^{2+}$  level: the plasma membrane  $\text{Ca}^{2+}$  ATPase pumps transporting  $\text{Ca}^{2+}$  from inside the cell into the extracellular space and the sarcoplasmic reticulum  $\text{Ca}^{2+}$  ATPase pumps transporting  $\text{Ca}^{2+}$  into the SR (Miller et al, 1997; Karaki et al, 1997).

#### **1.4.2 Muscle contraction**

Smooth muscles are classified into phasic or tonic muscles based on their speed of activation and contraction (Somlyo and Somlyo, 1994). Phasic muscles (uterus, urinary bladder, intestinal muscle, etc) are normally activated by spontaneous action potentials or by neural stimulus. They contract and relax rapidly and cannot maintain large forces for long periods of time. On the other hand, tonic muscles (airways, blood vessels, etc) are usually activated by pharmacological or humoral agonists. These muscles respond gradually to stimuli, maintain tension for long periods of time with low energy expenditure and relax more slowly (Meiss, 1997).

In general, when smooth muscle contracts it can generate force without changing its length (isometric contraction) or it can also do it by changing its length or shape (isotonic or auxotonic contraction). Isometric contraction occurs when the impediment against a change in length is greater than the force generated by the muscle. The muscle is then capable of maintaining stable force for a long period of

time (steady-state) with relatively little energy consumption. In contrast, during isotonic contraction the muscle shortens in an active, load-dependant manner.

Smooth muscle contraction results from the chemical and physical interaction between its contractile proteins, actin and myosin. Activation of smooth muscle produces a rapid increase in  $[Ca^{2+}]_i$  caused by influx of extracellular  $Ca^{2+}$  and release from the SR. Once free in the cytosol, calcium binds to calmodulin (CaM) creating the complex  $Ca^{2+}$ -CaM that then binds and activates the enzyme myosin light chain kinase (MLCK). When activated, MLCK catalyzes the phosphorylation of the regulatory light chains of myosin (RLC), which allows the myosin ATPase to be activated by actin. Increased activity in the actin-activated myosin ATPase initiates cross bridge cycling and therefore, muscle contraction. During the cross bridge cycling myosin heads bind to the actin filament. The now attached cross bridges undergo conformational changes that result in the sliding of the thin filament relative to the thick filament, therefore, generating force. During the contraction, the cross bridges cyclically attach and detach from the actin filament using ATP as the source of energy for the mechanical work. Relaxation of the muscle occurs when  $[Ca^{2+}]_i$  decreases due to calcium extrusion or uptake by the SR. Decreased  $[Ca^{2+}]_i$  causes inactivation of MLCK with the consequent dephosphorylation of the RLC by myosin light chain phosphatase (MLCP) and cross bridge detachment (Word et al, 1997; Pfitzer, 2001).

The preceding scheme of events shows that smooth muscle contraction is primarily regulated by the activities of MLCK and MLCP that leads to RLC phosphorylation/dephosphorylation. The MLCK: MLCP activity ratio is known to be

mainly controlled by  $\text{Ca}^{2+}$ ; however, some other regulatory mechanisms can modulate this ratio resulting in alterations of  $\text{Ca}^{2+}$  sensitivity of RLC phosphorylation (Word et al, 1997). It has also been shown that under certain conditions, smooth muscle relaxes at high levels of myosin RLC phosphorylation. The mechanism responsible for this phenomenon is not clear yet. In this regard, it has been proposed that a small heat shock protein (HSP20) is responsible for the inhibition of the actomyosin interaction of phosphorylated myosins (Pfitzer, 2001).

### **1.5 Airway smooth muscle and its function**

In the upper airway, at the macroscopical level, ASM is located in the posterior wall of the trachea. There, the muscle is found attached to the ends of the incomplete C-shaped cartilaginous rings. In the lower airways, ASM is found circumferentially surrounding the lumen of the bronchi in a helix–antihelix pattern encasing the airway (Amrani et al, 2002; Stephens 2001). Microscopically, the layer of smooth muscle lies deep to the mucosa and becomes increasingly prominent as the airway diameter decreases (Amrani et al, 2002). Although ASM of the upper and lower airways appears similar at the cellular level, the orientation of the fibers and their organization into bundles is different. In the trachea there is a unified layer of thick bundles of SM characterized by minimal branching and transverse orientation, whereas in the lower airways, the muscle bundles are small and the cells are irregularly orientated (Stephens, 2001). Despite these differences, it has been demonstrated that bronchial smooth muscle shows similar contractile characteristics to tracheal smooth muscle (Stephens et al, 1998).

The specific role of ASM in the healthy state is not entirely clear, however, it is believed that ASM tone controls the diameter of the conducting passages with the consequent control of the resistance to airflow within the respiratory tree, therefore, it plays a homeostatic role to stabilize airways and airspaces (Seow et al, 2001). Although the physiological function of ASM has not been completely identified, the importance of studying its function and structure sits on the fact that alterations in ASM contractility are believed to be in part responsible for many pathological conditions like asthma and COPD.

## **CHAPTER 2. Airway smooth muscle plasticity in health and disease**

### **2.1 Introduction**

Smooth muscle, like many tissue types, is responsive to a wide variety of normal and pathological stimuli. Adaptation of smooth muscle to changes in functional demand is a fundamental biological property, without which most of our organs' capacity to function with changing external requirements would be severely limited. With the case of ASM, adaptation to externally imposed length and load variations includes changes in shortening velocity, power output and muscle ultra-structure. Although the mechanism of adaptation in smooth muscle is not entirely clear, it probably involves plastic rearrangement of the contractile apparatus and cytoskeleton of the muscle (Seow and Fredberg, 2001).

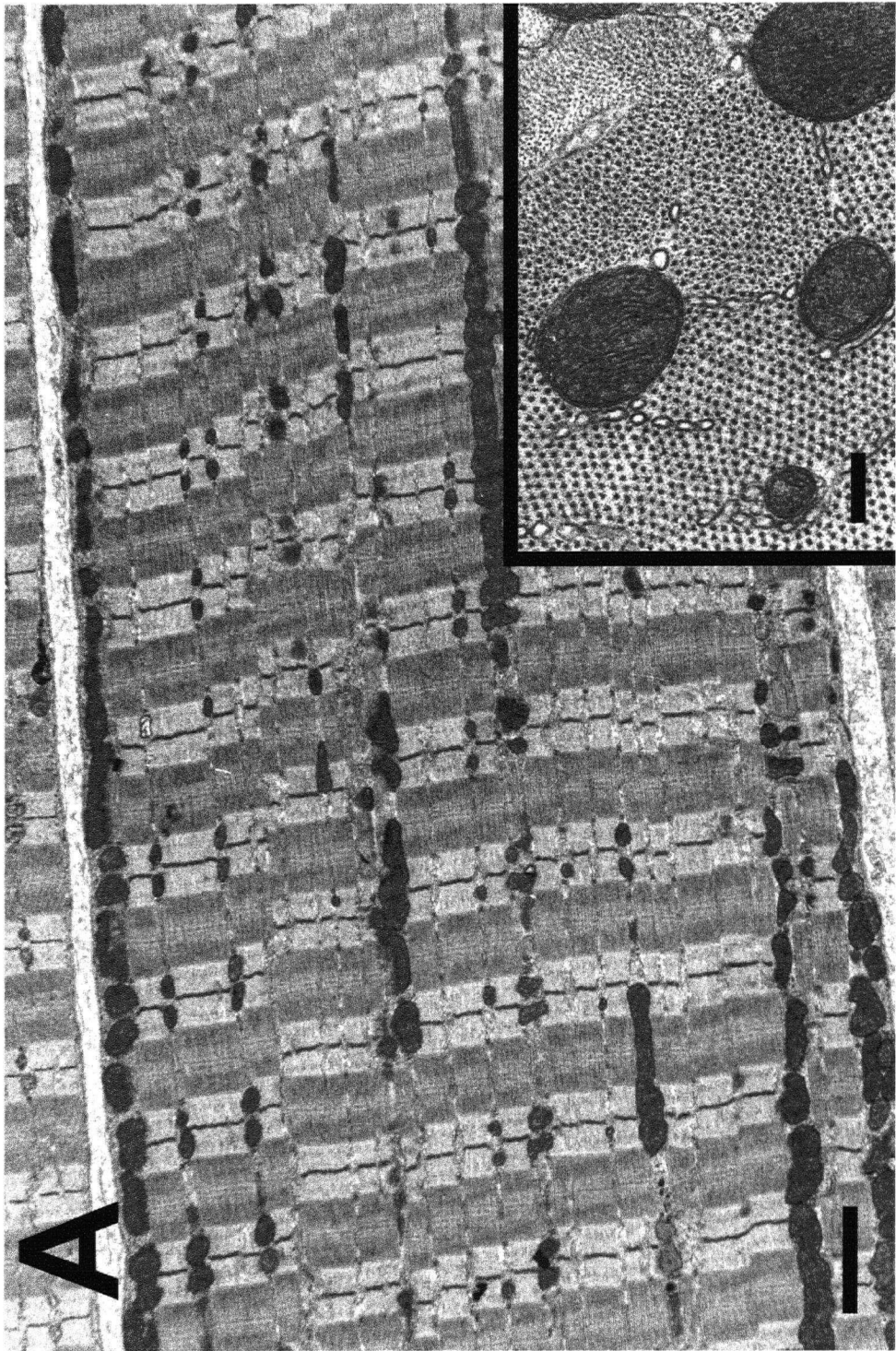
### **2.2 Mechanics of airway smooth muscle**

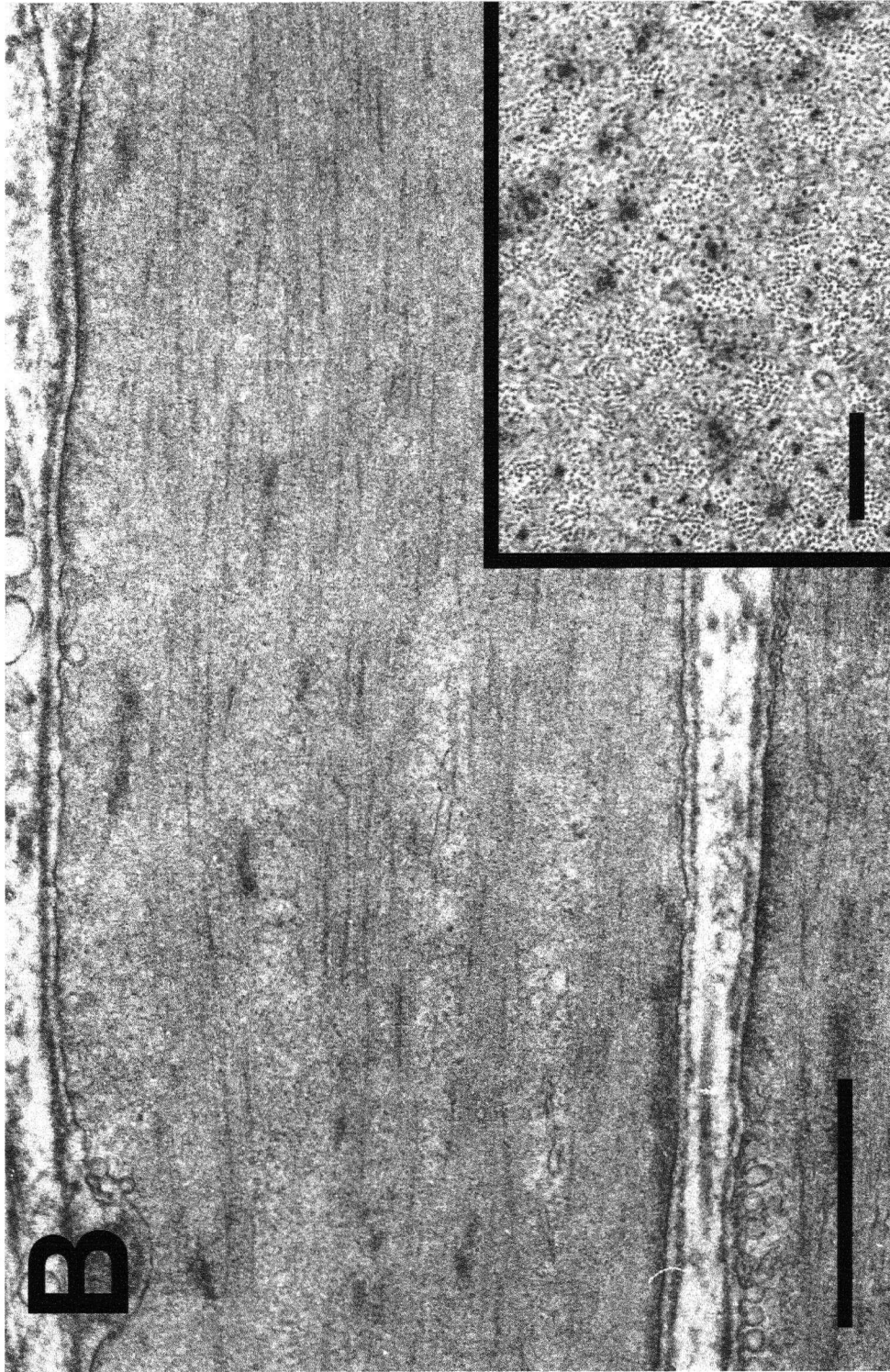
Smooth muscle mechanics can be described in a variety of different ways; these include force generation, shortening velocity, power output and stiffness. These mechanical attributes can be explored using various experimental methods. Length and tension (L-T) measurements under isometric conditions give information about the ability of the muscle to stiffen and support load and may inform us about the extent of overlap between contractile filaments. On the other hand, force and velocity (F-V) measurements evaluate the maximal rate of shortening and power production of

the muscle, and may inform us about the degree of activation and the geometric arrangement of contractile units (Stephens, 2001).

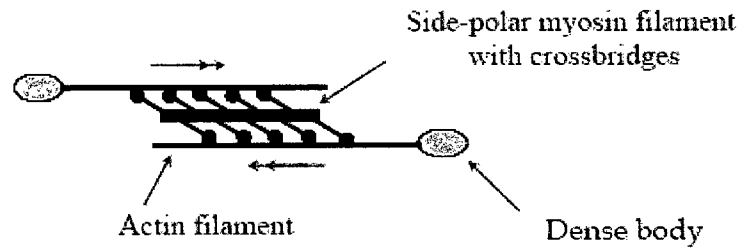
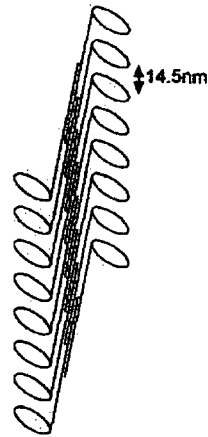
Muscle force is the simplest mechanical parameter to measure. When the measured force is normalized by the cross-sectional area ( $F/CSA$ ) of the muscle, it is called stress. Active stress provides insights into the workings of the contractile apparatus of the muscle as it is closely related to the number of active cross-bridges. Passive force is believed to stem from the cytoskeleton and the parallel elastic component (PEC) that consists of connective tissue surrounding the muscle (Meiss, 1997; Stephens, 2001). The total force or stress generated by the muscle is the combination of the active and passive forces.

Shortening velocity of the muscle is a measurement that provides information about the level of activation and regulatory state of the muscle. Velocity of shortening is closely related to the enzymatic activity of the cross-bridges (Meiss et al, 1997). In combination, force and shortening velocity measurements provide information on the nature of the contractile proteins and the basic organization of the contractile apparatus of the muscle, as well as the physical structure of the muscle tissue. In smooth muscle, this structure-function correlation is still poorly understood, mainly because smooth muscle lacks the regular sarcomeric organization observed in skeletal muscle (Fig. 4A and 4B). However, it is believed that the contractile filaments in smooth muscle are not entirely random in structural arrangement and that there are assemblies known as contractile units (Fig. 5), where thick filaments seem to be a key component (Gabella, 1997; Cooke et al, 1972; Cooke et al, 1987; Lambert et al, 2003).





**Figure 4. A. Electron micrographs of a skeletal muscle cell.** The contractile apparatus is highly organized into structures known as sarcomeres. Overlapping of myosin and actin filaments confer the muscle with the characteristic appearance of “striations” in the longitudinal sections. In the cell cross-section (inset), one can observe the uniform distribution of the contractile filaments myosin and actin. (TEMs of skeletal muscle were kindly provided by Dr. William Ovalle). Calibration bar in the longitudinal section:  $2\mu\text{m}$ , and in the cross-section (inset):  $0.2\mu\text{m}$ . **B. Electron micrographs of a smooth muscle cell.** Note that there is no recognizable pattern of sarcomere-like organization in the longitudinal section. In the cross-section (inset), myosin and actin filaments seem to be randomly distributed in a disorganized fashion. Calibration bar in longitudinal section:  $2\mu\text{m}$ , and in cross-section (insets):  $0.2\mu\text{m}$

**A****B****Side-polar**

**Figure 5. A. Schematic representation of a contractile unit of smooth muscle.**

Note that the thick filament possesses a side-polar architecture that allows it to move actin filaments and dense bodies in opposite directions (double arrows). Adapted from Lambert et al, 2003.

**B. Illustration of nonhelical, side-polar myosin filament.** It

has been suggested that these side-polar filaments are built from stacked monolayers of myosin molecules having a side-polar arrangement. The existence of these side-polar filaments has only been shown in solution (in vitro) studies. Adapted from Craig et al, 1977.

In ASM velocity measurements at different time points after muscle activation have shown that the velocity declined after it reached a peak early in contraction and while the force was still rising (Kamm et al, 1985; Seow et al, 1986; Seow et al, 2000). At least two different explanations have been put forward regarding this observation.

One explanation is based on the observation that the time course of the regulatory myosin light chain phosphorylation coincides with the time course of velocity change. It is postulated that during an isometric contraction, with the onset of contractile stimulus, cross-bridges cycle relatively rapidly, leading to rapid force increase. As the force approaches the plateau, the rapidly cycling (phosphorylated) cross bridges are progressively replaced by slowly cycling (dephosphorylated) bridges. These slow cycling bridges, also called latch bridges, are force-bearing bridges that consume only about one quarter of energy that the rapidly cycling bridges consume. The decrease in the bridge cycling rate leads to a proportional decrease in the shortening velocity of the muscle while force is maintained (Dillon et al, 1981; Stephens, 2001).

Another explanation of the velocity change is based on the assumption that myosin filaments lengthen during the time course of an isometric contraction (Ford et al, 1994; Seow et al, 2000). It is argued that force produced by the muscle is proportional to the number of cross-bridges cycling in parallel. During muscle activation the number of cross-bridges in parallel increases at the expense of the number of cross-bridges in series. The lengthening of the filaments results in fewer filaments arranged in series spanning the muscle length (Fig. 6). Because the overall shortening velocity of the muscle is proportional to the number of contractile filaments in series, the

decrease in the number of filaments in series leads to a decrease in shortening velocity (Ford et al, 1994; Seow et al, 2000).

The two theories that attempt to explain the decrease in muscle velocity during isometric contraction are not mutually exclusive. Throughout the course of this dissertation more evidence that supports the argument of plastic rearrangement of the contractile elements in activated ASM is presented.

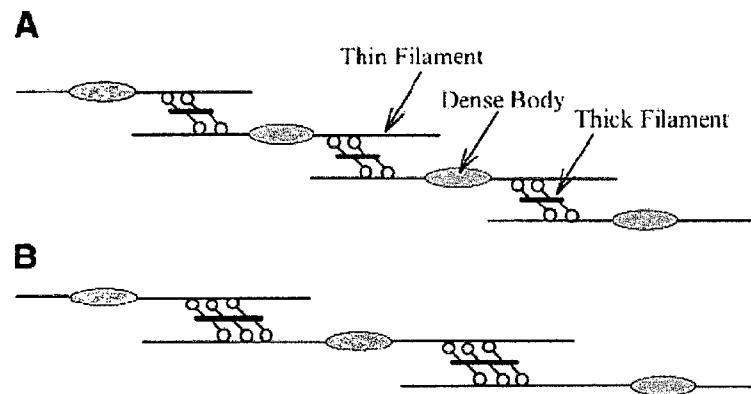


**Figure 6. Schematic representation of the series-to-parallel transition of thick filament lattice of airway smooth muscle.** The diagram illustrates the possible scenario where, after muscle activation, there is a transition from series (A) to parallel (B) of the thick filament lattice. Elongation of the thick filaments cause more cross-bridges in parallel to cycle and generate force. At the same time, by having longer filaments the cell can accommodate less of them in series within its cell length. Less thick filaments (contractile units) in series will translate to a decrease in the shortening velocity during muscle activation. Adapted from Seow et al, 2000.

### **2.2.1 Plastic adaptation to large changes in cell length**

Smooth muscle has the ability to function over a larger range of length than skeletal and cardiac muscle. This perhaps is important for the normal physiological functioning of some hollow organs, where large volume changes are necessary (Uvelius, 1976; Wingard et al, 1995). Uvelius (1976) described the ability of smooth muscle from rabbit urinary bladder to work over a large (~7 fold) range of length, and demonstrated that the change in muscle length is a reflection of changes in individual cell lengths. The same ability to work over a large range of length under physiological conditions was also shown to be present in swine carotid vascular smooth muscle (Wingard et al, 1995). In the airways this plastic property is not an exception, although it does not seem to serve any important physiological function. Rather, it seems that ASM adaptability to large changes in length only serves to cause troubles. In diseases like asthma and COPD, there are many conditions under which airway smooth muscle could be adapted to pathologically short lengths, e.g. chronic inflammation of the airway wall that decreases resting muscle length, acute inflammatory reactions with constant stimulation of the muscle, just to mention a few (Seow et al, 2001).

The plastic adaptation of ASM to large changes in length was first described in detail in 1995 by Pratusевич et al. The authors systematically evaluated some mechanical variables like tetanic force, shortening velocity and compliance of canine tracheal smooth muscle preparations. By examining the mechanical properties of ASM strips at two and threefold length range, the authors found that isometric force generation is (relatively) independent of muscle length, while shortening velocity is proportional to

muscle length. To explain their findings, Pratusевич et al. proposed the “plasticity theory” of airway smooth muscle. This theory or hypothesis suggests that ASM undergoes structural changes by varying the number of contractile units (thick filaments) in series in order to function over a large range of lengths. By reorganizing the number of thick filaments in series the muscle is able to keep the optimal overlap of thick and thin filaments (Fig. 7). Therefore, the plastic rearrangement of the contractile units allows the muscle to optimize its mechanical performance, that is, force generation and shortening velocity at a given muscle length (Pratusевич et al, 1995; Ford et al, 1994).

The plastic adaptation of ASM after a change in length was shown to be relatively fast (~30 min) if the muscle was periodically stimulated (Pratusевич et al, 1995). However, adaptation of ASM also occurs when the length of the muscle is passively changed with no subsequent stimulations (Wang et al, 2001; Naghshin et al, 2003), although longer time is required. In 2001, Wang et al. demonstrated a bi-directional shifting of the L-T curve after 24 hours of passive lengthening and shortening of ASM (Fig. 8). The changes in the L-T curve after the 24-h passive adaptation of the shortened muscles did not appear to be permanent as it could be reversed in 50 min after periodic stimulation of the muscle (Wang et al, 2001). In contrast, Naghshin et al. (2003) showed that irreversible adaptation of passively shortened ASM occurs after 7-8 days, and that the shifting of the L-T curve is directly proportional to the time the muscle spends at a shorter length. It was concluded that the number of contractile units in series probably changes due to chronic shortening or lengthening of the muscle, but that the filament overlap is likely kept at its optimal state (Naghshin et al, 2003).

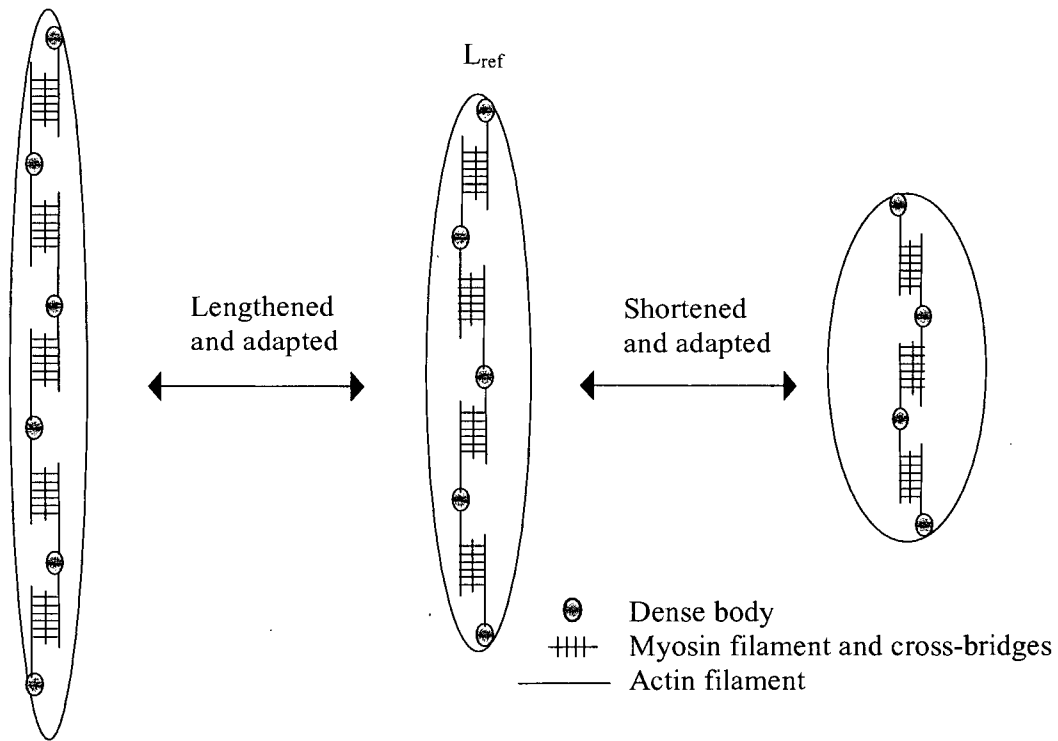


**Figure 7. Schematic representation of plastic length adaptation of ASM by rearrangement of the contractile units.** The diagram shows the hypothetical scenario of contractile unit rearrangement when the muscle is adapted to the new lengths. The model is based on the assumption that the number of contractile units in series will increase or decrease after adaptation of the muscle at a longer or shorter length respectively. The overlap of thick and thin filaments is kept optimal; therefore, force generation is preserved while shortening velocity becomes length dependant.

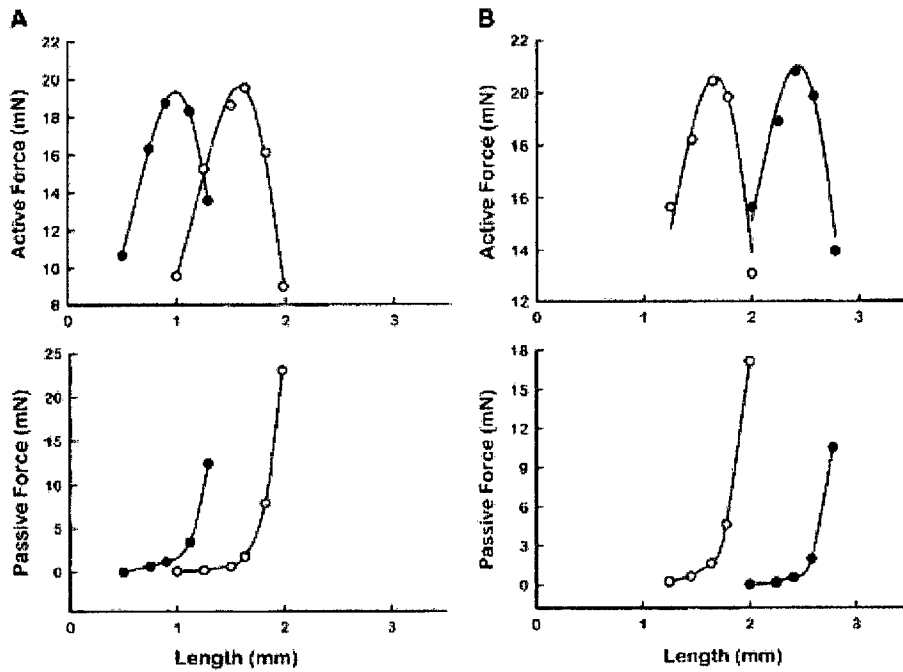


**Figure 8. Length-tension curves of passively shortened and lengthened rabbit trachealis.** When passively shortened (A) and passively lengthened (B) trachealis smooth muscle shows a shift of the L-T curve to shorter or longer lengths, respectively (closed circles). Adaptation of ASM to the passively imposed change in length can be explained by rearrangement of the contractile units in series. By deleting or increasing contractile units in series, the smooth muscle cell is able to preserve the optimal overlap of myosin-actin filaments, which in turn, preserves maximal force generation. Adapted from Wang et al, 2001.

In other studies, Gunst et al (1983; 1986; 1995) have shown that when ASM is adapted at a reference length and then shortened, there is a decrease in force development and shortening velocity proportional to the size of the shortening step (Gunst, 1983; 1986; Gunst et al, 1995). It was also observed that by letting the muscle sit at the new shorter length for a period of time, subsequent stimulations resulted in the recovery of force generation and shortening velocity (Gunst, 1983; 1986; Gunst et al, 1995). In addition to the adaptative changes in the contraction dynamics of ASM at a shorter length, Gunst et al. (1995, 2001) also observed marked alterations in the muscle stiffness (Gunst et al, 1995, 2001). ASM becomes significantly stiffer and less extensible after isometrically contracted at a shorter length, which suggests that the cytoskeletal structure of ASM cell changes when the muscle is activated at different lengths (Gunst et al, 1995, 2001, 2003). This process of cytoskeletal reorganization is believed to involve the remodeling of cytoskeletal structures that anchor actin filaments (i.e. dense plaques and dense bodies) as well as the remodeling of the actin filaments themselves (Gunst et al, 2003).

Together, these studies have shown that the plastic adaptation of ASM to different lengths is a complicated phenomenon that requires the reorganization of the contractile machinery and remodeling of the cytoskeletal structure of the muscle.

This phenomenon of adaptation has very important clinical implications in the area of respiratory diseases where chronic and excessive airway narrowing is present. This matter will be discussed in more detail in the next sections of this thesis.

### **2.2.2 Comparison of smooth muscle mechanical properties with those of skeletal muscle**

In contrast with smooth muscle, skeletal muscle exhibits a fixed and constant organization of its contractile machinery in structures known as sarcomeres. These sarcomeres are stable structures arranged in series and in parallel with one another in a muscle fiber. Sarcomere stability confers skeletal muscle the mechanical characteristics that set it apart from smooth muscle. In skeletal muscle, the active length range of a muscle fiber is determined by the number of sarcomeres in series while the maximal active force is proportional to the number of sarcomeres in parallel.

According to the sliding filament theory (Huxley and Niedergerke, 1954) sarcomere force depends on the amount of overlap of the contractile filaments (myosin-actin). The length, at which maximal force is generated, is referred to as the optimal length of the sarcomere. For lengths shorter than the optimal length, the force generated is submaximal. At lengths greater than the optimal length, active force decreases with the stretching of the muscle (Huxley and Niedergerke, 1954; Huxley, 2000). When chronically lengthened or shortened, skeletal muscle adapts to its new length by changing the numbers of sarcomeres in series (Williams et al, 1978; Farkas et al, 1983; Jakubiec-Puka et al, 1991). This adaptation has been shown to only occur after ~12-48 hours of passively lengthening or shortening the muscle if intermittent stimulation is applied (Jakubiec-Puka et al, 1991). On the other hand, if the muscle is passively lengthened or shortened and no stimulation is applied, the process of adaptation may not occur, and if it does, it happens very slowly (6-8 weeks).

Adaptation or remodeling of skeletal muscle to a new length, evidently serves as a mechanism to ensure that myosin-actin overlap remains optimal. Even though skeletal muscle is able to adapt to a new length, the mechanism by which this muscle adapts seems to be different from that of smooth muscle, in which adaptation occurs in a short period of time (~30 min) as previously described. Therefore, a fixed sarcomere-like structure cannot be used to explain the rapid plastic adaptation that occurs in smooth muscle after a change in length. A more dynamic and malleable structure is needed to facilitate the fast adaptation of smooth muscle. In this regard, it has been suggested that myosin polymerization/depolymerization plays an important role in muscle activation (Gillis et al, 1988; Godfrain-Debecker et al, 1988; Wantanabe et al, 1993; Xu et al, 1997) and in the process of smooth muscle adaptation to changes in length (Seow et al, 2000).

### **2.3 Airway smooth muscle in disease**

As described in previous sections ASM does not seem to have a specific physiological role in normal or healthy airways. However, ASM dysfunction has been implicated in the pathophysiology of chronic airway diseases such as asthma and COPD. Asthma and COPD are diseases characterized by airways hyperresponsiveness, that is, excessive airway narrowing in response to airway challenge with pharmacological agonists or irritant stimuli. Therefore, under these pathological conditions the most striking feature is the excessive narrowing of the airways, but the exact mechanism by which ASM contraction contributes to this exaggerated airway narrowing is not clear.

It remains unclear whether airway narrowing is exclusively caused by changes in the ASM phenotype, changes in the amount of muscle or changes/rearrangement of the contractile elements of the muscle or if it is a product of the combination of all these factors. It is believed that due to chronic inflammation of the airways, ASM is constantly activated and shortened, which in the long run directly contributes to and perpetuates airway narrowing (Moreno et al, 1986). As previously described, ASM has the ability to plastically adapt to new lengths by possibly rearranging its contractile apparatus. If this is true, then by sitting at a shorter length as it occurs in chronic inflammation, ASM could adapt to this shorter length and enhance airway narrowing. Thus, once we understand the mechanisms regulating changes in the contractile activity and the plastic adaptation of healthy ASM we will be able explore the mechanisms involved in the development of pathological conditions like asthma or COPD.

### **2.3.1 Deep inspiration and how ASM responds to mechanical strain**

With normal breathing, ASM is subjected to constant mechanical oscillations, which are believed to have an important impact on the ability of the muscle to function properly (Shen et al, 1997; Wang et al, 2000; Wang et al, 2002). In normal subjects these oscillatory strains have been shown to relax the contracted ASM (bronchodilatory effect), whereas in asthmatic patients the strains do not seem to have the same relaxing effect (Wheatley et al, 1989). Deep inspiration (DI) has also been shown to have a bronchoprotective effect on subsequently stimulated normal airways

(Malmberg et al, 1993), but in asthmatic airways DI elicited before stimulation has no effect (Scichilone et al, 2001).

It is believed that DI and tidal breathing affect the airways mainly by stretching the ASM layer and that the lack of response observed in asthmatic airways is caused either by mechanical decoupling of lung parenchyma and airway wall components from the muscle layer or by an abnormal response to strain by ASM (Gunst, 1983; Fredberg, 2001).

The bronchodilatory effect of DI and tidal breathing in healthy airways can be explained by the disruption of the cross-bridge dynamics and the consequent decrease in force generated by the muscle (Gunst, 1983; Fredberg et al, 1997). It has been suggested that the strain caused by DI perturbs the equilibrium of myosin binding causing the cross-bridges to detach from the actin filaments prematurely. Thus, by decreasing the number of attached cross-bridges, mechanical strain decreases the active force (Fredberg et al, 1997,1999). Even though the perturbed equilibrium of myosin binding can explain the bronchodilatory effect of DI on the normal airways, it cannot explain the bronchoprotective effect.

By applying oscillatory strain to relaxed ASM and mimicking the cyclic lengthening of the muscle during tidal breathing or consecutive DI, it has been found that ASM temporarily loses its ability to generate maximal force after length perturbation. This could explain, at least in part, the *in vivo* observation of the bronchoprotective effect of DI (Wang et al, 2000, Kuo et al, 2001). Wang et al. (2000) showed that force depression is linearly related to the amplitude of oscillation (Figure 9), and that large-

amplitude oscillations cause a transitory loss of force that cannot be explained by the perturbed cross-bridge binding equilibrium because the oscillation is applied to relaxed muscles where there is little cross-bridge interaction. After the oscillatory strain has ended, ASM is able to recover its ability to generate force if the muscle is allowed to adapt at a fixed length without further length perturbation. Later structural studies demonstrated that the decrease in force generation associated with length oscillation is accompanied by a proportional decrease of thick filament density -the number of thick filaments per cell cross-sectional area- in the ASM cells (Kuo et al, 2001). The thick filament density was shown to recover to the pre-oscillation levels as the muscle recovered its ability to generate maximal force (Figure 10). Wang et al. (2003) also demonstrated that maximal shortening velocity of ASM slightly but significantly increases when length oscillation is applied in the relaxed state (Wang et al, 2003).

All together, the findings of Wang et al (2000, 2001, 2002) and Kuo et al (2001) led to the suggestion that the disruption in force generation, decrease of thick filament density and increase in shortening velocity caused by length oscillation applied to relaxed muscles involve possible rearrangement, fragmentation, and partial dissolution of the contractile filaments in the muscle. The altered response of the ASM to mechanical strain could be due to a failure in the process of rearrangement of the contractile units and could explain the absence of the bronchoprotective effect of DI in asthmatic patients.

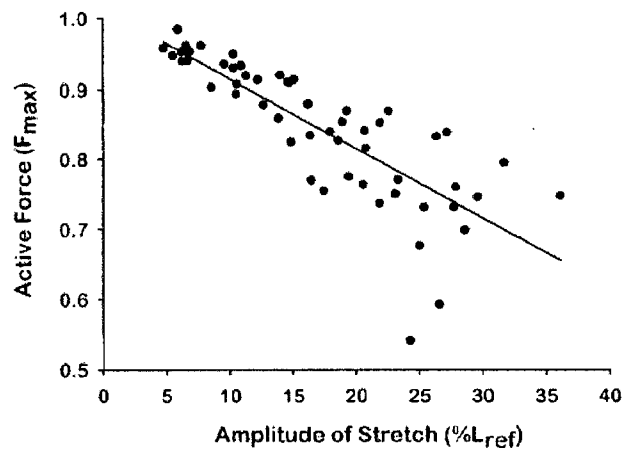


**Figure 9. Effect of oscillatory amplitude on ASM force generation.** The graph shows the linear relation of amplitude of oscillation and force depression on ASM subjected to length oscillation. Adapted from Wang et al, 2000.

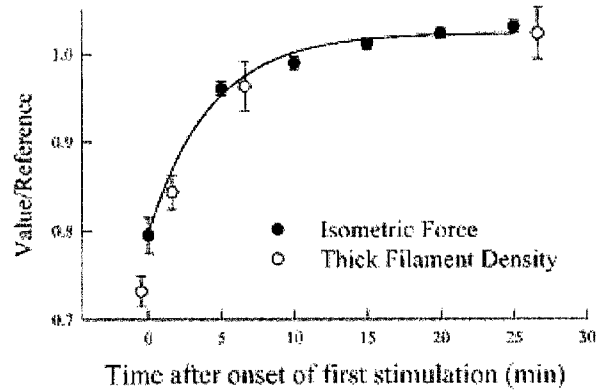


**Fig. 10. Isometric force and thick filament density recovery after ASM length oscillation.** The graph displays the time course of changes in isometric force and myosin thick-filament density after length oscillation. Adapted from Kuo et al, 2001.

## **CHAPTER 3. General hypothesis and specific aims**

### **3.1 Research focus**

The goal of this thesis research is to further our understanding of how smooth muscle contracts. A specific question being addressed is, what subcellular ultrastructural changes are responsible for the mechanical function observed at the whole cell level? ASM has an important pathophysiological role in diseases like asthma and COPD; to understand the pathophysiology, we need to first understand the normal structure and function of the tissue.

As it is referred to in the preceding sections, this thesis focuses on the relation between morphology and mechanical properties of ASM during contraction and adaptation to length changes. The studies presented here were carried out under the general hypothesis that the contractile apparatus and cytoskeleton in ASM are highly malleable and that there is active rearrangement of the contractile filaments upon activation and during length adaptation so that the optimal overlap between the contractile filaments is maintained.

Several questions that are dealt with in this thesis:

- How is the ASM contractile machinery organized *in vivo*?
- How are the mechanical properties and plastic behavior of ASM correlated to structural changes and vice-versa?

- What regulatory mechanisms are involved in the process of ASM's plastic adaptation to new lengths?
- What implications do the structural and functional findings have in terms of ASM's role in obstructive airway diseases?

### **3.2 General and specific hypotheses**

Based on the findings from previous studies in our laboratory on the mechanics and ultra-structure of ASM, a general hypothesis was adopted for this thesis research; the hypothesis is that the contractile apparatus and cytoskeleton of airways smooth muscle is highly malleable and that they undergo constant remodelling to accommodate large changes in the cell geometry and to optimise the cell's contractile function.

The following are specific hypotheses regarding the correlation of structure and function of ASM:

- Dynamic myosin and actin reorganization involving protein polymerization and depolymerization plays a key role in reorganization of the contractile filaments (myosin and actin) that in turn contributes directly to force development during muscle activation and to the process of plastic adaptation to length change where maximal isometric force is rendered length independent.

- Intracellular resting calcium level is necessary for a basal level of thick filament formation and stability in intact airway smooth muscle; increase in intracellular calcium concentration associated with muscle activation facilitates further thick filament formation through calcium-dependent myosin regulatory light chain phosphorylation.
- Adaptation of ASM to different lengths involves a change in the number of contractile units in series and in parallel, and a change in the contractile filament length for maintaining the optimal overlap of actin and myosin filaments.

### **3.3 Specific aims**

The present thesis is based on two published papers (Herrera, A. M., K.-H. Kuo, and C. Y. Seow. Influence of calcium on myosin thick filament formation in intact airway smooth muscle. *Am. J. Physiol. Cell Physiol.* 282: C310-C316, 2002; Herrera AM, Martinez EC, and Seow CY. Electron microscopic study of actin polymerization in airway smooth muscle. *Am J Physiol Lung Cell Mol Physiol.* 286(6): L1161-8, 2004) and a manuscript on which I am the lead author. The specific aims are therefore organized in three main groups.

### **3.3.1 Determination of thick filament stability and factors affecting thick filament formation in vivo**

The thick filament density in cell cross-sections were assessed in intact ASM to quantify the changes in thick filament mass under various conditions: 1) fully adapted and relaxed; 2) fully adapted and contracted; 3) immediately after a period of length oscillation; 4) fully recovered after the length oscillation; 5) in the absence of basal level of intracellular calcium.

### **3.3.2 Determination of thin filament stability and factors affecting thin filament formation in vivo**

The thin filament density in cell cross-sections was assessed in intact ASM to quantify the changes in thin filament mass under the same conditions outlined for thick filament quantification (above).

### **3.3.3 Determination of contractile unit reorganization in ASM adapted to different lengths**

The changes in contractile unit arrangement was assessed functionally by measuring the length-force relationships at different muscle lengths and structurally by quantifying the thin and thick filament densities, as well as the density of dense bodies. The functional and structural data were used to produce specific models that

illustrate changes in contractile unit rearrangement associated with muscle adaptation to different cell lengths.

## **CHAPTER 4. General methods and experimental protocols**

### **4.1 Tissue preparation**

Porcine tracheal smooth muscle was used for all the studies described in this thesis.

The tracheas were obtained from a local abattoir. Immediately after their removal from the animals, the tracheas were placed in physiological saline solution at 4°C. Rectangular smooth muscle strips (~6 x ~1.5 x ~0.3 mm in dimension) were dissected from the tracheas. Special care was taken to obtain clean (free of connective tissue) smooth muscle strips for structural analysis. The strips were attached to aluminum foil clips at both ends. One end of the muscle strip was placed over a stationary hook inside the muscle bath, and the other end was connected to the lever arm of a servo-controlled force/length transducer. The muscle bath contained physiological saline solution (PSS) with pH 7.4 at 37°C, bubbled with a gas mixture (5% CO<sub>2</sub>-95% O<sub>2</sub>), with a composition (in mM) of 118 NaCl, 5 KCl, 1.2 NaH<sub>2</sub>PO<sub>4</sub>, 22.5 NaHCO<sub>3</sub>, 2 MgSO<sub>4</sub>, 2 CaCl<sub>2</sub>, and 2g/l dextrose. During the periods of equilibration and experiment the PSS in the muscle bath was changed every 5 minutes.

The experimental apparatus consisted of a servo-controlled force/length lever system with a force resolution of 10 µN and a length resolution of 1 µm. The analog signals were converted to digital signals via a National Instrument analog-to-digital converter and were recorded by a computer. The computer also controlled the sequence of events during the experiments.

## 4.2 Mechanical measurements of the muscle properties

In all the experiments the strips of smooth muscle were equilibrated in the PSS at 37°C and electrical field stimulation (EFS) was applied once (for 12 s) every 5 min until the isometric force production reached a steady state. This process took about 1 hour per strip of muscle. During equilibration, a reference length of the muscle ( $L_{ref}$ ) was established by stretching the muscle to approximately the *in situ* length, at which the resting tension was 1–2% of the maximal isometric force. The EFS was provided by a 60-Hz alternating current stimulator with platinum electrodes. The maximal isometric force generation ( $F_{max}$ ) of each muscle at  $L_{ref}$  was recorded; the muscle was then ready for the next step of the experimental protocol or for fixation for structural analysis.

As part of the experimental protocol some strips of muscles adapted at  $L_{ref}$  and other lengths were activated with Acetylcholine (Ach) to obtain a steady plateau of muscle contraction. The Ach concentration used for the contractile activation of the muscle was  $10^{-4}$  M. The isometric contraction and force generation produced by Ach were followed for ~300 seconds. The muscles were then fixed under contractile activation for structural study.

### 4.3 Electron microscopy

All muscle preparations were primarily fixed for 15 min while they were still attached to the experimental apparatus. Care was taken not to disrupt the muscle mechanically during the fixation. The primary fixing solution contained 2% glutaraldehyde, 2% paraformaldehyde, and 2% tannic acid in 0.1 M sodium cacodylate buffer that was pre-warmed to the same temperature as the bathing solution (37°C). After the initial fixation, the strip was removed from the apparatus, cut into small blocks ~1x ~0.5x ~0.3 mm in dimension, and put in the primary fixing solution for 2 h at 4°C on a shaker. The blocks were then washed three times in 0.1 M sodium cacodylate (30 min). In the process of secondary fixation, the blocks were put in 1% OsO<sub>4</sub>-0.1 M sodium cacodylate buffer for 2 hours, followed by three washes with distilled water (30 min). The blocks were then further treated with 1% uranyl acetate for 1 h (en bloc staining), followed by washes with distilled water. Increasing concentrations of ethanol (50, 70, 80, 90, and 95%) were used (10 min each) in the process of dehydration. Ethanol (100%) and propylene oxide were used (three 10-min and 15-min washes, respectively) for the final process of dehydration. The blocks were left overnight in the resin (TAAB 812 mix, medium hardness) and then embedded in molds and placed in an oven at 60°C for 8–10 h. The embedded blocks were sectioned on a microtome with a diamond knife and placed on 400-mesh copper grids. The section thickness was ~90-100 nm. The sections were then stained with 1% uranyl acetate and Reynolds lead citrate for 4 and 3 min, respectively. The images of the cross sections of the muscle cells were obtained with a Phillips 300 electron microscope.

#### 4.4 Morphometric analysis

Sampling and analysis for all the experiments described in this dissertation were carried out “blind”. The codes indicating experimental conditions were revealed only after the analysis of each group was finished. A range of 25-60 electron micrographs of muscle cell cross sections per trachea (~5-15 sections per preparation) were analysed for each experiment. A specialized image analysis software (Image Pro-Plus 3.0) was used to help in the manual counting of the thick and thin filaments by marking and keeping track of the number of filaments counted (tag-point counting).

In some studies, thick filaments were counted in the whole cell cross section. The total number of thick filaments was then divided by the cytoplasmic area of the cell to obtain the thick filament density. The cytoplasmic area of the cells was equivalent to the total area of the cell cross section minus areas occupied by nuclei, mitochondria, and other organelles. In other studies, the computer program randomly placed 10 circles with an area of  $0.1734 \mu\text{m}^2$  on each micrograph (Fig. 11). Circles that fell on the areas occupied by nucleus, organelles, plasma membrane or extracellular space were excluded from the study; only the circles that fell on cytoplasmic areas with mostly thick and thin filaments, and occasionally dense bodies, were counted. The area occupied by dense bodies was not included in the calculation of filament density. Of the 10 circles generated by the computer, about 3-4 of them met the criteria. Thick and thin filaments were counted and the resulting number was divided by the area of the circle to obtain the thick and thin filament density.

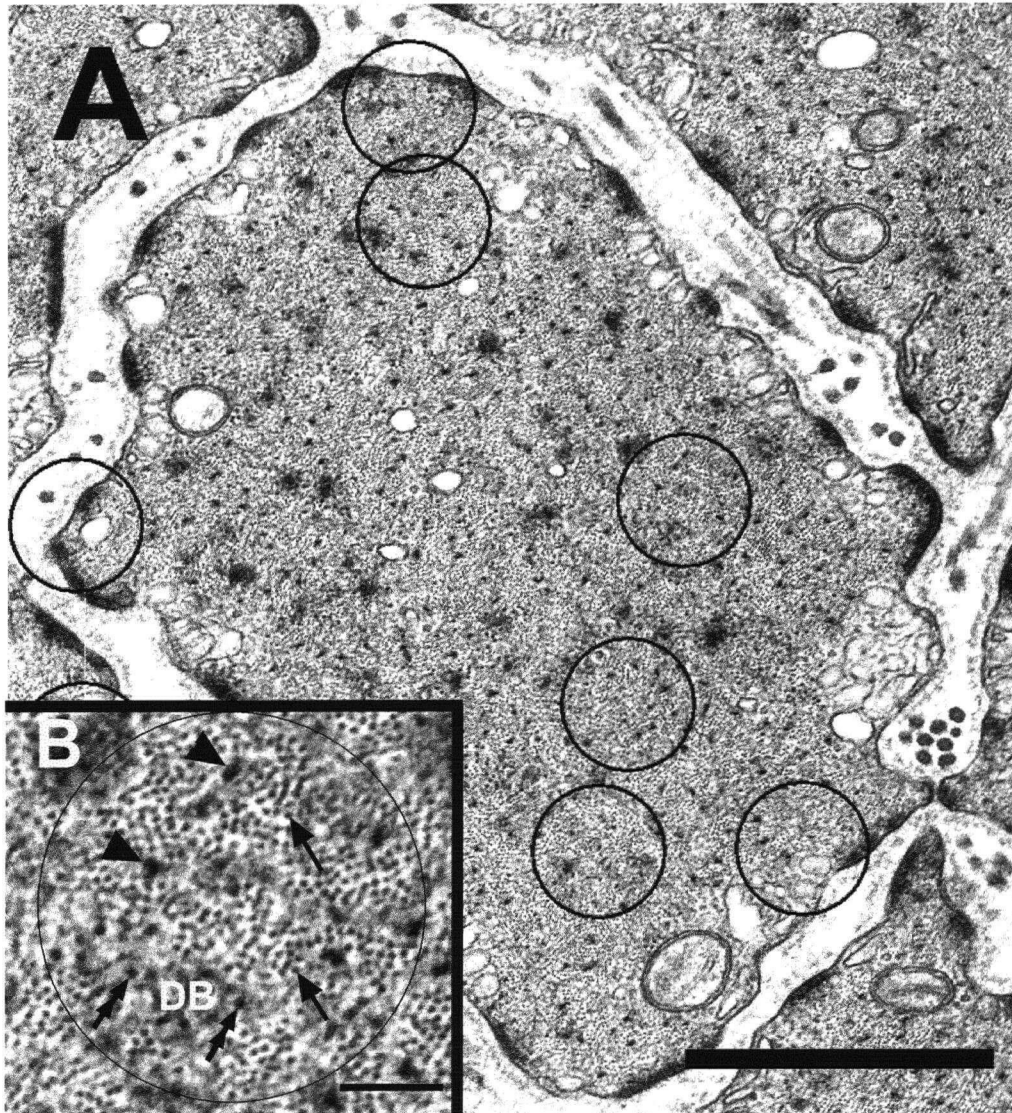


**Figure 11. Example of randomly selected areas for morphometric analysis.**

**A.** An electron micrograph showing a transverse section of a porcine trachealis cell fixed at its in situ length and in the relaxed state. The circles were randomly placed by the computer; only the circles that cover cytoplasmic area with no inclusion of major organelles were selected for filament counting. Calibration bar: 1  $\mu\text{m}$ .

**B.** (Inset). An enlarged circle in A. Arrowheads point to myosin filaments; arrows point to actin filaments; double arrows point to intermediate filaments. DB: dense body. Calibration bar: 0.1  $\mu\text{m}$ .

#### **4.5 Statistical analysis**

The analysis and comparison between the groups were performed by one-way or two-way ANOVA. N was the number of animals (tracheas) used. Data from each animal were averaged first before the means from different animals were averaged. Statistically significant difference corresponds to a  $p$  value  $<0.05$ .

## **CHAPTER 5. Myosin thick filament stability**

### **5.1 Thick filament formation *in vitro***

It has been known that smooth muscle thick filaments are structurally different from those of skeletal muscle. In smooth muscle, myosin molecules aggregate into “side-polar” filaments (Fig. 5B) in contrast with the bipolar conformation found in the thick filaments of skeletal muscle (Craig et al, 1977). The side-polar filaments have no central bare zone and are formed mainly by the antiparallel overlap of myosin tails, which confers the filaments with the ability to further elongate by the addition of more myosin molecules (Craig et al, 1977, Kendrick-Jones et al, 1987). By using isolated myosin II molecules in solution, it was found that myosin exists in two different conformational states classified according to their sedimentation coefficient into 10S and 6S (Trybus et al, 1982). The 10S myosin is a dephosphorylated monomer (assembly-incompetent form) with its tail folded into equal thirds. This folded monomer unfolds to a 6S conformation when the myosin regulatory light chain (RLC) is phosphorylated (Trybus et al, 1982, Trybus et al, 1984, Craig et al, 1983). The 6S is an extended monomer that is more suitable to form antiparallel dimers and therefore, to assemble into filaments. (Trybus et al, 1982, Trybus et al, 1984, Craig et al, 1983). The transition between myosin conformational states was found to be influenced by different factors like pH, ionic strength,  $\text{MgCl}_2$  concentration, but mainly by the  $\text{Ca}^{2+}$ -dependent phosphorylation of myosin RLC (Trybus et al, 1982, Trybus et al, 1984, Craig et al, 1983). Phosphorylation of the myosin RLC has been shown to be closely coupled with the initiation of

contraction in smooth muscle (Kamm et al, 1985). As a result, phosphorylation of the myosin RLC seems to have a dual regulatory role on smooth muscle myosin by affecting its conformational state and its enzymatic activity (Trybus, 1989). By studying myosin molecules in solution researchers have shown that  $\text{Ca}^{2+}$ -dependent phosphorylation of myosin RLC directly contributes to the thick filament assembly *in vitro*; however, it does not seem to directly contribute to the thick filament stability *in vivo*. In 1981, Somlyo et al. showed that even in the un-phosphorylated state, myosin thick filaments are abundantly present in the relaxed smooth muscle (Somlyo et al, 1981). Therefore, the question of how exactly the polymerization and depolymerization of smooth muscle myosin are regulated *in vivo* remains unanswered.

## **5.2 Smooth muscle myosin thick filament stability *in vivo***

It has been suggested that myosin thick filaments in relaxed smooth muscle are partially dissolved and reaggregate upon activation (Gillis et al, 1988; Godfrain-De Becker et al, 1988; Watanabe et al, 1993; Xu et al, 1997). Functional studies of ASM have shown that thick filament lengthening could account for the increase in isometric force and the decrease in shortening velocity during the sustained phase of contraction (Seow et al, 2000). It was observed in ASM that within at least a threefold length range and when the muscle was allowed to adapt to the lengths at which it was studied, isometric force was independent of muscle length, and shortening velocity and power output were positively correlated to muscle length (Pratusevich et al, 1995). The observations suggest that the

number of in-series contractile units (of which myosin thick filaments are an essential component) could be variable. In a more recent study, Kuo et al (2001) have observed that the thick filaments in intact airway smooth muscle dissolved partially when subjected to mechanical perturbation (Kuo et al, 2001). There are, therefore, many lines of evidence supporting a notion that myosin thick filaments in smooth muscle are labile; partial disassembly/reassembly of the thick filaments could allow the muscle to quickly adapt to externally imposed mechanical strains that reshape the cell.

### **5.3 Objectives and specific protocol**

As a first step toward understanding what regulates ASM cellular plasticity in terms of thick filament formation, the present studies were carried out to examine myosin evanescence during muscle activation and length adaptation and to determine the stability of the thick filaments in relaxed ASM depleted of calcium and subjected to mechanical perturbation.

#### **5.3.1 Muscle activation and length adaptation protocol**

Before the trachealis preparations were chemically fixed for electron microscopic examination, they were equilibrated at a preset length for about 1 hour. During the equilibration period, the muscles were stimulated (with electric field stimulation, 60 Hz)

periodically to produce 12-s tetani at 5-min intervals. The preparations were considered equilibrated when it developed a stable maximal isometric tetanic force. Tracheas from three animals were used for the experiments. There were 4 experimental conditions under which the preparations were fixed (after equilibration): 1) relaxed and unstrained (at the in situ length); 2) activated at the in situ length; 3) relaxed and strained (at 1.5x the in situ length); 4) activated and strained (at 1.5x the in situ length). For the preparations fixed under an activated state, the final stimulation was produced by addition of 0.1 mM of acetylcholine to the muscle bath. The muscle was fixed at the plateau of isometric contraction 120 s after the addition of acetylcholine. Acetylcholine (instead of electric field stimulation) was used in the final contraction to ensure that activation of the muscle was maintained during fixation. Muscle preparations were fixed for EM using a conventional protocol described previously in chapter 4.

### **5.3.2 Extracellular calcium removal and length oscillation protocol**

For this part of the thick filament study, a bath solution different from the normal PSS described earlier was used. Zero-calcium saline solution (same composition as PSS, but with no added calcium) contained 1 mM EGTA and was bubbled with the same gas mixture to maintain the pH at 7.4.

Tracheas from four animals were used for the experiments. Four strips of muscle per trachea were dissected and fixed under four different conditions, as illustrated in Fig. 12.

A muscle strip fixed at *time 1* was used as the control. At *time 2*, a strip of muscle was fixed after five stimulations over a period of 25 min in zero-calcium PSS. Isometric force diminished during the time course of stimulation and was not detectable after the third stimulation. At *time 3*, a 5-min period of length oscillation was applied to the muscle while it was still in zero-calcium PSS. The amplitude of stretch associated with the oscillation was 30% *in situ length*. At *time 4*, the muscle was allowed to recover after the oscillation in normal PSS. During the period of recovery (25 min), the muscle was stimulated electrically once every 5 min. Full recovery of isometric force occurred after the first couple of stimulations. The muscle strip was fixed after relaxation from the fifth contraction. Note that all preparations were fixed in the relaxed state in this group of experiments. The same protocol was repeated four times for four groups of muscle preparations from four tracheas. Results from each of the four strips under the same condition from four different animals were averaged to obtain the final data. Muscle preparations were fixed for EM using a conventional protocol described previously in chapter 4.

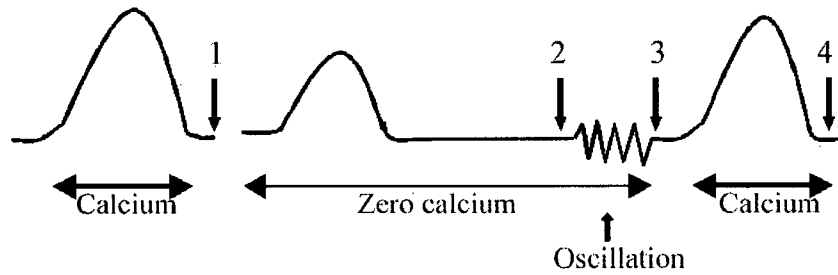


**Figure 12. Experimental protocol for extracellular calcium removal and length oscillation.** The diagram illustrates time points during the course of experiment when the muscle samples were fixed for electron microscopic examination. Contraction of muscle was elicited by a 12 sec EFS. Note that the samples were all fixed in resting state.

### **5.3.3 Morphometric analysis protocol**

As described in chapter 4, for all the experiments, sampling and analysis were carried out “blind”. The codes indicating experimental conditions were revealed only after the analysis of each group was finished. Each analyzed image contained a whole cell cross section. Some of these micrographs contained cross sections of cells with nuclei, central clusters of mitochondria, and some or no other organelles. This protocol of sampling of cross sections was used to ensure that the ultra-structure in different regions of a cell was examined. Myosin thick filaments were identified by eye and manually counted in the whole cell cross section. A potential inaccuracy in identifying the thick filaments was due to the variable size of the thick filament cross sections. The thick filaments, on average, have a diameter of about 15–20 nm. However, the filaments have tapered ends, and the diameter at both ends is therefore smaller than that in the middle. The thick filaments, however, can be identified by the “rosette” of thin filaments surrounding them under most circumstances, regardless of their size. It is still possible though that the number of thick filaments was underestimated with our counting method, but because the same criteria were used in counting all groups, the underestimation should be the same in all groups.

For the muscle activation and length adaptation study, a total of 20 electron micrographs of muscle cell cross sections per trachea were analyzed (5 per preparation). A specialized image analysis software (Image Pro-Plus 3.0) was used to help in the manual counting of the thick filaments by marking and keeping track of the number of filaments counted

(tag-point counting). For the analysis of thick filament density change in the relaxed muscle in the presence and absence of calcium and mechanical perturbation, a total of 240 images of cross sections of the muscle cells were analyzed. Fifteen micrographs per strip of muscle (60 images/animal) were selected. The cell cross-sectional areas were measured with a morphometric digital device made by Carl Zeiss.

In all the studies, the thick filament density was obtained by dividing the number of thick filaments by the total area of the cell cross section minus areas occupied by nuclei, mitochondria, and other organelles (cytoplasmic area). The density in the central region of a cell cross section was assessed by placing a circle (such as the ones in Fig. 11) in the central region of a cell cross section, counting the number of thick filaments within the circle and dividing the number by the circle area. The peripheral density was assessed by randomly placing a circle in the peripheral region of a cell cross section, counting the number of thick filaments in the circle and dividing the number by the circle area.

#### **5.4 Effects of muscle activation and length adaptation on thick filament density**

Figure 13 shows an example of airway smooth muscle cell cross sections fixed in the relaxed state (Fig. 13-A) and at the plateau of acetylcholine-elicited contraction (Fig. 13-B). Cross-sectional densities of the thick filaments under various conditions are shown in Figure 14. Both contractile activation and adaptation of the muscle at the longer length caused a significant increase in the thick filament density. The distribution of the thick

filaments in a cell cross section was relatively even in the relaxed state; in the activated state the distribution was less even with small clusters formed in various regions in a cell, but there was no systematic aggregation of thick filaments in the central or peripheral regions (Fig. 13-B).

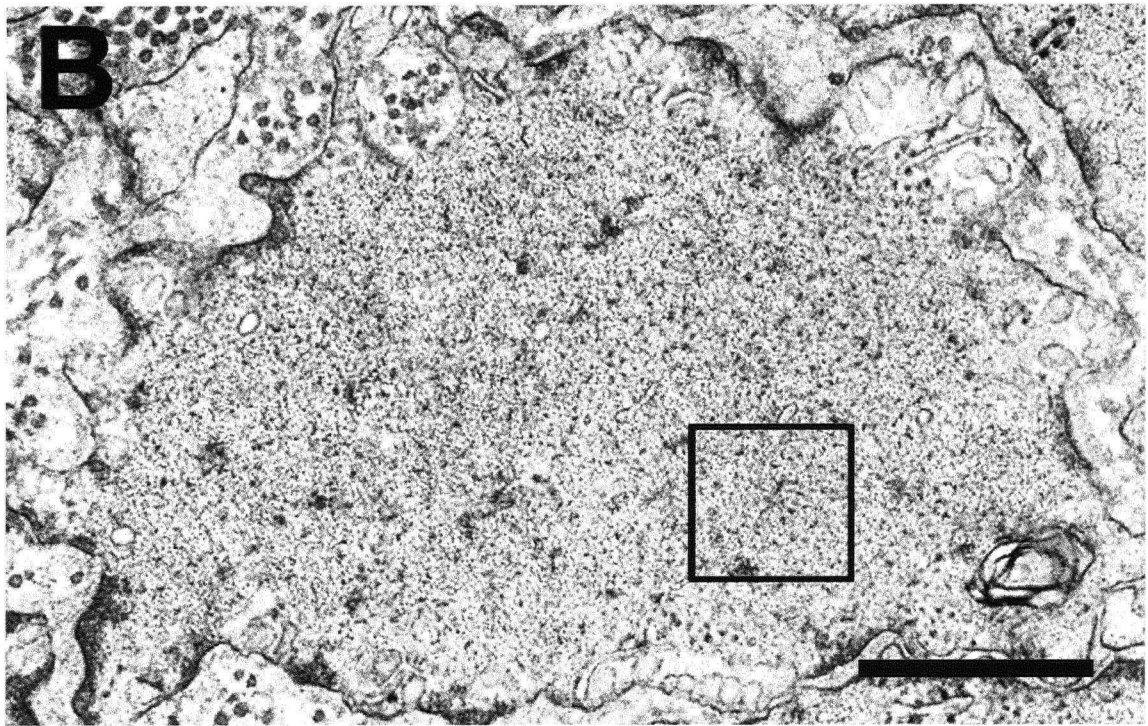
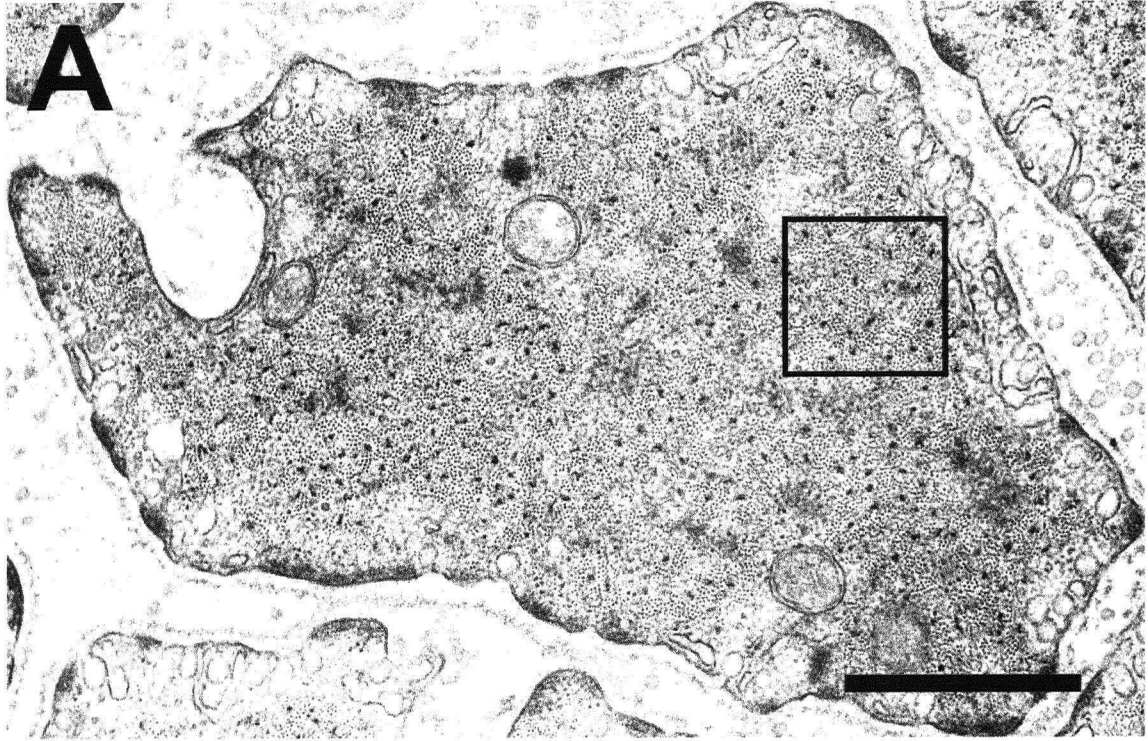
After length adaptation at 1.5x the *in situ* length, thick filament density significantly increased by  $25.05\% \pm 0.33$  (SEM) and  $39.1\% \pm 1.26$  in the relaxed and activated muscles, respectively. Contractile activation resulted in a significant increase in the thick filament density; in cells activated at *in situ* length, the density increased by  $63.3\% \pm 1.9$  (SEM), and in cells activated at 1.5x the *in situ* length, the density was found to increase by  $81.7\% \pm 5.67$  (Fig.14).

Although the thick filament distribution in the activated muscle is not as even as in the relaxed state, there was no significant difference in the thick filament density in the central and peripheral regions of the cells cross sections.

The results indicate that there was a 25-39% increase in thick filament density after lengthening and adaptation of the muscle at 1.5x the *in situ* length. At the same time, there was a 63-82% increase in thick filament density due to contractile activation, depending on the adapted length of the muscle cells (Fig. 14). It appears therefore, that the formation of thick filaments is facilitated by muscle lengthening and to a greater extent by contractile activation.

The average isometric force after adaptation of the muscles at in situ length ( $43.7 \pm 7.3$  mN (SEM)) and at 1.5x the in situ length ( $48.2 \pm 7.2$  mN) was not significantly different ( $p > 0.05$ , paired T test).

The values of the cross-sectional areas at in situ length and at 1.5x the in situ length were  $7.01 \pm 0.25$  (SEM)  $\mu\text{m}^2$  and  $5.7 \pm .18$   $\mu\text{m}^2$  respectively. The decrease of cell cross-sectional area after stretching the muscle to 1.5x in situ length was of  $23.3\% \pm 0.58$ . These results indicate that the ASM cell volume is conserved at different lengths.



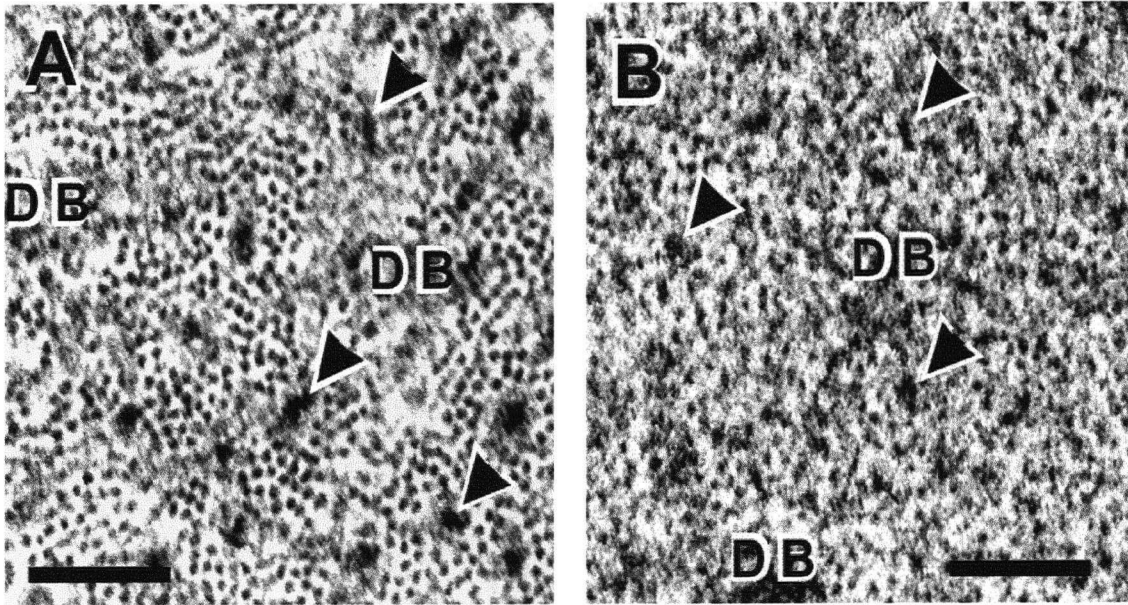


**Figure 13. Structural comparison of relaxed and activated ASM cells.** **A.** Example of a cross section of porcine trachealis cell fixed at the in situ length in the **relaxed** state. The square area is enlarged to show myosin filaments (arrowheads) and DB: dense bodies. **B.** Example of a cross section of porcine trachealis cell fixed at the in situ length in the **activated** state. The square area is enlarged to show myosin filaments (arrowheads) and DB: dense bodies. Calibration bars indicate 1  $\mu\text{m}$  (main pictures) and 0.1  $\mu\text{m}$  (magnifications).

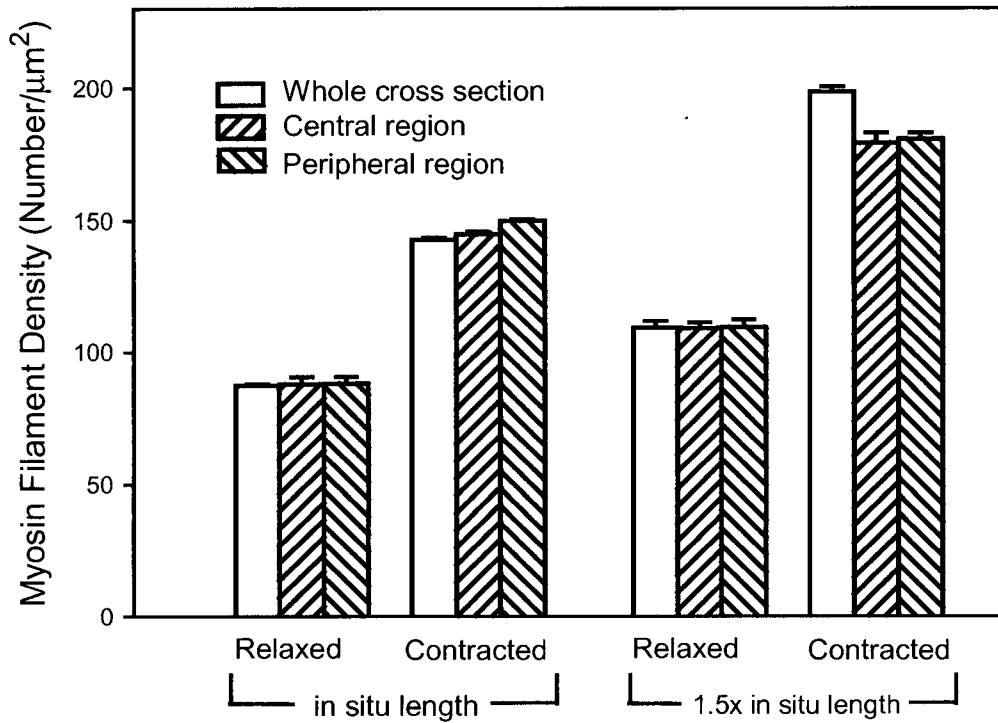


**Figure 14. Myosin (thick) filament densities in different regions of cross-sectional areas of trachealis cells.** Statistical analysis indicates no regional difference. The four groups (relaxed and contracted trachealis at two lengths) are however significantly different from one another (ANOVA,  $p < 0.05$ ). For each group, 5 cells from each of the 3 animals were used in the morphometric measurements. Means  $\pm$  SEM are plotted.

#### **5.4.1 Series-to-parallel transition of thick filament lattice due to muscle activation**

Lability of myosin thick filaments has been demonstrated in some intact smooth muscle preparations (Gillis et al, 1988; Godfraind-De Becker, 1988; Watanabe et al, 1993; Xu et al, 1997), including that of ASM (Kuo et al, 2001). The labile nature can be seen in the variation of the thick filament density in cross sections of cells fixed under different experimental conditions (Gillis et al, 1988; Kuo et al, 2001; Xu et al, 1997). The 63% increase in myosin filament density in contracted airway smooth muscle (compared with the density in the relaxed state) observed in the present study is similar to the 60% increase in thick filament density seen by Gillis et al (Gillis et al, 1988), but it is greater than the 23% increase in density due to activation in rat anococcygeus found by Xu et al (Xu et al, 1997). In contrast, in guinea pig taenia coli, no significant increase in thick filament density has been found (Xu et al, 1997). The difference in the observed myosin evanescence has been attributed to the difference in the “active state” in resting muscles (Gillis et al, 1998; Xu et al, 1997). Taenia coli normally does not exist in a truly relaxed state because of its ability to spontaneously contract. The thick filaments may not have a chance to disassemble in such a muscle. Anococcygeus muscle, on the other hand, has a long quiescent period in between contractions; this may allow the thick filaments to partially depolymerize. The airway smooth muscle preparation that we used has an extremely low resting activity, judging from the absence of active tone and zero myosin light chain (MLC) phosphorylation found in this preparation (Mitchell et al, 2001). This may explain the significant difference in the thick filament density between the relaxed and contracted states found in this study. Other explanations, however, cannot be

excluded; the variation in myosin evanescence may be due to differences in properties of myosin molecules and other cellular properties associated with different types of smooth muscle. It has been reported in rat anococcygeus that the cell cross-sectional area decreases when the muscle contracts (Gillis et al, 1998; Xu et al, 1997). The cell shrinkage was not observed in guinea pig taenia coli (Godfraind-De Becker, 1988), at least not consistently (Xu et al, 1997). No significant change in the cell cross-sectional area due to activation was found in this study, and therefore no correction for the area variation was carried out. To summarize, activation of ASM resulted in a 63% increase in the amount of myosin filaments seen in muscle cell cross sections at in situ length and 82% in muscle cell cross sections at 1.5x in situ length; the activation-dependent increase in the filament density may be related to the increase in MLC phosphorylation during muscle activation.

In ASM it has been observed that shortening velocity declines during the rise of force after muscle activation (Kamm et al, 1985; Seow et al, 1986; Seow et al, 2000). It has been proposed that the decrease in velocity is due to myosin filaments lengthening during the time course of an isometric contraction (Ford et al, 1994; Seow et al, 2000). If this is true, lengthening of the thick filaments during muscle activation will be translated to an increase of the thick filament number per  $\mu\text{m}^2$  of cell transverse area (thick filament density). Based on previous functional studies, the calculated thick-filament lengthening required to slow velocity during the rise in tetanic force is about ~55% (Seow et al, 2001). In the present study we found a significant increase of the thick filament density

after muscle activation (63%) that is close to the density estimated by Seow et al (Seow et al, 2001).

The results from this part of the study strongly suggest the occurrence of a series to parallel change in the smooth muscle filament lattice during muscle activation. This transition is most likely to be brought on by the elongation of thick filaments during the tetanus.

#### **5.4.2 Is there plastic rearrangement of contractile units?**

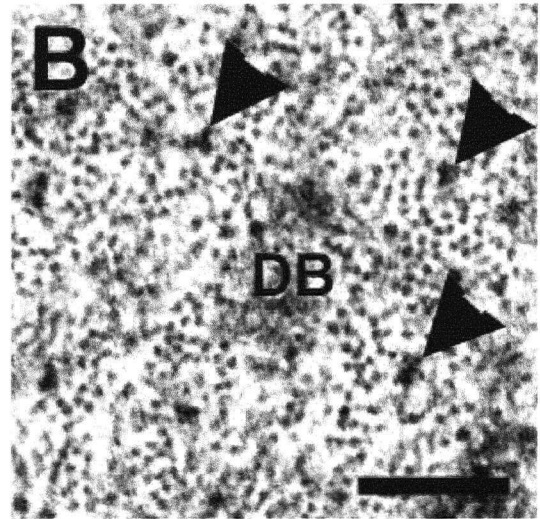
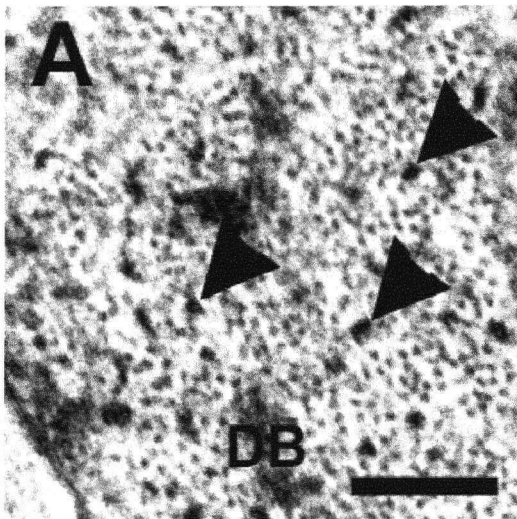
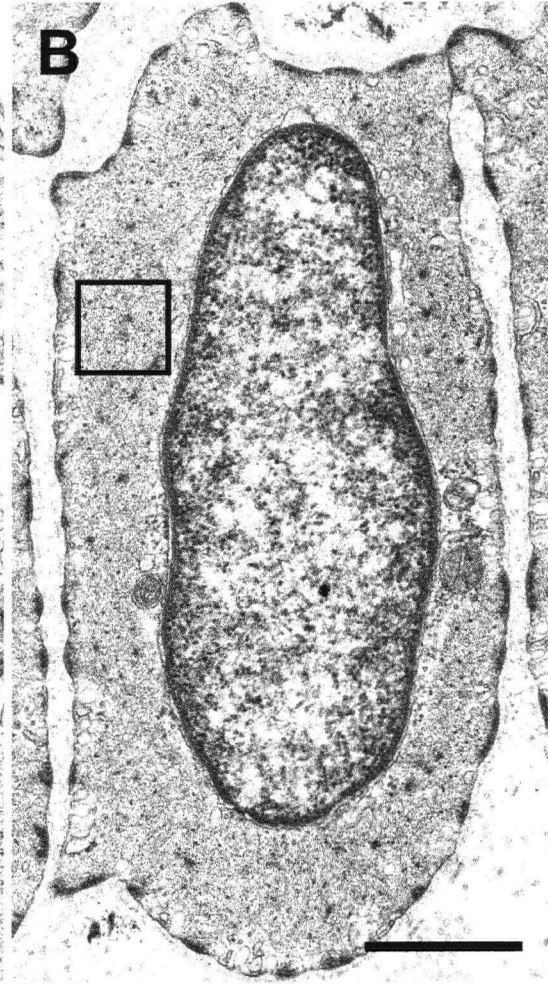
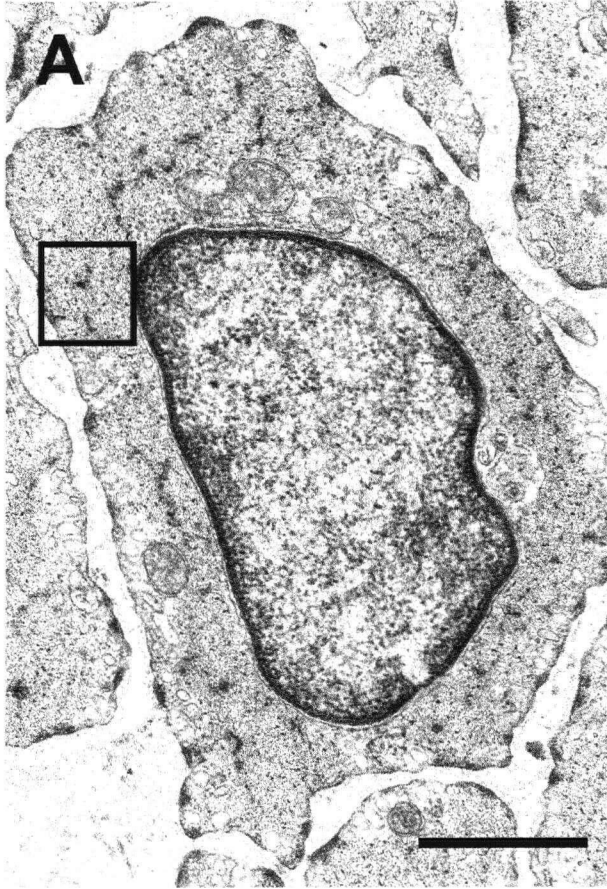
Early studies by Ford et al (1994) and Pratusевич et al (1995) have shown that isometric force of tracheal smooth muscle is independent of muscle length (after adaptation) and that velocity increases at long lengths (Ford et al, 1994; Pratusевич et al, 1995). Based on the results from these studies it was suggested that the number of contractile units (of which the thick filaments are an essential component) in series increases by lengthening of the muscle (Pratusевич et al, 1995). This theory proposes that the total amount of myosin filaments will increase when the muscle is adapted to a longer length and that adaptation of the muscle to large changes in cell length may be facilitated by the ability of smooth muscle thick filaments to depolymerize and repolymerize (Pratusевич et al, 1995). The random distribution of the thick filaments within cell and the possible polymerization of myosin molecules into filaments after increasing the cell length will most likely produce an increase in the total myosin filament content (Kuo et al, 2003). At

present, the most reliable method to indirectly estimate the myosin filament content, provided that the cell volume is conserved, is by finding the thick filament density in ASM cell cross-sections. In the current study, we found a significant increase (25%) of the thick filament density after stretching and adapting the muscle to 1.5x the *in situ* length. In the activated muscle, the thick filament density increase at 1.5x the *in situ* length was of 39%, value that agrees with the previously reported (35%) by Kuo et al (2003). In the present study we also observed that the isometric force developed by the muscle at 1.5x the *in situ* length was not different from that of the muscle at *in situ* length. Thus, the increase in the total content of myosin filaments is not associated with an increase in the number of filaments in parallel, but instead an increase of the total filaments in series. This is not the first time an increase in the thick filament density after adaptation at a longer length has been reported in ASM (Kuo et al, 2003). However, the results presented here provide more evidence that confirm that myosin filament content in ASM is regulated by muscle length and, that a plastic rearrangement of the contractile units (myosin filaments) in series occurs during the process of length adaptation.

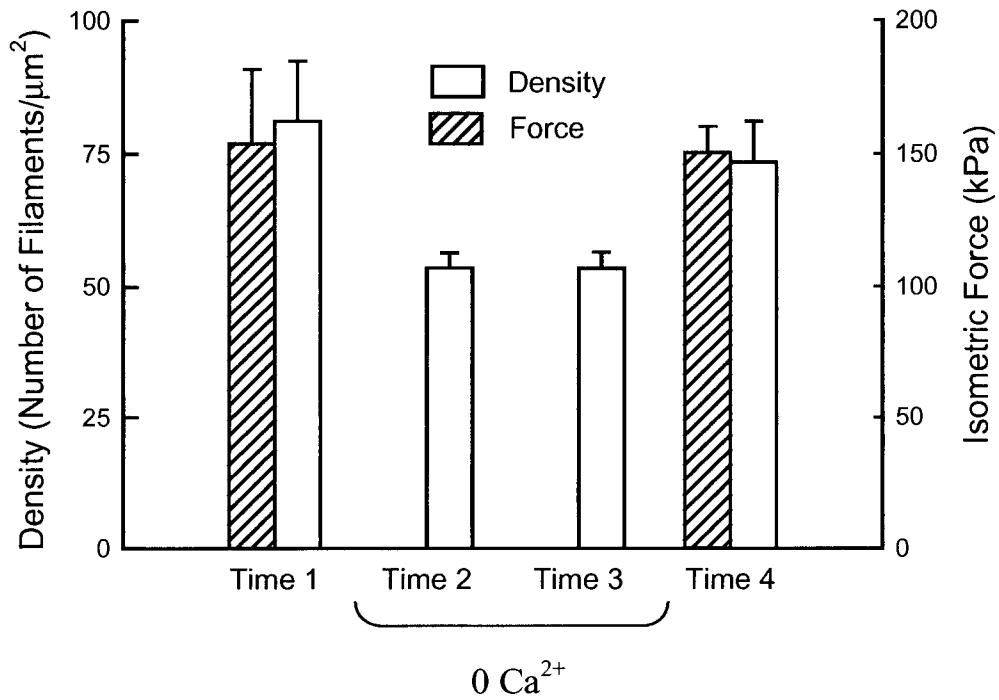
### **5.5 Influence of calcium on myosin thick filament formation**

Figure 15 shows two examples of airway smooth muscle cell cross sections fixed at *time 4* (Fig. 15-A) and *time 2* (Fig. 15-B). As shown in Fig. 12, *time 4* indicates the time point at which the muscle preparation had recovered from being in zero-calcium PSS and subjected to length oscillation. The isometric force, thick filament density, and other

morphometric appearances of the cross sections at *time 4* were not different from those at *time 1*, indicating that the experimental protocol did not cause permanent cell damage. *Time 2* indicates the time point at which the muscle preparation produced no isometric force due to the lack of calcium. Figure 16 shows the averaged ( $n=4$ ) thick filament densities for the samples fixed at the four time points shown in Fig. 12. One-way ANOVA showed that the variation in thick filament density is significant ( $P < 0.05$ ). The thick filament density decreased significantly by 35% after extracellular calcium removal. However, there was no difference ( $P = 0.67$ ) between the groups at *times 1* and *4*. Also, no significant difference ( $P = 0.59$ ) was found between the groups at *times 2* and *3*. Isometric force of the muscle was totally abolished in zero-calcium PSS. The force, however, recovered fully after reincubation of the muscle in normal PSS; isometric force produced by the muscle at *times 1* and *4* was not different ( $P = 0.9$ ) (Fig. 16). One-way ANOVA showed that there was no significant difference ( $P = 0.5$ ) among the cross-sectional areas.



**Figure 15. Examples of electron micrographs of muscle cell cross-sections for the extracellular calcium removal study.** **A.** Muscle sample fixed after a period of recovering from being in zero-calcium PSS and subjected to length oscillation (**Time 4** in Fig. 12). The square area is enlarged to show myosin filaments (arrowheads) and DB: dense bodies. Arrowheads point to myosin thick filaments surrounded by actin thin filaments. **B.** Muscle sample fixed after extracellular calcium removal (**Time 2** in Fig. 12). The square area is enlarged to show myosin filaments (arrowheads) and DB: dense bodies. Arrowheads point to myosin thick filaments surrounded by actin thin filaments. Calibration bars indicate 1  $\mu\text{m}$  (main pictures) and 0.1  $\mu\text{m}$  (magnifications).



**Figure 16. Thick filament density and isometric force associated with the 4 conditions in the extracellular calcium removal study.** The 4 conditions are indicated by the 4 time points in Fig. 12. Isometric tetanic force was elicited by 12 s EFS. At Time 2 and 3, force was zero. Means and standard errors are plotted.

### **5.5.1 Is myosin RLC phosphorylation directly involved?**

The underlying mechanism for the thick filament lability in intact smooth muscle is not clear. Studies of isolated myosins in solution have suggested that calcium-dependent phosphorylation of the myosin RLC was essential in the formation of the thick filaments (Kendrick-Jones et al, 1987; Trybus et al, 1982). The present finding of a substantial increase in myosin filament density upon muscle activation (described in the previous section) supports the notion that myosin light chain (MLC) phosphorylation could enhance thick filament formation. However, this does not mean that dephosphorylation of the light chain will cause total dissolution of the thick filaments. Thick filaments have been found in relaxed, dephosphorylated muscles (Somlyo et al, 1981; Tsukita et al, 1982). Results from the present study also indicate that thick filaments exist in relaxed ASM, even after removal of extracellular calcium and in the presence of the calcium-chelating agent EGTA. Calcium removal, however, does lower the thick filament density significantly (35%; Fig. 16). An intriguing question is whether this decrease in the filament density is due to a decrease in the level of MLC phosphorylation below its normal resting level. This is not likely considering that the normal resting level of phosphorylation in our preparation is virtually zero (Mitchell et al, 2001). Also, in a recent study Qi et al (2002) used wortmannin (a potent inhibitor of MLC kinase) to examine the effect of MLC phosphorylation on thick filament formation; they found that inhibition of MLC phosphorylation by wortmannin in the presence of calcium did not cause a reduction in the thick filament density from its normal resting level (although length oscillation was able to reduce the filament density under this condition, and

recovery of the density required removal of wortmannin) (Qi et al, 2002). The reduction in thick filament density (without mechanical agitation) associated with calcium removal therefore is likely due to disruption of some pathways that rely on a normal resting calcium level.

In conclusion, removal of calcium resulted in a 35% decrease in the filament density from its normal resting level; this change in filament density appears to be independent of MLC phosphorylation.

### **5.5.2 Is there myosin monomer-polymer equilibrium *in vivo*?**

The condition of zero extracellular calcium with EGTA likely creates a nonphysiological state for the muscle. The present experiment, however, demonstrated that a normal resting level of calcium was important for preservation of filamentous myosins in relaxed airway smooth muscle. It is interesting to observe that spontaneous calcium release (that does not contribute significantly to the global intracellular calcium concentration) appears to be essential for myofibrillogenesis in striated muscle. Blockade of the transient calcium release disrupts myosin thick filament assembly in the developing *Xenopus* myocytes (Ferrari et al, 1998). It is not known whether the occasional calcium “sparks” observed in resting smooth muscle have the same function in maintaining integrity of the thick filaments in the relaxed state. In a previous study (Kuo et al, 2001) it was shown that mechanical oscillation imposed on relaxed airway smooth muscle (in the presence of

normal extracellular calcium) resulted in a transient reduction in the thick filament density. The density (and isometric force) recovered fully after a period of 25–30 min during which the muscle was stimulated electrically once every 5 min (Kuo et al, 2001). In the present study, the same oscillation protocol was used but with the muscle bathed in zero-calcium PSS. Figure 16 shows that the amount of decrease in myosin thick filament density after oscillation (Fig. 12, *time 3*) was the same as that after removal of calcium without oscillation (Fig. 12, *time 2*). This is somewhat surprising considering that mechanical oscillation has been shown to be able to “break up” the labile (presumably nonphosphorylated) thick filaments in relaxed muscles (Kuo et al, 2001). It has been shown under *in vitro* conditions that there is equilibrium between filamentous and monomeric myosins (Kendrick-Jones et al, 1987), and once a critical concentration of monomeric myosins is reached, thick filaments will form even if the myosins are not phosphorylated. It is possible that the amount of thick filaments seen under zero-calcium conditions in the present study represents the minimum amount of thick filaments maintained by the equilibrium. Mechanical agitation may be able to cause dissolution of the filaments, but the equilibrium force would quickly reestablish the minimum concentration of thick filaments. It also is possible that the intracellular pathway that conveys the mechanical signal leading to dissolution of the thick filaments is calcium dependent; with removal of calcium, this pathway may not be functional, resulting in the insensitivity of thick filament density to mechanical stretch.

## **CHAPTER 6. Actin dynamics in ASM plasticity**

### **6.1 Actin regulation in smooth muscle**

Actin is a major cytoskeletal and contractile protein in muscle and non-muscle cells. It plays an important role in such diverse functions as motility, cytokinesis, contraction and control of cell shape. Actin exists in cells in one of two forms: globular or G-actin, which is not polymerised; and filamentous or F-actin, which is the polymerised form. Although it has been recognized for some time that actin polymerization and depolymerization associated with the contraction-relaxation cycle in smooth muscle is important for normal function of the tissue (Adler et al, 1983; Mauss et al, 1989), details of the actin dynamics and its relation to the basic mechanism of contraction have just begun to emerge. Many pathways have been implicated in the regulation of actin in smooth muscle. It appears that one of the pathways mediating the activation-associated actin reorganization is through activation of the small GTPase Rho and its subsequent activation of Dia1/profilin, which induces the formation of actin stress fibres and mediates the formation of actin filaments (Watanabe et al, 1999; Hedges et al, 1999; Lesh et al, 2001; Matrougui et al, 2001; Halayko et al, 2001; Tang et al, 2003). Another pathway that mediates the actin reorganization is thought to be via activation of p38 MAP kinase and its subsequent phosphorylation of the 27-kDa heat shock protein (HSP27) (Larsen et al, 1997; Hedges et al, 1999; Yamboliev et al, 2000; Gerthoffer et al, 2001). Phosphorylation of HSP27 has been shown to be involved in the regulation of actin polymerization, focal adhesions and cellular interaction with the extracellular

matrix. Therefore, the p38 MAP kinase/HSP27 complex is thought to also play an important role in modulating smooth muscle contraction (Yamboliev et al, 2000).

## **6.2 Mechanical properties of thin filaments in ASM**

Prevention of actin polymerization has been shown to severely reduce force production in many types of smooth muscle (Tseng et al, 1997; Filipe et al, 2002; Shaw et al 2003).

In ASM it has been shown that there is a substantial pool of globular actin molecules in the relaxed state and polymerization of these molecules occurs during contractile activation (Mehta et al, 1999). In cultured ASM cells it has been shown that oscillatory strain increased actin filament formation (Smith et al, 2003); this however has not been demonstrated in intact tissue. The actin filament formation associated with contractile activation is accompanied by an increase in the stiffness of the cytoskeleton; even after the contribution to the stiffness by actomyosin cross-bridges is excluded (An et al, 2002). These studies suggest that in the relaxed state actin filaments are likely partially dissolved and may not be firmly attached to the dense bodies/plaques or focal adhesion plaques, and the cytoskeleton may be malleable as a result. This interpretation is consistent with earlier findings from functional studies that showed plastic behaviour in these cells (Gunst et al, 1995; Pratusевич et al, 1995). The ability of the muscle to plastically reorganize its contractile apparatus and therefore optimize its contractile function has been attributed to malleability in both the cytoskeleton (Fabry et al, 2001) and the contractile filament arrays embedded in the cytoskeleton (Kuo et al, 2003).

Although there is strong functional evidence supporting plastic deformation of ASM cells subjected to large strains (both static and oscillatory), ultrastructural details associated with the remodelling of cytoskeleton/contractile apparatus are still vague, especially the details regarding actin filament formation and distribution within the muscle cell.

### **6.3 Objectives and experimental protocol**

The main objective of this project is to elucidate the role of actin polymerization/depolymerization in the process of reorganization of the cellular cytoskeleton and rearrangement of contractile units during the course of length adaptation in airway smooth muscle.

To gain insights into the role of actin polymerization in the cell's adaptation to external forces, the present study was carried out to quantify the densities of actin filaments in electron micrographs of transverse sections of intact airway smooth muscle fixed under a variety of experimental conditions.

### **6.3.1 Protocol for thin filament quantification after muscle activation and length adaptation**

Tracheas from 3 animals were used for this experiment. The muscle preparations were first equilibrated at near *in situ* length as previously described in Chapter 4. There were 5 experimental conditions under which the preparations were fixed (after equilibration): 1) relaxed and unstrained (at the *in situ* length); 2) activated at the *in situ* length; 3) relaxed and strained (at 1.5x the *in situ* length); 4) activated and strained (at 1.5x the *in situ* length); 5) relaxed at the *in situ* length and post-oscillation (the length-oscillation frequency was 0.5 Hz, the peak-to-peak amplitude of strain was 60% of the *in situ* length, the oscillation was centred around the *in situ* length which meant that the cells were subjected to a 30% stretch beyond their *in situ* length, the duration of oscillation was 5 min). Muscle activation and fixation for electron microscopy (EM) were performed as described in Chapter 4 and 5.

For the thin filament quantification, sampling and analysis were carried out “blind”. The codes indicating experimental conditions were revealed only after the analysis of each group was finished. A total of 25 electron micrographs of muscle cell cross sections per trachea were analyzed (5 per preparation). A specialized image analysis software (Image Pro-Plus 3.0) was used to help in the manual counting of the thin filaments by marking and keeping track of the number of filaments counted (tag-point counting). The computer program randomly placed 10 circles with an area of  $0.1734 \mu\text{m}^2$  on each micrograph (Chapter 4, Figure 11). The thin filaments were counted by the tag-point

quantification method in each of the non-excluded circles placed in the cytoplasmic areas on the cells. According to standard morphological methods, the filaments that fell on the edge of the circles were counted as half. The total numbers of thin filaments counted were divided by the area of the circle (minus area of dense bodies, if there were any) to obtain the thin filament density.

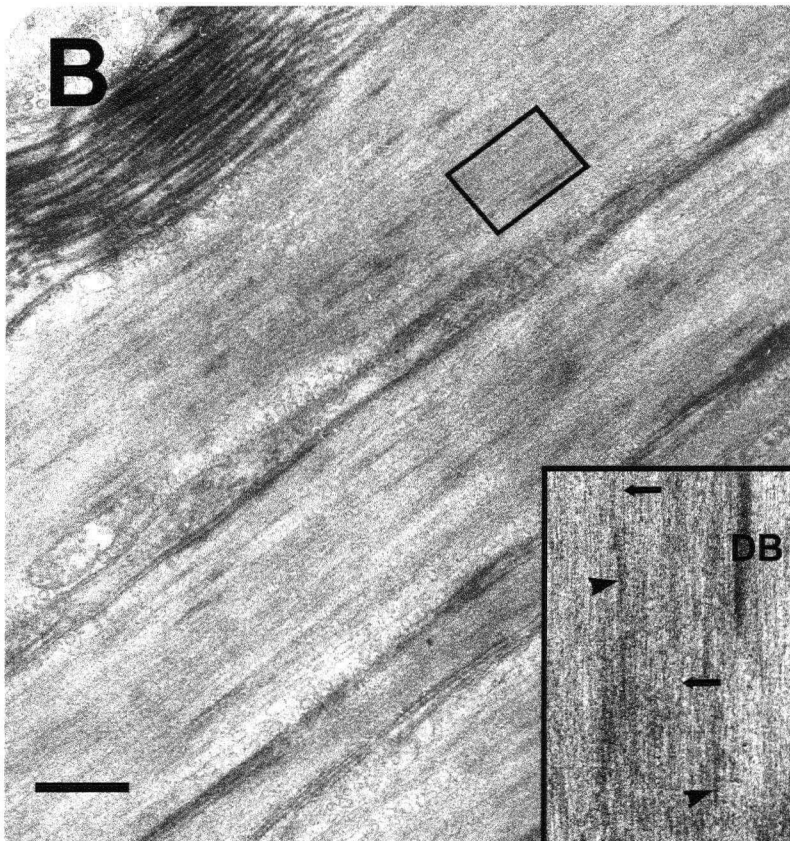
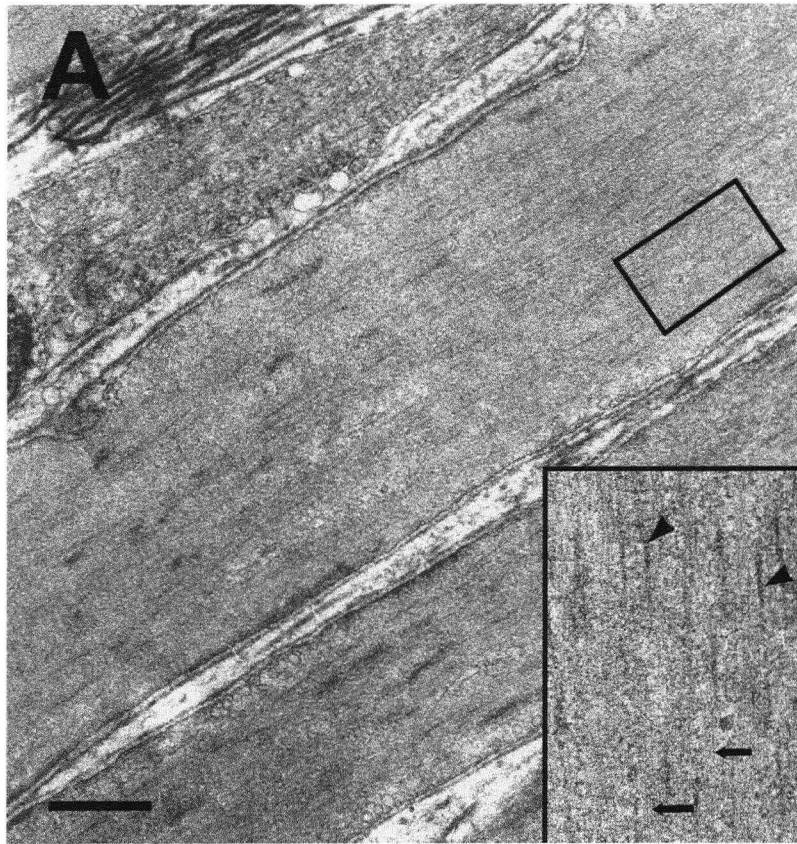
#### **6.4 Thin filament density changes in response to muscle activation, length adaptation and mechanical strain**

Figure 17 shows longitudinal sections of trachealis cells fixed in the relaxed (A and C) and contracted states (B and D). In the activated state the filaments were aligned with the longitudinal axes of the cells that in turn were aligned with the axis of force transmission at the time the tissue was fixed. In the relaxed state, although most filaments lay parallel to the common longitudinal axis of the cell bundle, some filaments lay with small angles to the longitudinal axis. Excluding the regions occupied by organelles, there was no evidence for regional aggregation or large degree of uneven distribution of filaments in the activated cells compared to the relaxed cells.

Cross-sectional densities of the thin filaments under various experimental conditions are shown in Fig. 18. Contractile activation resulted in a significant increase in the thin filament density; in cells activated at in situ length, the density increased by  $19.5\% \pm 3.9$  (SEM), whereas in cells activated at 1.5x the in situ length, the density increase was

30.1%±10.1. Length adaptation of the muscle at 1.5x in situ length produced a significant increase (10.6%±1.9 (SEM)) in thin filament density.

In cells fixed in the relaxed state at the in situ length after a period of length oscillation, there was a small but significant increase in the thin filament density (9.1%±1.8); this happened despite a decrease (18.4 %± 2.6(SEM)) in the thick filament density.



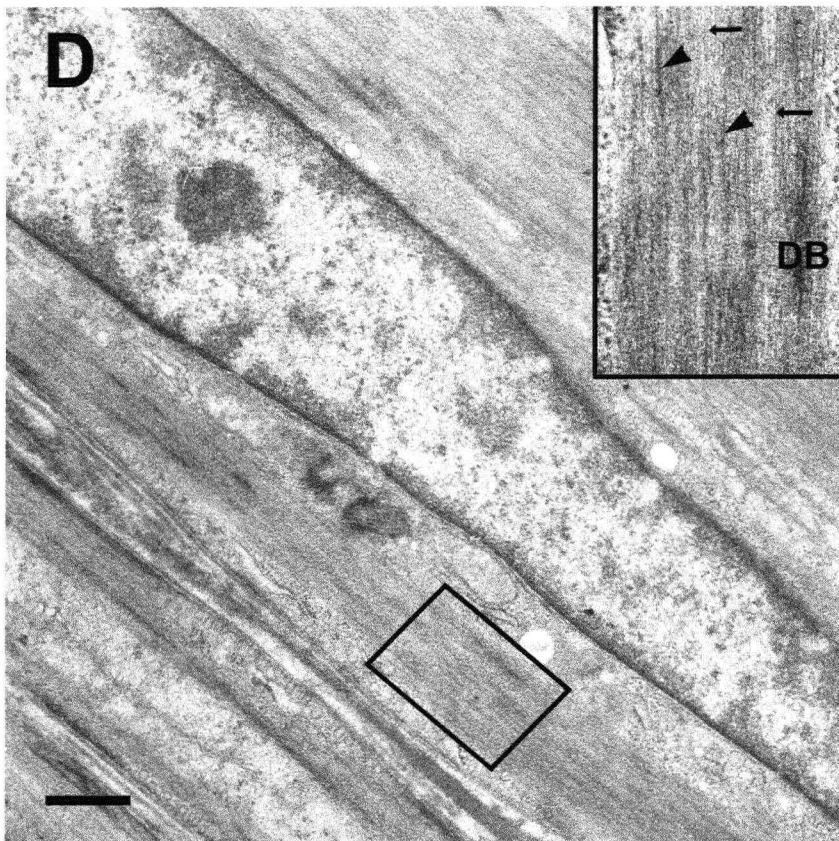
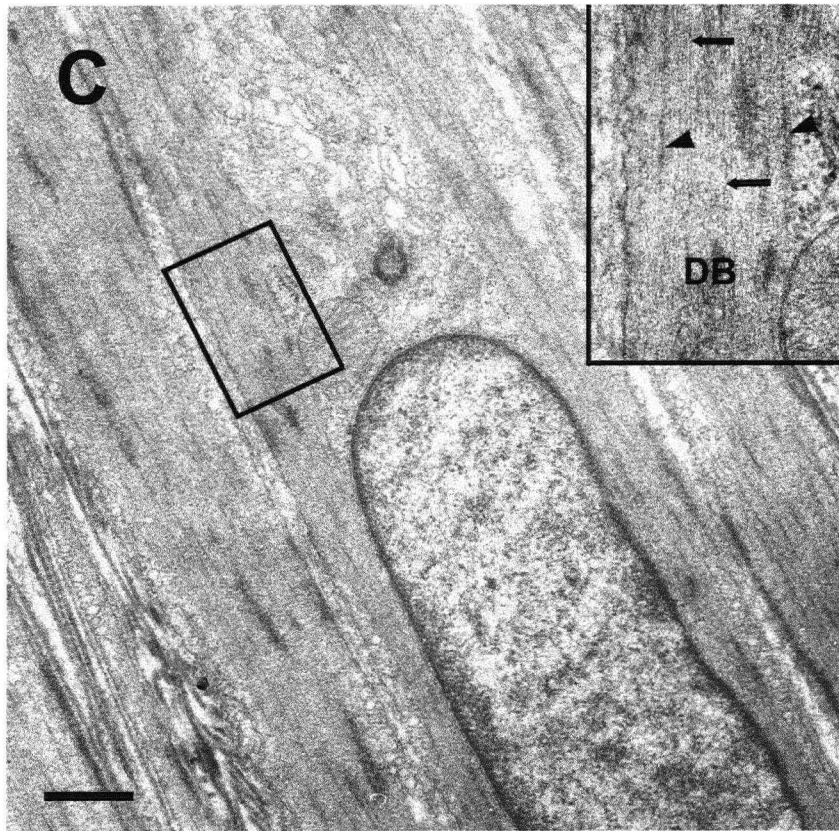


**Figure 17. Electron micrographs showing longitudinal sections of trachealis cells fixed at in situ length in the relaxed (A and C) and contracted (B and D) states. In the magnified insets, arrowheads indicate myosin filaments; arrows indicate actin filaments. DB: dense body. Note that there is no regional aggregation or large degree of uneven distribution of filaments in the activated cells compared to the relaxed cells. Calibration bar represents 1  $\mu\text{m}$ .**

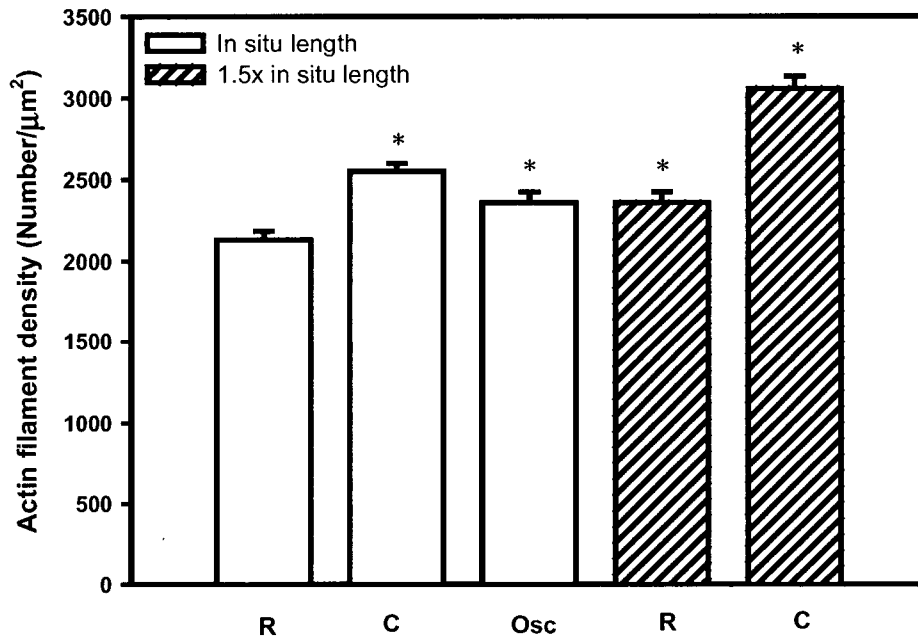


**Figure 18. Thin filament density associated with different muscle states.** The densities were assessed in randomly selected cytoplasmic areas. The bars indicate the 5 conditions under which the muscle preparations were fixed. R: relaxed (control), C: contracted, Osc: post-oscillation. For each condition, 5 cells from each of the 3 animals were used in the morphometric analysis. Means  $\pm$  SEM are plotted. Asterisks indicate statistically significant ( $p < 0.05$ ) difference from control. See text for results of further statistical analysis.

## 6.5 Thin filament regional distribution in the strained and activated muscles

To quantitatively describe regional distribution of thin filaments in cell cross sections, we examined the density of thin filaments near dense bodies (DB), near the peripheral regions, and near the central region of the cell cross sections. These density values were then compared to each other and to the average density measured from randomly selected areas from the respective preparations. Fig. 19 shows an example of an area that contained a dense body (that occupied ~15% of the area within the circle) selected for examination for thin filament density around the dense bodies. The central and peripheral thin filament densities were assessed in the same way as described for thick filament density assessments (described above).

The filament density was examined under 4 conditions: relaxed vs. contracted at 1.0x and 1.5x the in situ length. For the comparisons of densities near the DB's, six micrographs from each group were used and in each micrograph thin filaments in 3 circles were counted. The percentages of areas occupied by the dense bodies within the circles for the relaxed and contracted groups are  $16.1 \pm 0.1$  and  $14.8 \pm 0.1$ , respectively. They are not statistically different ( $p= 0.3$ ). For the comparisons of central and peripheral thin filament densities, six micrographs from each group were used and in each micrograph thin filaments within one circle placed in the central region of the cell cross section and one circle placed in the peripheral region were counted. Fig. 20 summarizes the comparisons.

Thin filaments were more concentrated near the dense bodies; increased by  $11.6\% \pm 2.8$  (SEM) and  $11.5\% \pm 3.9$  in the relaxed and activated cells, respectively. Upon activation, the density near a dense body increased by  $19.2\% \pm 1.9$  (SEM), nearly identical to the increase in density in the randomly selected area during activation ( $19.5 \pm 3.9$ ). Two-way ANOVA revealed that the elevated thin filament densities around dense bodies and after contractile activation are significant ( $p < 0.05$ ), and there is no statistical interaction between DB-area specific and contractile state associated thin filament densities. The distribution of thin filaments in a cell cross section appeared to be even and there was no systematic aggregation of the filaments in the central or peripheral areas after the cells had been activated or stretched (Fig. 20).

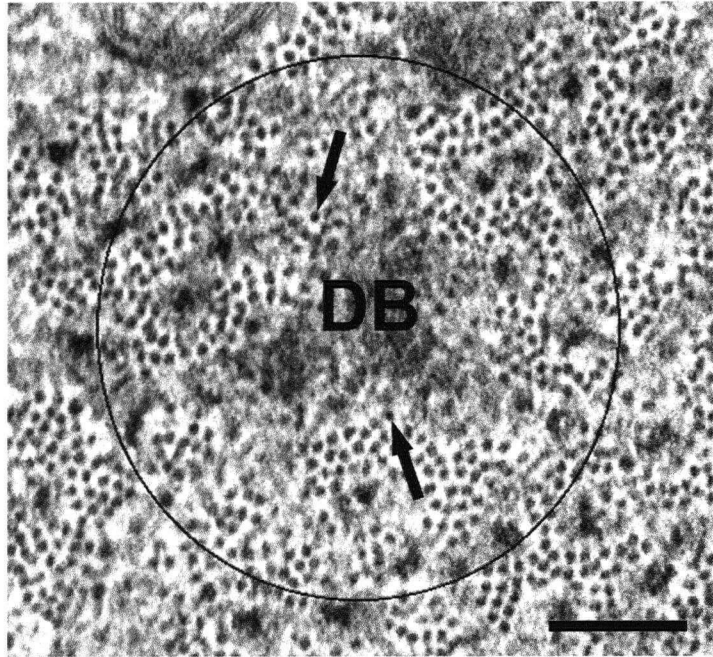


**Figure 19.** An example of a cytoplasmic area surrounding a dense body of a relaxed trachealis muscle. Areas like the one shown here were used for counting the thin filaments (arrows). DB, dense body. Calibration bar indicates 0.1  $\mu\text{m}$ .

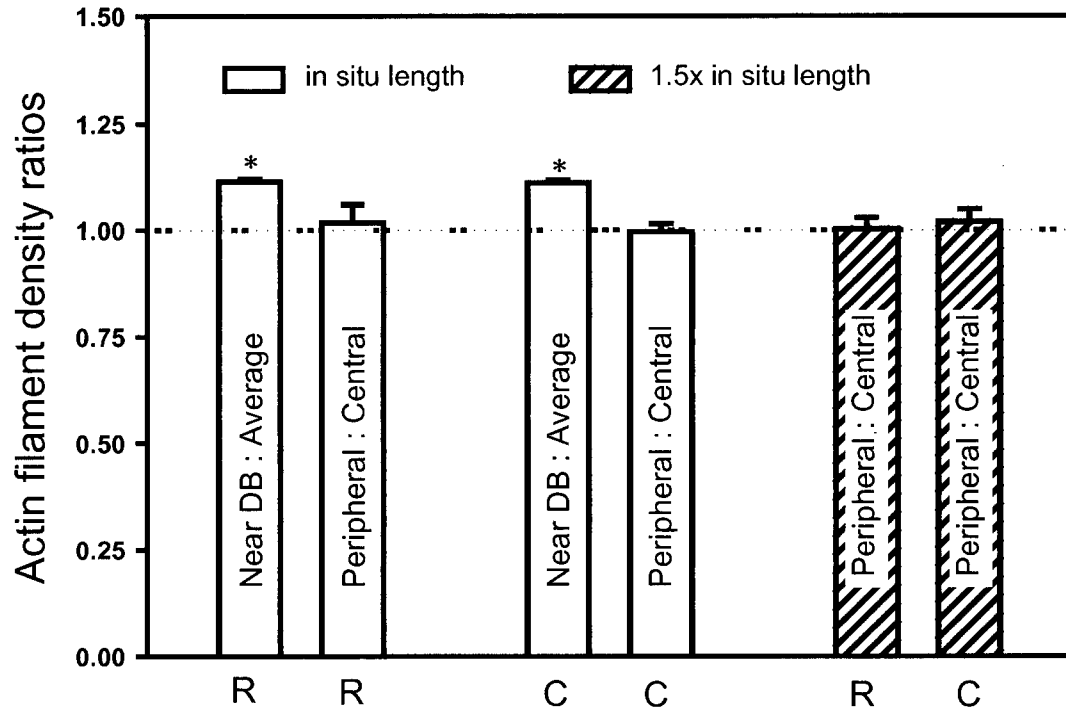


**Figure 20. Ratios of actin filament densities measured in different regions of cell cross-sectional areas.** The thin filament density near dense bodies (DB) is significantly higher ( $p < 0.05$ ) compared to the average density assessed in randomly selected areas (from Fig. 3). The densities in the central and peripheral areas in the cross-sections of trachealis cells fixed in the relaxed (R) and contracted (C) states at different lengths are not statistically different. Means and SEM are plotted.

## 6.6 Thin filament role in ASM plasticity

The dynamics of cytoskeletal structure of smooth muscle has received considerable attention recently and has been recognized as one of the key mechanisms that enable smooth muscle cells to adapt to large changes in length or to migrate (Obara et al, 1994; Mehta et al, 1999; Lesh et al, 2001; An et al, 2002; Cipolla et al, 2002; Filipe et al, 2002; Tang et al, 2002; Shaw et al, 2003). Findings of this study have revealed some previously unknown aspects of actin polymerization in ASM and their possible roles in the muscle's adaptation to external strain and generation of active force.

Before we discuss the results in detail, it is important to point out limitations of our measurements. There was a small change in the angle of alignment of contractile filaments with the cell's longitudinal axis during contractile activation (as the filaments became more parallel to the axis of force transmission, Fig. 17-1 and 17-2); this could affect the filament density count in cell cross sections. However the angles were in general relatively small and it is not likely to change the conclusion of this study (although it may alter quantitatively the density values). The filament density measured in a cell cross section at different cell lengths is directly proportional to the mass of the filaments in the cell, if the cell volume is constant. Since the filament mass is determined by the average length and number of the filaments, the filament density ( $D$ ) is a product of filament length ( $L$ ) and number ( $N$ ), i.e.,  $D = L \times N$ . Unfortunately we cannot differentiate a density change due to a change in filament length from that due to a change in the number of filaments. An increase in filament density can only be

interpreted as a result of three possible changes: 1) an increase in the number of filaments; 2) an increase in filament length (of existing filaments) or 3) a mix of the above two possibilities.

#### **6.6.1 Activation-dependent thin filament density and its regional variation**

Actin polymerization during contractile activation has been examined by many investigators using a variety of methods; pharmacological inhibition of the transition from globular (G) to filamentous (F) actin has been extensively used in the studies of both intact and cultured smooth muscle cells (Adler et al, 1983; Mauss et al, 1989; Obara et al, 1994; Lesh et al, 2001; Filipe et al, 2002; Shaw et al, 2003); immuno-staining of both G and F actins has also been used (Cipolla et al, 2002; Fultz et al, 2000; Hirshman et al, 2001); biochemical quantification is another method used to assess the composition of G and F actins (Mehta et al, 1999; Tang et al, 2003). The above-mentioned studies examined the “global” changes in the contents of G and F actins in muscle cells; the methods used in these studies lacked the resolution to pinpoint where within the cytoplasm the polymerization or depolymerization of actin occurs in response to specific stimuli. The results presented in the present study revealed for the first time the difference in actin filament densities in the subcellular domains. The thin filament density near the cytoplasmic dense bodies was found to be slightly higher than the density in the cytoplasmic areas without dense bodies (Fig. 20). This small but significant increase in density suggests that there was a tendency for thin filaments to

bundle together near dense bodies; this is perhaps related to the appearance of “myofibrils” within individual smooth muscle cells found in longitudinal sections where thin filaments attach to dense bodies in a horse-tail fashion (Bagby, 1983). The densities in the central and peripheral areas of cell cross sections were however not altered by contractile activation or stretching of the cells (Fig. 20).

Although a significant increase in thin filament density was found to accompany contractile activation (Fig. 18), there was no out-of-proportion regional increase (Fig. 20). The present finding is consistent with the interpretation that the actin polymerization is more or less even globally, not localized to any particular subcellular domains in a cell cross section. Polymerization of myosin thick filaments due to contractile activation, on the other hand, is rather inhomogeneous (Chapter 5, Fig. 13B), as also reported by us previously (Herrera et al, 2002; Kuo et al, 2003). The clustered aggregation of thick filaments in activated cells however does not show systematic concentration of thick filaments in the central region of the cell or vice versa (Chapter 5, Fig. 14).

It is still not clear why polymerization of actin is needed in smooth muscle during activation. There appears to be abundant thin filaments packed within the cytosol, even in the relaxed state. It has been postulated that lengthening of thin filaments might be needed for focal adhesion (Gerthoffer et al, 2001). The non-localized thin filament lengthening/formation observed in the present study suggest that the polymerization may have a function of facilitating thin/thick filament interaction and therefore force generation, although it would appear that the relatively sparse thick filaments would be

the limiting factor in this regard and that the additional thin filament formation that accompanies contractile activation would not have a major effect. More studies are needed to clarify this issue.

The present finding of 20-30% increase in thin filament density is greater than that estimated in other studies (Mehta et al, 1999). We have no clear explanation for the discrepancy. There are a number of factors that could contribute to the variation. Smooth muscle preparations are known to have resting tone and the tone varies from preparation to preparation. If the resting tone is high, the measured increase in thin filament polymerization due to contractile activation may be underestimated because of the high starting level of polymerized thin filaments. Another source of variation is the alignment of thin filaments with the longitudinal axis of the cell. The filament alignment in the relaxed state may not be as perfect as that in the activated state; this could lead to overestimation of thin filament density increase (due to contractile activation) because a non-perpendicular thin filament found in a relaxed cell cross section may not be recognized as such.

#### **6.6.2 Length-dependent thin filament density**

The results presented in Fig. 18 indicate that the thin filament density is higher in muscle cells adapted at a longer length. In the relaxed state, a 50% increase in length resulted in  $10.6\% \pm 1.9$  (SE) increase in thin filament density. In the contracted state, the density

increase was even greater ( $20.1 \pm 5.8$ ). It appears that there is synergy between contractile activation and increased strain in augmenting actin polymerization. Statistical analysis (two-way ANOVA) however revealed that, although the significantly increased ( $p < 0.05$ ) thin filament formation can be attributed separately to contractile activation and increased cell length, there is no statistically significant interaction between activation and cell-length in determining the extent of actin polymerization. We have previously shown in the same trachealis preparation that the cell volume is conserved at different cell lengths (Kuo et al, 2003). If the thin filaments (which are short compared to the cell length) are evenly distributed within the cell volume and if there is no polymerization or depolymerization of the filaments, the density of thin filaments at randomly selected cross-sections should be the same at different cell lengths. An increase in density therefore indicates an increase in the G-to-F actin transition. Polymerization of myosin filaments was also favored at longer lengths (Chapter 5, Fig. 14), as we have previously found (Kuo et al, 2003). In our previous study we also found that both muscle power and shortening velocity increased with adapted length while isometric force was not changed (Kuo et al, 2003). A simple explanation of the finding is that there were additional contractile units (thick filaments) added in series to the contractile apparatus of a cell adapted to a longer length. Because in smooth muscle there are many more thin filaments compared to thick filaments (see Chapter 5, Fig. 13), one could argue that there may be enough thin filaments for the additional contractile units needed at longer cell lengths (without additional formation of thin filaments). The present finding indicates that this may not be the case. It appears that despite a large excess of thin filaments (compared to thick filaments), actin polymerization/depolymerization is still required as

part of the process of cell adaptation to different lengths. As discussed above, actin polymerization may be involved in anchoring the cytoskeleton to focal adhesion sites (Gerthoffer et al, 2001), although it is not clear why such polymerization is required.

### **6.6.3 Thin filament lability versus thick filament lability**

Lability of myosin filaments in smooth muscle has been recognized ever since the ultrastructure of the muscle was examined under electron microscope (see a review by Bagby, (Bagby, 1983)). Although it is still controversial as to the extent of lability, it is generally accepted that, compared to those in striated muscle, thick filaments in smooth muscle are structurally less stable. Lability of actin filaments is less well documented. It has been recognized only recently that polymerization/depolymerization associated with the contraction/relaxation cycle in smooth muscle may facilitate plastic adaptation of the muscle to externally applied stress and strain (Gunst et al, 1995; Mehta et al, 1999). In Chapter 5 the described results indicate that there was 63-82% increase in thick filament density due to contractile activation, depending on the adapted length of the muscle cells (Fig. 14). The increase in thin filament density was about 20-30% under the same conditions (Fig. 18). It appears therefore that the formation of thick filaments is facilitated by contractile activation to a greater extent.

Another difference between thin and thick filaments in terms of their structural stability is shown in the filaments' responses to oscillatory strain. By applying periodic (0.5 Hz)

30% stretches to a relaxed trachealis preparation for 5 minutes, the thick filament density was found to decrease by  $18.4 \pm 2.6$  (SE) whereas the thin filament density was found to increase by  $9.1 \pm 1.8$  (Fig. 18). Mechanical agitation that caused thick filaments to fall apart apparently had an opposite effect on the thin filaments. In cultured airway smooth muscle cells subjected to long-term oscillatory strain, it has been reported that there was a large increase in the amount of F-actin and that the increase was associated with RhoA activation (Smith et al, 2003). It is not known whether the increase in thin filament density observed in the present study is related to RhoA activation. It is clear though that short-term oscillatory strain did not cause depolymerization of thin filaments, as it did with thick filaments.

## **CHAPTER 7. Contractile apparatus organization in the ASM cell**

*Experiments and data acquisition for this project were carried out in collaboration with laboratory coworkers: Dr. Brent McParland, Agnes Bienkowska and Ross Tait.*

### **7.1 Are there sarcomeres in smooth muscle?**

The ability of smooth muscle cells to shorten is the most important attribute that allows the muscle tissue to carry out its physiological function and any abnormal enhancement or diminution in the shortening ability regularly leads to dysfunction of the organ that contains the smooth muscle. The sliding-filament, cross-bridge mechanism of contraction described for skeletal muscle (Huxley, 1957) is believed to be also responsible for smooth muscle contraction (Guilford et al, 1998). The sarcomeres of striated muscle have been well characterized in terms of their structure and function (Gordon et al, 1966), the equivalent basic contractile units in smooth muscle, however, are still poorly understood. Structural evidence suggests that the myosin thick filaments in smooth muscle are side-polar (Small, 1977; Cooke et al, 1987), with 14-15 nm periodicity along the entire filament length and no central (cross-bridge) bare zone (Fig. 5), in contrast to the bi-polar thick filaments found in striated muscle that possess a central bare zone. If indeed the thick filaments in smooth muscle are side-polar, the structure of the muscle's contractile unit will necessarily be different from the sarcomeric structure adopted by striated muscle. The structural difference will in turn confer unique functional characteristics on smooth muscle.

## 7.2 Objectives and experimental protocol

To understand the basic mechanism of contraction in smooth muscle we need to know the structural components that make up a contractile unit and how it works. In the present study, the relationship between isotonic load and the amount of shortening in ASM was examined; the experiments were designed to detect any load-independent shortening in a length range where filament overlap was maximal or near maximal. Absence of such a load-independent shortening will constitute strong evidence against the existence of bipolar thick filaments (with a central bare zone) in smooth muscle. Because of the adaptive nature of ASM (Pratusevich et al, 1995), we also examined the relationship of load versus isotonic shortening in the same muscle cells adapted to different lengths. The large change in the relationship associated with length adaptation found in this study suggests that the structure of the contractile apparatus was altered as a result of accommodating the muscle cells at different lengths. We also examined the muscle's structure and shortening ability immediately after a quick step-increase in length and compared the acute changes associated with the length increase to the changes after the muscle had been fully adapted to the stretched length. The comparison revealed a dynamic contractile apparatus of airway smooth muscle that is in many aspects fundamentally different from the sarcomere structure of striated muscle.

### **7.2.1 Determination of the relationship between isotonic loads and the respective amounts of shortening in muscle cells shortening from different initial resting lengths**

This group of experiments was carried out to examine the ability of tracheal smooth muscle to generate force (or carry load) after a certain amount of shortening, and to determine the minimum length to which the muscle could shorten. It was assumed that the amount of overlap between the thick and thin filaments was a major determining factor for force generation by the muscle and that a cross-bridge bare zone in the thick filaments would allow the muscle to shorten over a length interval equivalent to the width of the bare zone without diminishing the maximal force (load-independent shortening).

Before a trachealis preparation was ready for the experiment, it was equilibrated for about 1 hour at one of the two lengths: 1) 1.5 times the in situ length ( $L_{in\ situ}$ ), and 2) 0.75  $L_{in\ situ}$ . During the equilibration period, the muscle was electrically stimulated periodically to produce 12-s tetani at 5-min intervals. The preparation was considered equilibrated when it developed a stable maximal isometric tetanic force with negligible resting tension. Six muscle preparations from six pigs were used for this group of experiments. Three of the muscle preparations were equilibrated at 0.75  $L_{in\ situ}$ ; the other three at 1.5  $L_{in\ situ}$ . Five isotonic loads were used to generate a curve that described the relationship between the isotonic loads and the corresponding maximal shortenings; the loads were 90%, 70%, 50%, 30% and 10% of the maximal isometric force ( $F_{max}$ ). At lighter loads (<50%  $F_{max}$ ) maximal shortening was reached in less than 12 seconds of

stimulation; at heavier loads, longer stimulation time (up to 27 seconds) was needed to obtain maximal shortening. For the muscle preparations equilibrated at  $1.5 L_{in situ}$ , the load-shortening relationship was first obtained with the muscle shortening (against the 5 isotonic loads, randomly applied,) from the initial length of  $1.5 L_{in situ}$ . The same preparations were then equilibrated at  $0.75 L_{in situ}$  until their isometric force reached a stable, maximal level; this process took about 30-40 minutes (6-8 isometric contractions). The load-shortening relationship was then obtained with the muscle shortening from  $0.75 L_{in situ}$  against 5 isotonic loads (10-90%  $F_{max}$  as before; the  $F_{max}$  however was that obtained at  $0.75 L_{in situ}$ ). In between isotonic contractions, at least one isometric contraction was elicited to determine the level of isometric force. Shortening at low isotonic loads often resulted in a reduction in the isometric force in the subsequent isometric contraction. Several isometric tetani (in 5-min intervals) were often required to bring the isometric force back to the initial level (a process called adaptation) before the isotonic contraction was elicited. For the muscle preparations equilibrated at  $0.75 L_{in situ}$ , the load-shortening relationships were obtained in the reversed order as that described for the preparations equilibrated at  $1.5 L_{in situ}$ ; i.e., a load-shortening relationship was obtained first at  $0.75 L_{in situ}$ , followed by adapting the same muscle preparation at  $1.5 L_{in situ}$  and then obtaining the load-shortening relationship from that length. (Results from the two groups were not statistically different and were combined in the final analysis).

It is important to point out the difference between *equilibration* and *adaptation*. A muscle preparation was always "equilibrated" before an experiment to allow the muscle cells to recover from mechanical and metabolic perturbations caused by dissection, low temperature, and lack of perfusion. The equilibration period for the trachealis

preparations was about an hour. Adaptation, on the other hand, referred to a time-dependent process where a muscle preparation recovers from a change in length. In our previous studies, the muscle properties measured before a length change and after sufficient time was allowed for the muscle to “adapt” to the length change include isometric force, shortening velocity, muscle power output, rate of ATP utilization, and myosin filament mass (Kuo et al, 2003; Herrera et al, 2004). The changes were interpreted by a model where plastic rearrangement of the contractile filaments occurred as a result of length adaptation (Lambert et al, 2004). Adaptation or re-adaptation of a muscle preparation to different lengths was performed only after the muscle preparation had been equilibrated. The protocol for adaptation of trachealis preparations was as follows. After a change in length, the muscle preparation was stimulated electrically to produce a brief tetanus (12 s) and this was repeated once every 5 minutes until the maximal isometric force reached a steady value (normally it returned to the value before the length change). Adaptation typically required 30-40 minutes.

The maximal rate of shortening was measured from each isotonic shortening trace to gain insights into the force-velocity relationship and mechanisms underlying the changes in the relationship at different muscle lengths in adapted and non-adapted states. The maximal velocity of shortening during an isotonic contraction occurred between 200-400 ms after the onset of isotonic shortening; the shortening velocities were therefore measured in that time interval and plotted against the corresponding isotonic loads. The force-velocity data were fitted with the Hill’s hyperbolic force-velocity equation (Hill, 1938) of the form:  $V = b (F_{\max} - F)/(F + a)$ , where  $V$  is the shortening velocity,  $F_{\max}$  is

the maximal isometric force,  $F$  is the isotonic load, and  $a$  and  $b$  are the Hill's constants. The non-linear curve fits were performed using the SigmaPlot® (Version 8.02) program.

### **7.2.2 Determination of the load-shortening relationship at $L_{in situ}$ and after a 10% quick stretch**

This group of experiments was carried out to examine the effects of a small acute length change ( $0.1 L_{in situ}$  in amplitude) on the ability of the muscle to shorten in the absence of extensive adaptation of the muscle to the length change. The rationale was that a small stretch might not trigger the adaptation response in the muscle; we had previously seen such a response elicited in smooth muscle subjected to a large change in length (Pratusевич et al, 1995; Seow, 2000; Wang et al, 2000; 2001; Kuo et al, 2001; 2003). The isotonic contraction immediately following a quick stretch was intended to minimize the time for any possible muscle adaptation to occur. If smooth muscle behaved like striated muscle, the maximally shortened length of the muscle during an isotonic shortening should be the same with or without a quick stretch applied before the onset of shortening (Edman, 1980).

For this group of experiments, muscle preparations ( $n=6$ ) were adapted at  $L_{in situ}$ . Isotonic contractions against the various isotonic loads (ranging from 10-90%  $F_{max}$ , as described above) were elicited at an initial length of  $1.0 L_{in situ}$  to obtain a reference load-shortening curve. A "test" curve was obtained in the same way except that just before the isotonic

contraction, the muscle preparation was rapidly stretched (within 100ms) by 10% of  $L_{in\ situ}$ . The relationships between isotonic load and maximal shortening with or without the pre-contraction quick-stretches were then compared. The shortening velocities were measured during the time interval of 200-400 ms after the onset of isotonic shortening for the  $L_{in\ situ}$  group (reference). For the stretched group, because there was a transient increase in passive tension immediately after the quick stretch, shortening velocities in this group were measured at a later time interval to allow the increase in passive tension to disappear as the muscle shortened. The length at which the velocities were measured in the pre-stretched group was the same as the length in the reference group (without stretch) when the velocities were measured. That is, in the stretched group, shortening velocities were measured at the time the muscle had shortened by an additional 10% of  $L_{in\ situ}$ , compared to the un-stretched reference group.

### **7.2.3 Measurement of isotonic shortening and ultrastructural change after a 30% quick stretch**

This group of experiments was carried out to examine both structural and functional changes associated with a step increase in length. The experimental protocol is schematically illustrated in Fig. 21. Five trachealis preparations from 5 animals were used for this group of experiments. The muscle preparations were first adapted at  $L_{in\ situ}$ .  $F_{max}$  and passive force associated with  $L_{in\ situ}$  were measured. This was then followed by an isotonic shortening ( $\Delta L_1$ ) against a 30%- $F_{max}$  load. After the isometric force had

recovered from the isotonic shortening (this usually took 1-5 isometric contractions at 5-min intervals, not shown in Fig. 21), a quick stretch with amplitude of  $0.3 \cdot L_{in\ situ}$  was applied to the muscle. This was followed immediately by an isometric contraction; the maximal isometric force ( $F'_{max}$ ) and passive force of the isometric contraction (at  $1.3 \cdot L_{in\ situ}$ ) were then measured. The muscle was then return to the original length ( $L_{in\ situ}$ ), and was adapted again at that length. Based on the measured isometric force at  $1.3 \cdot L_{in\ situ}$ ,  $30\% \cdot F'_{max}$  was applied to the muscle during an isotonic shortening ( $\Delta L_2$ ) elicited immediately after a 30% quick stretch from  $L_{in\ situ}$ . The muscle was then allowed to adapt at  $1.3 \cdot L_{in\ situ}$  and regain the isometric force; this normally took 3-5 isometric contractions (not shown in Fig. 21). After the muscle had been fully adapted at  $1.3 \cdot L_{in\ situ}$ , the maximal isometric force ( $F''_{max}$ ) was measured; a final isotonic shortening at  $30\% \cdot F''_{max}$  ( $\Delta L_3$ ) was then elicited.

For structural examination, the muscle preparations were fixed for electron microscopy (EM) under 3 conditions: 1) Fully adapted at  $L_{in\ situ}$  (reference), as indicated by the arrow labelled "A" in Fig. 21; 2) immediately after a  $0.3 \cdot L_{in\ situ}$  quick stretch from  $L_{in\ situ}$ , as indicated by the arrow labelled "B" in Fig. 21; and 3) fully adapted at  $1.3 \cdot L_{in\ situ}$ , as indicated by the arrow labelled "C" in Fig. 21. The reason for using a larger step-size of stretch ( $30\% \cdot L_{in\ situ}$ ) was that the structural change associated with a small length change might be too small to be accurately quantified by the EM morphometrics. The disadvantage of using a large stretch was that the physical disruption associated with the length change could cause disintegration of thick filaments, as suggested by previous

observation (Kuo et al, 2001), and this would make interpretation of the results more difficult.

For the morphometric analysis sampling and analysis were carried out “blind”. The codes indicating experimental conditions were revealed only after the analysis of each group was finished. Six electron micrographs of muscle cell cross sections per condition per trachea were analyzed. The thick and thin filament densities were estimated by using the same method as described previously in Chapter 4, 5 and 6.

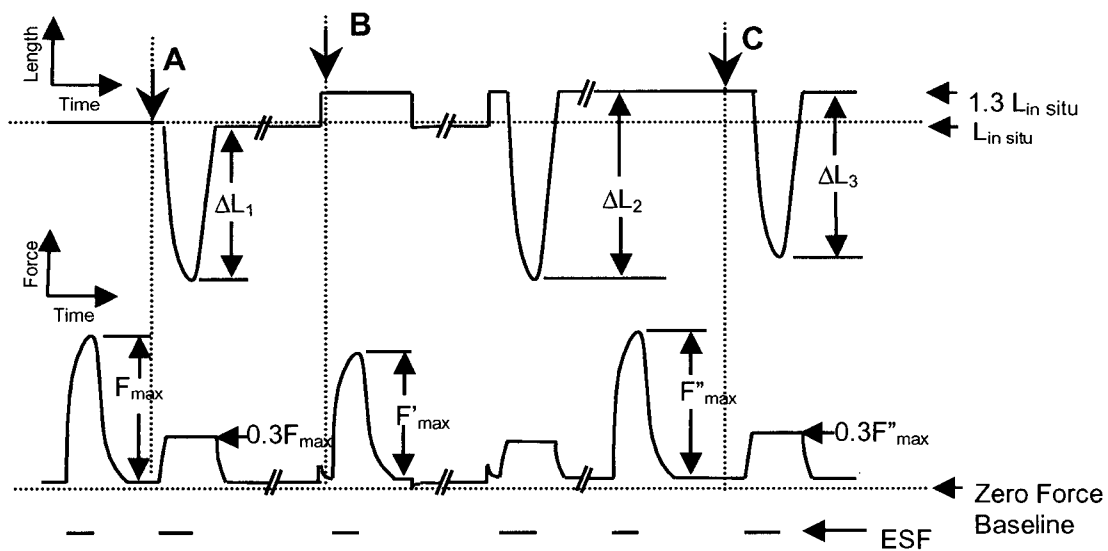


**Figure 21. Schematic illustration of the experiment protocol for the length step change experiment.** Upper solid trace: length vs. time; lower solid trace: force vs. time. EFS: electric field stimulation.  $\Delta L$  represents isotonic shortening. Large arrows labelled A, B, and C indicate the time and condition at which the muscle preparations were fixed for electron microscopic examination of ultra-structure; they were all fixed in the relaxed state. The breaks in the trace indicate time durations excluded in the plot where the muscle preparations were allowed to fully recover (or adapt) after a passive length change or active shortening. The adaptation protocol consists of brief isometric tetani (12-s duration) elicited once every 5 minutes for up to 40 minutes.

### 7.3 Isotonic shortening from different adapted lengths

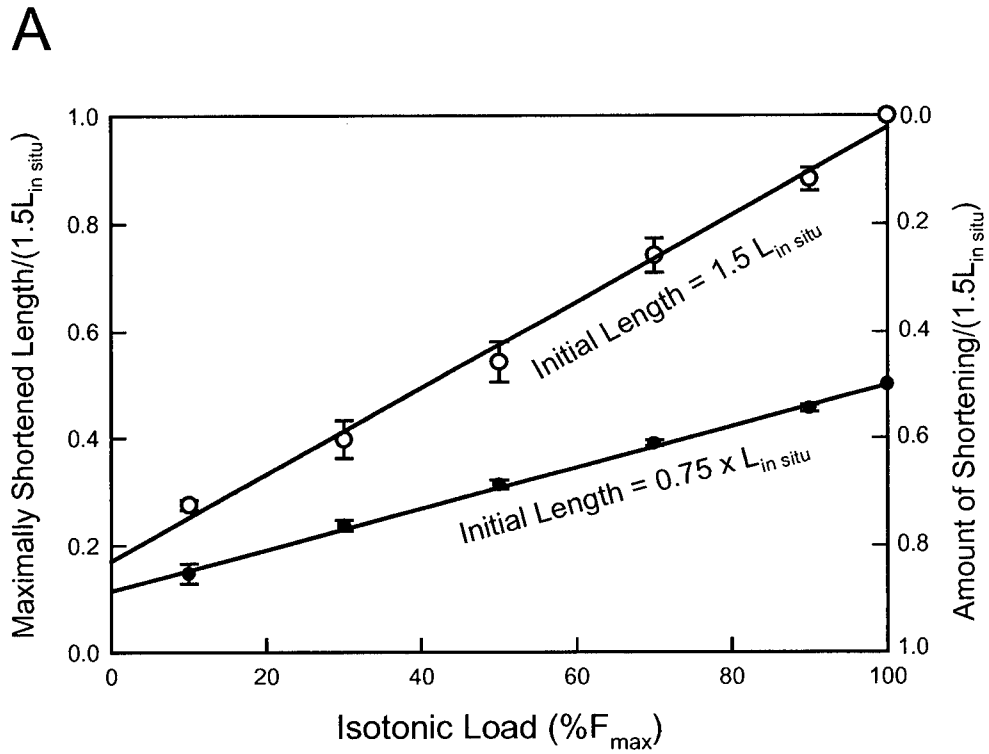
Fig. 22-A depicts the relationship between the amount of isotonic shortening (or maximally shortened length, which equals the initial muscle length minus the amount of isotonic shortening) and isotonic load in muscle preparations adapted to different lengths. Each preparation was adapted and studied at 2 lengths, 0.75 and 1.5  $L_{in situ}$ . The results were averaged from six pairs of measurements in six muscle preparations from six tracheas. A linear relationship was obtained at both muscle lengths; there was no load-independent shortening within the length range examined. The extrapolated zero-load “y-intercepts” of the fitted lines, normalized by 1.5  $L_{in situ}$ , are  $0.116 \pm 0.006$  and  $0.168 \pm 0.021$  respectively for the 0.75 and 1.5  $L_{in situ}$  lines (Fig. 22-A). They are statistically different ( $p < 0.05$ ). The slopes are  $0.0038 \pm 0.0001$  and  $0.0081 \pm 0.0003$  (in units of  $1.5L_{in situ} / \% \text{ isotonic load}$ ) respectively for the 0.75 and 1.5  $L_{in situ}$  lines. They too are different ( $p < 0.05$ ).

Fig. 22-B depicts the relationship between shortening velocity and isotonic load. A non-linear curve fit with the Hill's Hyperbola was performed for the data collected at an initial muscle length of 1.5  $L_{in situ}$  (open circles). The fitted curve was then scaled down vertically (i.e., velocity scaling) by a factor of 0.61 to fit the data collected at an initial length of 0.75  $L_{in situ}$ . The increase in shortening velocity from doubling the adapted muscle length (from 0.75 to 1.5  $L_{in situ}$ ) therefore is  $1/0.61$ , or 1.64 fold. There was no resting tension at 0.75  $L_{in situ}$ . The average resting tension at 1.5  $L_{in situ}$  (fully adapted) was  $0.0168 \pm 0.0044 F_{max}$ . Force-velocity data obtained at this length were not corrected

for this low level of resting tension, which likely would disappear upon shortening of the muscle.

### **7.3.1 Relationship between maximally shortened length under zero external load and initial (adapted) muscle length**

From the data presented above, it is clear that muscle preparations adapted at a shorter cell length will have a shorter maximally shortened length. The relationship between maximally shortened length at zero external load and the initial, adapted muscle length is explicitly plotted in Fig. 23. The relationship can be described by a linear equation of the form: Maximally shortened length = 0.103 + 0.101 x (Initial length), with all lengths normalized by  $L_{in\ situ}$ .



**Figure 22-A. Isotonic shortening from different adapted lengths.** Maximally shortened length or maximal amount of shortening (as a fraction of 1.5x  $L_{in situ}$ ) of tracheal smooth muscle adapted at 1.5 and 0.75  $L_{in situ}$ , plotted as functions of isotonic load. The isotonic loads were expressed as percentages of the maximal isometric forces ( $F_{max}$ ) generated at the adapted lengths of 1.5 and 0.75  $L_{in situ}$ .

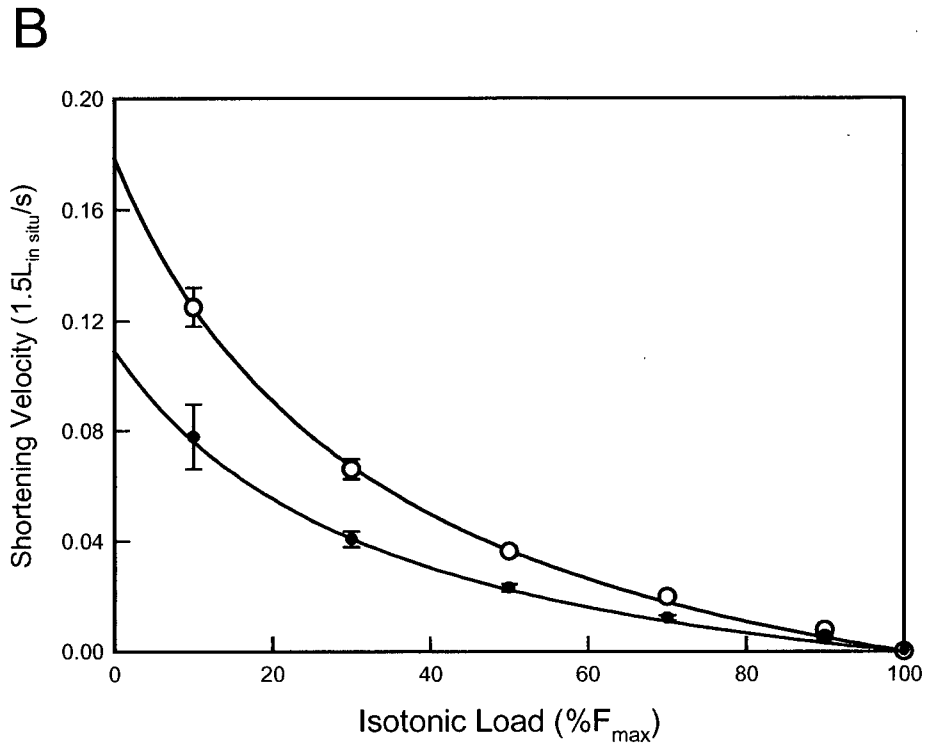


**Figure 22-B. Isotonic shortening from different adapted lengths.** Shortening velocity of tracheal smooth muscle adapted at 1.5 (open circles) and 0.75 (filled circles)  $L_{in situ}$ , plotted as functions of isotonic load. The velocities were measured from the corresponding isotonic contractions described for panel A. The line through the open circles represents a rectangular hyperbola (the Hill Equation) that best fit the data. The line through the filled circles is obtained by scaling the line through the open circles vertically by a factor of 0.61. Six muscle preparations were used; each preparation was adapted in alternating order at initial lengths of 1.5 and 0.75  $L_{in situ}$  before the isotonic contractions were elicited. The isometric forces ( $F_{max}$ ) at 1.5 and 0.75  $L_{in situ}$  were  $158.4 \pm 26.4$  (kPa) and  $147.6 \pm 21.6$  (kPa) respectively, not significantly different from each other. Means and standard errors of means are plotted.

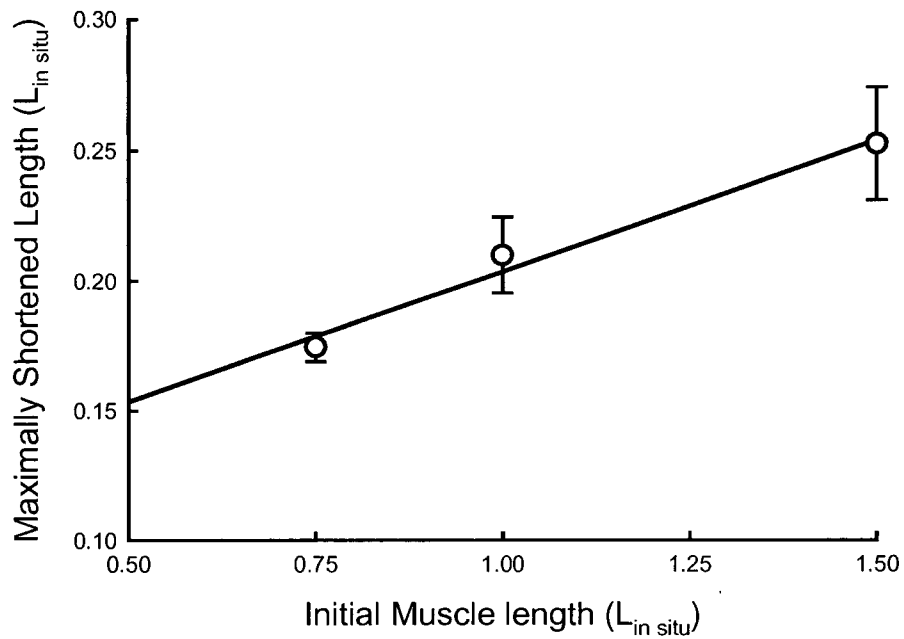
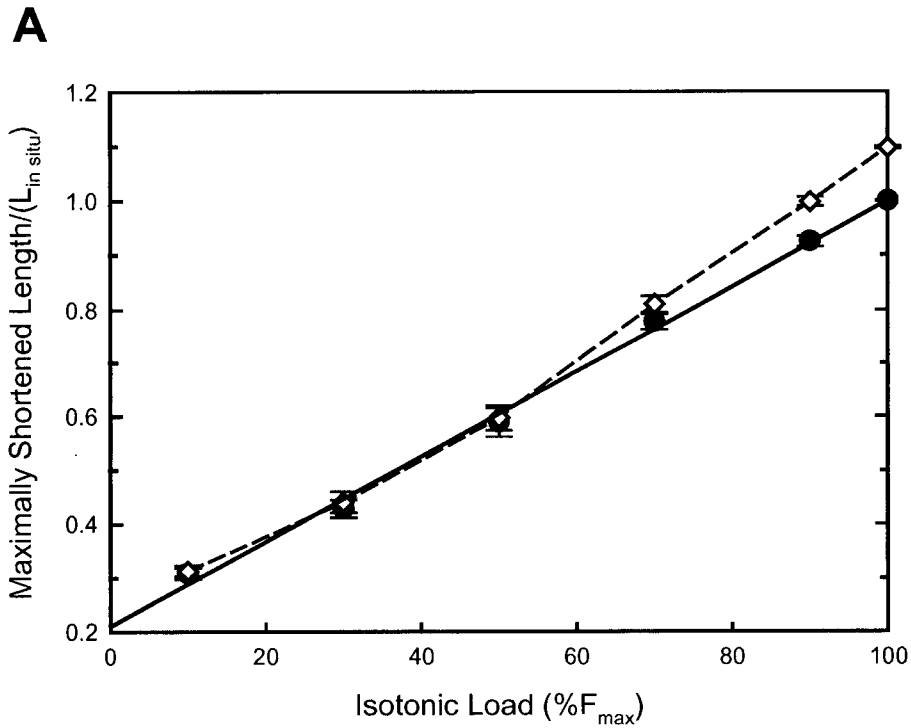


**Figure 23. Maximally shortened length at zero external loads as a function of the initial (adapted) muscle length.** The plotted data were extracted from the data presented in Fig. 22 and 24. The best-fit line has a “y-intersect” of  $0.103 (L_{in\ situ}) \pm 0.016$  (SE) when extrapolated to zero initial length, and a slope of  $0.101 \pm 0.014$ .

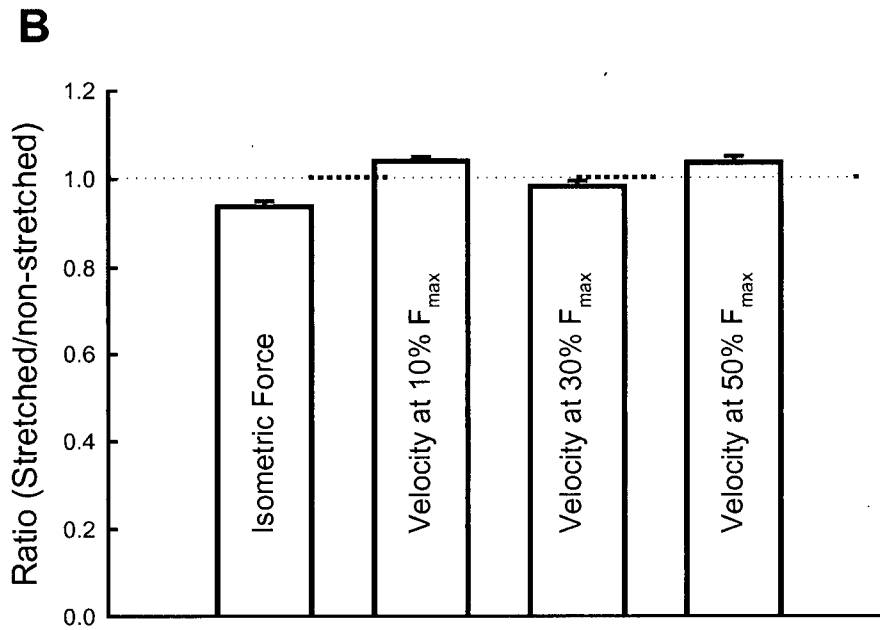
#### 7.4 Isotonic shortening after a 10% ( $0.1 \cdot L_{in\ situ}$ ) quick stretch

Fig. 24-A depicts the relationship between the maximally shortened length and the isotonic load in muscle preparations shortening from the adapted length ( $L_{in\ situ}$ ) and after a  $0.1 \cdot L_{in\ situ}$  quick stretch. The quick stretch was applied just before the muscle was activated. The data from the non-stretched controls (filled circles) were fitted with a straight line (solid) with a slope of  $0.0079 \pm 0.0002$  ( $L_{in\ situ} / \% \text{ isotonic load}$ ) and a zero-load “y-intercept” of  $0.210 \pm 0.0147$  ( $L_{in\ situ}$ ). The data obtained after the quick stretch (diamonds) were connected with straight (dash) lines. Data points at isotonic loads of 10%, 30% and 50%  $F_{max}$  from the stretched and non-stretched sets were not different statistically (Fig. 24-A). On the other hand, at isotonic loads greater than 50%  $F_{max}$ , the lengths at the maximally shortened state are different (ANOVA,  $p < 0.05$ ).

Shortening velocities at the three lower isotonic loads ( $< 50\% F_{max}$ ) were compared between the stretched and non-stretched groups; the velocity ratios (stretched/non-stretched) were  $1.040 \pm 0.009$ ,  $0.982 \pm 0.013$ , and  $1.037 \pm 0.014$  for the 10%, 30%, and 50%  $F_{max}$  isotonic loads respectively (Fig. 24-B). One-way ANOVA indicated that the ratios were not different from unity. There was a slight but significant decrease ( $6.3 \pm 1.3\%$ ) in maximal isometric force immediately after the  $0.1 \cdot L_{in\ situ}$  stretch (Fig. 24B).



**Figure 24-A. Isotonic shortening after a 10% ( $0.1 \cdot L_{in\ situ}$ ) quick stretch.** Maximally shortened length (as a fraction of  $L_{in\ situ}$ ) of tracheal smooth muscle adapted at  $L_{in\ situ}$  (filled circles) and after a quick stretch by 10%  $L_{in\ situ}$  (open diamonds), plotted as functions of isotonic load. The solid line is the linear regression through the filled circles; the dash lines are straight lines connecting the adjacent diamonds.



**Figure 24-B. Isotonic shortening after a 10% ( $0.1-L_{in situ}$ ) quick stretch.** Ratios of force and velocity values obtained from pre- and post-stretched muscle preparations. The force ratio is significantly different from unity ( $p < 0.05$ ); analysis for the three velocity ratios indicates no difference from unity. Means and SE of means are plotted ( $n=6$ ).

## 7.5 Isometric force generation and isotonic shortening after muscle lengthening

The isometric force and the amount of isotonic shortening under the experimental conditions depicted in Fig. 21 are shown in Fig. 25. Isometric force elicited immediately after the quick stretch ( $F'_{\max}$ ) was  $13.3 \pm 4.6\%$  ( $p < 0.05$ ) lower than the control ( $F_{\max}$ ). The force decrease was fully recovered after the period of adaptation ( $F''_{\max}$ ). The loads for the isotonic shortenings  $\Delta L_1$ ,  $\Delta L_2$ , and  $\Delta L_3$  were 30% of  $F_{\max}$ ,  $F'_{\max}$  and  $F''_{\max}$  respectively. Note that  $\Delta L_2$  and  $\Delta L_3$  were shortenings generated by muscle cells with a starting length of  $1.3L_{\text{in situ}}$ , whereas  $\Delta L_1$  was generated by muscle cells shortening from  $L_{\text{in situ}}$ . All shortenings were normalized by  $L_{\text{in situ}}$ .  $\Delta L_2$  is nearly exactly  $0.3L_{\text{in situ}}$  greater than  $\Delta L_1$  ( $\Delta L_2 - \Delta L_1 = 0.305 \pm 0.032 L_{\text{in situ}}$ ) indicating that the  $0.3L_{\text{in situ}}$  stretch applied just before the isotonic contraction was “absorbed” into the total shortening and that the stretch had no effect on the final (minimum) length towards which the muscle shortened (and there was no sufficient time for the muscle to adapt to the length change). By allowing the muscle to adapt to the  $0.3L_{\text{in situ}}$  increase in length, the extra shortening ( $\Delta L_3 - \Delta L_1$ ) was reduced to  $0.24 \pm 0.037 L_{\text{in situ}}$ , significantly ( $p < 0.05$ ) different from the value of ( $\Delta L_2 - \Delta L_1$ ).

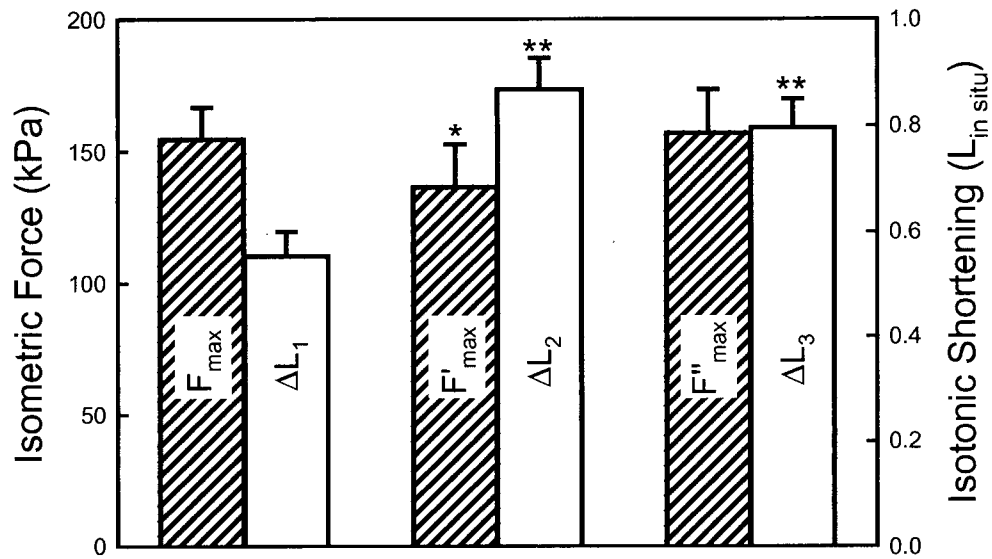


**Figure 25. Isometric force and isotonic shortening measured according to the experiment protocol outline in Fig. 21.**  $F_{max}$ ,  $F'_{max}$ ,  $F''_{max}$ ,  $\Delta L_1$ ,  $\Delta L_2$ , and  $\Delta L_3$  are defined in Fig. 21. Asterisks denote statistically significant difference from the respective references ( $F_{max}$  and  $\Delta L_1$ ). \*,  $p < 0.05$ ; \*\*,  $p < 0.01$ . The average length ( $L_{in\ situ}$ ) of the muscle preparations was  $4.51 \pm 0.25$  mm. See text for more statistical analysis and comparison.

### **7.5.1 Actin/Myosin filament ratio variations after a quick stretch and after adaptation at the stretched length**

The densities of myosin (thick) and actin (thin) filaments in transverse electron microscopic (EM) sections were quantified in micrographs such as those shown in Chapter 4, Fig. 11. The thick filament density, thin filament density and the ratio (thin/thick) of the densities in muscle preparations fixed at time points A, B, and C (indicated in Fig. 21) are plotted in Fig. 26. Immediately after the quick stretch, there was a significant decrease in myosin filament density (by  $27.3 \pm 2.5\%$ ); after adaptation at the stretched length, the density increased significantly by  $17.2 \pm 2.5\%$  (compared to the pre-stretched density). The actin filament density did not change significantly under the 3 conditions, although the increase ( $14.7 \pm 4.8\%$ ) after adaptation at the stretched length was significant at a p value of  $<0.1$ . The thin/thick filament ratio was significantly increased (by  $33.7 \pm 0.7\%$ ) immediately after the stretch; adaptation at the stretched length returned the ratio to the pre-stretch level.

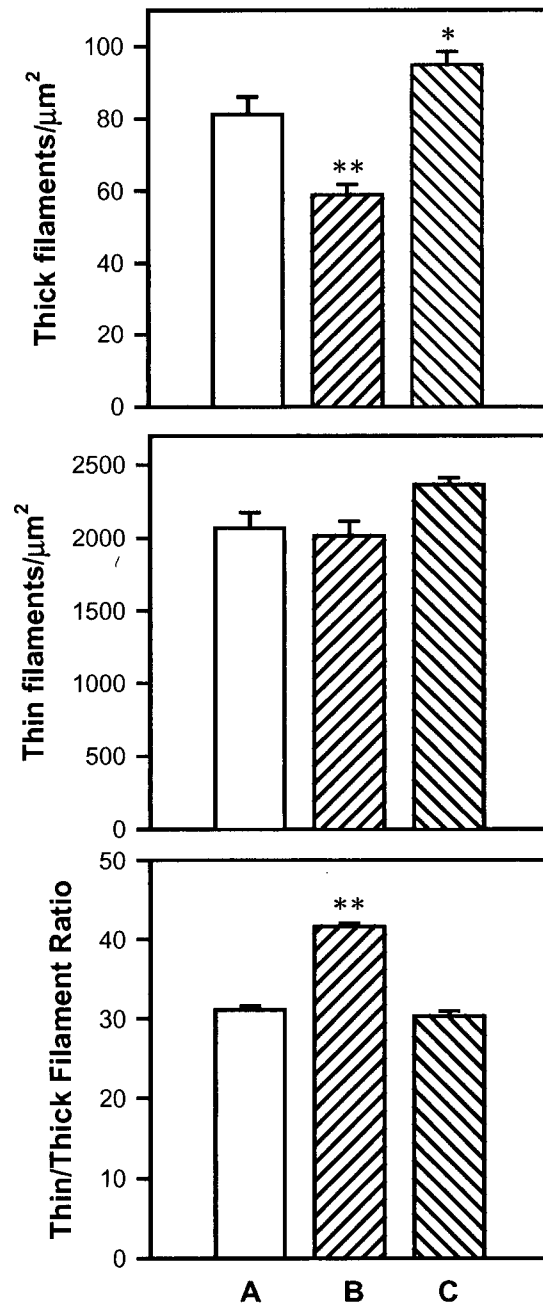


**Figure 26.** Myosin (thick), actin (thin) filament densities, and the density ratio in trachealis fixed at the 3 time points (A, B, and C) indicated in Fig. 21. Asterisks (\*) indicate statistically significant difference from control (A). \*,  $p < 0.05$ ; \*\*,  $p < 0.01$ .

Immediately after the quick stretch, many of the thick filaments adjacent to the dense bodies disappeared from the EM cross sections. Analysis of the distribution of the distance between dense bodies and their respective closest thick filaments (Fig. 27) revealed that the decrease in thick filament density was most pronounced within a 40-50 nm perimeter surrounding the dense body. The analysis indicated a shift in the distribution of the thick filaments about 10 nm away from the dense bodies after the stretch (Fig. 27). This apparent shift is a result of disproportional decrease in thick filament density around the dense bodies, with more thick filaments disappearing in the vicinity immediately adjacent to the dense bodies. After adaptation at the stretched length, the filament distribution profile returned to that observed before the stretch (Fig. 27). The decrease in thick filament density within a 60 nm perimeter of a dense body immediately after the quick stretch was  $29.1 \pm 1.4\%$ , slightly more than the average decrease across the whole cross section ( $27.4 \pm 2.1\%$ , Fig. 26) but not significantly different. As shown in Fig. 27, the frequency of observation of the nearest thick filaments occurring between 30-40 nm (away from the edge of a dense body) under the pre-stretch condition is 135 (out of 635 total observations); immediately after the quick stretch, the frequency decreased from 135 to 81 (adjusted for the total number of observations). This represents a 40% decrease, which is disproportionately greater than the decrease in average thick filament density ( $27.4\% \pm 2.1$ ) across the whole cell cross section, and indicates that many thick filaments might be pulled away from around the dense bodies in a quick stretch.

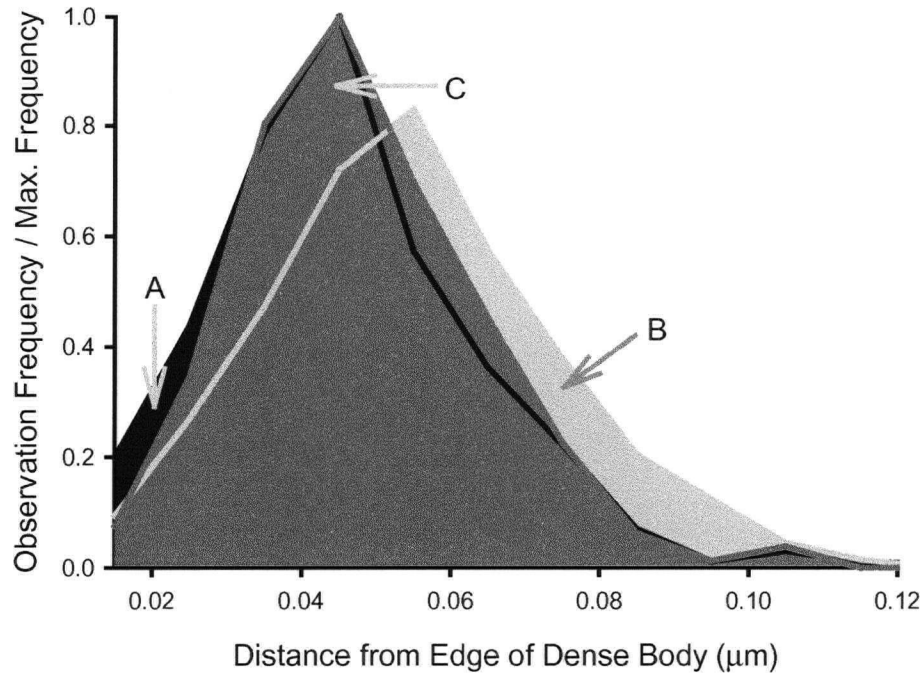


**Figure 27. Frequency polygons depicting the distribution of the distance between a dense body and the closest myosin filament.** The distance was measured from the center of the filament to the closest edge of the dense body. The observations were grouped into 0.01  $\mu\text{m}$  intervals. The black polygon shows the distribution obtained from the control group (pre-stretch, condition **A** indicated in Fig. 21); the light-grey polygon shows the distribution obtained from the post-stretch group (condition **B** in Fig. 21); the dark-grey polygon shows the distribution obtained from the post-stretch and adapted group (condition **C** in Fig. 21). The numbers of dense bodies examined in groups A, B, and C were 635, 511, and 591 respectively. The maximum frequency (occurred in Group A) was 171. The plots were normalized by the maximum frequency observed in Group A and adjusted for the number of observations in each group (so that the areas of the polygons are equal).

## 7.6 A proposed model of contractile unit in smooth muscle

The most essential components that make up sarcomeres in striated muscle are the myosin thick filaments, the actin thin filaments and the Z-disks. The counterparts of these components are present in smooth muscle, albeit in variant forms. The dense bodies in smooth muscle are thought to be equivalent to Z-disks in the sense that they are anchoring bodies for thin filaments. Smooth muscle thick filaments are likely side-polar (Small, 1977; Cooke, Kargacin, Craig, Fogarty, and Fay, 1987), in contrast to the bipolar variety found in striated muscle. A contractile unit in smooth muscle therefore is likely different from a sarcomere in terms of its functional mechanism and how it is assembled. It was structural evidence like those shown in Fig. 28 that had led us to propose the model of contractile unit shown in Fig. 29. The model is different from those proposed previously (Hodgkinson et al, 1995; Schellenberg and Seow, 2003) in that predictions regarding mechanical behaviour can be derived from geometric considerations of the model, as elaborated below.

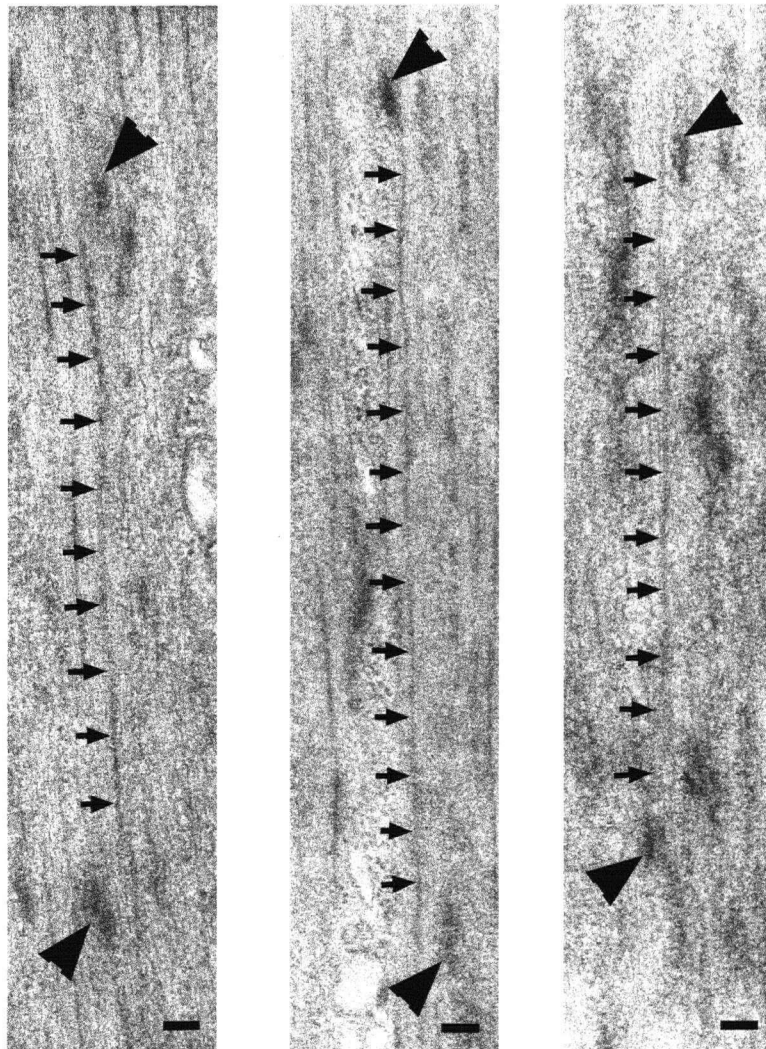
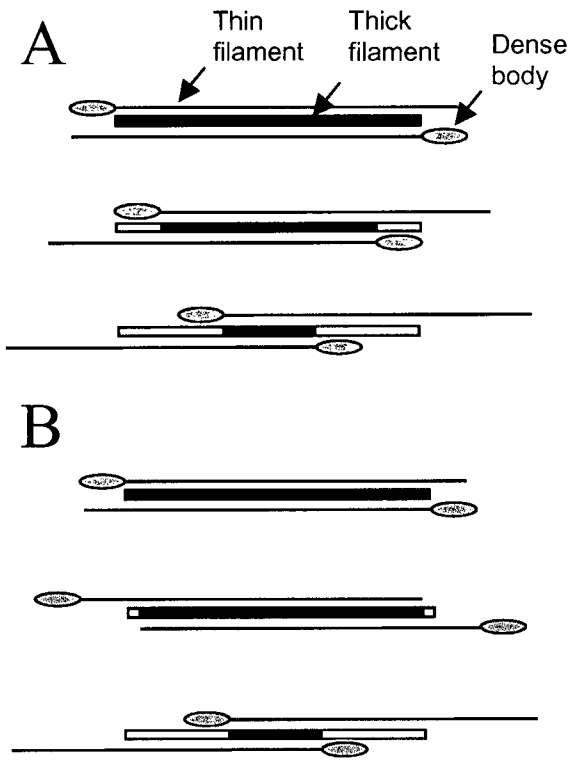


**Figure 28. Examples illustrating the spatial arrangement of myosin filaments and dense bodies that could be interpreted as a standard design of the contractile unit in smooth muscle:** a myosin filament spanning the distance between two dense bodies. The longitudinal EM sections were obtained from porcine tracheal smooth muscle cells fixed at their in situ length and in the relaxed state. The length of the thick filaments and the distance between the dense bodies are between 1.8-2.2  $\mu\text{m}$ . Large arrowheads indicate the relevant dense bodies; small arrowheads follow the myosin thick filaments. Calibration bar: 0.1  $\mu\text{m}$ .



1. Isometric contraction at max. force ( $F_{max}$ ).

2. Shortening against a 70%  $-F_{max}$  load.

3. Shortening against a 30%  $-F_{max}$  load.

1. Isometric contraction at max. force ( $F_{max}$ ).

2. Isometric contraction immediately following a 30%  $-L_{in situ}$  quick stretch.

3. Shortening against a 30%  $-F_{max}$  load after the quick stretch.

**Figure 29. Schematic representation of a contractile unit in smooth muscle under different conditions.** The solid portion of the thick filaments represents the segment between the dense bodies that overlaps completely with both of the thin filaments. It is assumed that only the cross bridges within the solid portion of the thick filaments can interact with the thin filaments properly to generate force. The length of the solid portion of thick filaments in a contractile unit therefore correlates directly to the ability of the muscle to carry load. Each numbered configuration represents an equilibrium (static) condition where external load equals the force produced by the contractile unit. **A.** Isometric contraction and isotonic contractions against different external loads. **B.** Isometric contractions at different lengths and isotonic contraction against an isotonic load.

### **7.6.1 Relationship between load on muscle and the amount of shortening**

At the plateau of an isotonic contraction where the muscle is maximally contracted, the force generated by the muscle equals the sum of all loads on the muscle. The loads on the muscle include the externally applied isotonic load and the internal load that may stem from distortion of extracellular matrix and cytoskeleton due to shortening (Bramley et al; 1995; Meiss, 1999). The mechanical equilibrium at the plateau of contraction (where shortening velocity is zero) offers an opportunity to examine the ability of a muscle to generate force at different lengths. If we assume that the structure of a contractile unit in smooth muscle resembles a sarcomere and if we assume that the in situ length of the trachealis muscle is within the plateau of the curve that characterizes the muscle's length-force relationship, shortening of the muscle within the force plateau will not change the maximal overlap between the thick and thin filaments and therefore there will be a force- or load-independent shortening. The amount of shortening will become dependent on the load when the muscle is operating on the ascending or descending limb of the length-force curve. The present data on the load-shortening relationship of trachealis muscle obviously cannot be explained by a sarcomere-like contractile unit because of the absence of a load-independent shortening (Fig. 24A). Attempts to find the load-independent shortening by setting the muscle to different initial lengths (Fig. 22A) also failed. Our finding indicates that no matter what the starting length was, the ability of the muscle to carry load was diminished as soon as the muscle shortened. Furthermore, the load-shortening relationship was linear regardless of the starting length.

The present data suggest that the myosin filament of smooth muscle being bipolar and with a central bare zone is highly unlikely. This has led us to consider the model presented in Fig. 29A. A variant form of the model is that the thick filament does not span end-to-end between the dense bodies, that is, there are non-overlap (between thick and thin filaments) zones in a fully adapted contractile unit. (Adaptation of the muscle will be discussed later). The existence of non-overlap zones could lead to load-independent shortening. To be consistent with the present finding of linear load-shortening relationship (regardless of the starting length), we have to assume that a thick filament spans the whole length of a contractile unit, and that there is no non-overlap zones in between the dense bodies in a normal (fully adapted) contractile unit, as depicted in Fig. 29A. Shortening occurring near the in situ length probably encounters very little internal load. A linear relationship between external load and the amount of shortening near  $L_{in\ situ}$ , according to the model in Fig. 29A, is expected. The linear relationship would be changed if increasing internal loads were encountered at shorter lengths. That is, the amount of shortening would be less than that predicted by the linear line at low (external) loads (Fig. 22A). It is therefore surprising to us that a curvilinear load-shortening relationship was not found in shortening trachealis.

There are several possible explanations. 1) The internal load has a linear relationship with length; 2) force generated by the muscle is a non-linear function of muscle length, which when combined with a non-linear internal load produces a linear overall load-shortening relationship; 3) the internal load is negligible in magnitude at muscle lengths greater than 10%  $L_{in\ situ}$ . The first possibility is not likely because if an internal load is

present in our preparation, it is likely to be non-linearly related to the muscle length (Meiss and Pidaparti, 2004). The second possibility is also unlikely, because even if by coincidence a linear relationship is produced by a combination of two non-linear components, the chance of this happening at three different initial lengths (Fig. 22A and Fig. 24A) is astronomically small. That leaves the third possibility as a likely explanation. The model presented in Fig. 29A appears to be the simplest that can accommodate all data collected in the present study. The requirement that a thick filament spans the whole length of a contractile unit and literally touches both dense bodies stems from the observation that a small amount of shortening of the muscle resulted in a decrease in the force generated by the muscle (Fig. 22A and 24A). If there were gaps between the thick filament and the dense bodies, the initial shortening of the contractile unit would result in the narrowing of the gaps at no cost to the force generating ability. Another requirement of the model is that only the portion of the thick filament between the dense bodies that overlaps with thin filaments (solid portion depicted in Fig. 29) is able to generate force; as the thick filament slides over and passes the dense bodies (white portions depicted in Fig. 29) it loses its ability to generate force, perhaps because there is no actin filament with the “correct” polarity available for interaction. The simplicity of the model lies in the mechanism that links the amount of filament overlap (or force generating ability) to the instantaneous length of the muscle in a direct and linear fashion, and straightforwardly accommodates the present data.

### 7.6.2 Muscle shortening after a quick stretch

The sliding-filament mechanism similar to that found in striated muscle has never been clearly demonstrated in intact smooth muscle. If such a mechanism exists in smooth muscle, an isotonic shortening with or without a preceding quick-stretch will arrive at the same final length (when the muscle is maximally shortened under a certain load). This is graphically illustrated in Fig. 29B. This prediction is supported by the results shown in Fig. 22 and Fig. 24, if we consider isotonic shortenings under loads less than 50%  $F_{\max}$ . (For loads greater than 50%  $F_{\max}$ , the longer contraction time required for the muscle to reach the shortening plateau may allow the mechanism of adaptation to play a role in determining the final length of the muscle. More discussion on the adaptive behaviour of the tracheal muscle is presented in the following section). The rapid shortening under light loads likely prevented substantial remodelling of the contractile apparatus from occurring in the <10 s duration of shortening (Fig. 22 and 24). The results from such contractions therefore can be explained by the “static” (non-adaptive) model in Fig. 29. A quick 10% stretch from  $L_{\text{in situ}}$  resulted in a 10% increase in isotonic shortening, so that the final shortened length was the same as that produced by the same muscle without a stretch (Fig. 24A, for loads  $\leq 50\% F_{\max}$ ). The shortening velocity should not be affected by such a stretch, as predicted by the model (Fig. 29) and supported by the data (Fig. 24B). With a larger stretch, similar results were obtained. In Fig. 25,  $\Delta L_2$  was obtained after a 30% quick stretch from  $L_{\text{in situ}}$  and was almost exactly  $0.3 L_{\text{in situ}}$  greater than  $\Delta L_1$ , indicating that the final length of the shortened muscle with or without the stretch was the same. Examination of thick filament density surrounding dense bodies in transverse cell

sections before and after a 30% quick stretch revealed that there was a density decrease associated with the stretch, and the decrease was most profound within a 30-50 nm perimeter surrounding the dense bodies (Fig. 27), suggesting that the stretch had pulled some of the dense bodies away from their accompanying thick filaments. If the stretch uniformly increased the distance between dense bodies in a muscle cell by 30% and left the thick filaments in the middle of the contractile units, we should see a more dramatic decrease in the thick filament density adjacent to the dense bodies. The smaller-than-expected density decrease suggests that the thick filaments might not stay in the middle of the contractile units during the stretch, and might skew to one side of the contractile unit with one end still in close association with the dense bodies. Some of the thick filaments might be torn apart in the middle during the stretch and the fragments remained close to the dense bodies. This scenario is possible considering that there was a large decrease in thick filament density across the whole cell cross section due to the stretch (Fig. 26), evidence of filament depolymerization. If we exclude the phenomena related to muscle adaptation away from the rest of our observations, the functional and structural data discussed above are consistent with the proposed model and could be regarded as evidence for the sliding-filament mechanism operating in smooth muscle.

### **7.7 Adaptation of smooth muscle to different lengths**

Many aspects of the muscle behaviour described in this study are related to the adaptive response of tracheal smooth muscle to changes in cell length, especially when the length

change is chronic in nature. It appears that the muscle has an innate tendency to optimize the contractile filament overlap at almost any (externally imposed) cell length and to maintain the ability to generate maximal force (Pratusevich et al, 1995; Gunst et al, 1995; Kuo et al, 2003). A good example is shown in Fig. 22. With a two-fold change in length, the maximal isometric force produced by the muscle (fully adapted at each length) was not different. The shortening velocity, on the other hand, was higher for the muscle adapted at the longer cell length (Fig. 22B). These findings are essentially the same as those found earlier (Pratusevich et al, 1995) and could be interpreted by a simple model where plastic adaptation alters the number of contractile units in series within a cell (Kuo et al, 2003; Lambert et al, 2004). The data presented in Fig. 22A provides further constraints on the model that we have developed in our earlier studies. As described in Fig. 30, the three possible rearrangements of contractile units within a cell, which has undergone a doubling in length, cannot be distinguished by our previous studies – they all predict no change in isometric force, and a  $\sim 5/3$  or 1.67-fold increase in shortening velocity, muscle power output, rate of ATP consumption, and myosin filament density (in a cell cross section). These predictions were all confirmed by Kuo et al (2003). With the new data presented in Fig. 22A, we are now able to refine the model. As described in Fig. 30, Model C appears to be the correct model in that it gives the best fit to the data (Fig. 31).

The mechanism for plastic adaptation to changes in cell geometry is largely unknown. It appears that not only reorganization of myosin filaments is involved (Kuo et al, 2001; Herrera et al, 2002; Qi et al, 2002; Kuo et al, 2003; Herrera et al, 2004), remodelling of

the cytoskeleton is also required (Gunst and Fredberg, 2003). Our inability to demonstrate unequivocally the proposed structural rearrangement accompanying cell length change, for example, in longitudinal electron microscopic sections, has forced us to rely on functional data such as those shown in Fig. 22 as basis of model proposal. The functional data, however, will be invaluable in guiding the search for and interpretation of structural evidence.

The concept of plastic adaptation in terms of myosin filament polymerization and reorganization presented in Fig. 30 not only helped in the interpretation of data shown in Fig. 22, it also helps to explain other findings of this study. In Fig. 24A, for shortenings under heavy loads ( $>50\% F_{\max}$ ), the amount of shortenings after a quick stretch were less than those expected, based on a model where a quick stretch increases the non-overlap portion between the thick and thin filaments (and explains the increase in shortening after a stretch in lightly loaded isotonic contractions). This observation, however, can be explained by considering the fact that during an isotonic contraction under a heavy load a muscle cell spends a longer period of time (after stimulation) in isometric mode (compared to that in an isotonic contraction under a light load) and this may allow the adaptation process to proceed to a significant extent before isotonic shortening starts. As illustrated in Fig. 31, adaptation after an increase in length leads to reduced amount of shortening. A similar observation was made in muscle cells after a 30% quick stretch, as shown in Fig. 25. By allowing the muscle to adapt to the 30% increase in length, the amount of shortening was reduced (from comparison of  $\Delta L_3$  to  $\Delta L_2$ ).

The thick filaments are structurally labile, especially in a relaxed muscle cell (Kuo et al, 2001; Herrera et al, 2004). The lability is evident in the present results. The thick filament density in cell cross sections was significantly reduced immediately after a 30% quick stretch (Fig. 26). This is likely due to depolymerization in some of the thick filaments. Adaptation of the muscle at the stretched length over a period of 30 min resulted in an extensive recovery of the thick filament density, consistent with the model prediction described in Fig. 30. The transient nature of thick filament density was also seen in Fig. 27. Immediately after the quick stretch, the density surrounding the dense bodies decreased. The decrease was greater than that expected from stretch-induced thick filament depolymerization alone; it could be due to the pulling of dense bodies away from the thick filaments, as depicted in Fig. 29B. After a 30-min period of adaptation, the density profile returned to the same shape and position as those before the stretch. This observation can be interpreted as supporting evidence for Model C proposed in Fig. 30 (i.e., lengthening of the thick filaments to span completely the contractile unit length). The actin thin filaments, on the other hand, appeared to be more stable and were not affected by the sudden change in length (Fig. 26).

An interesting observation (and model prediction) is that the maximally shortened length at any load was always shorter in muscles adapted to a shorter length (Fig. 22A). This unique smooth muscle property may have important clinical implications. Excessive shortening of ASM is implicated in the disease of asthma (King et al, 1999). Alterations in extracellular environment (due to airway inflammation and inflammation-associated tissue injury, for example) that result in adaptation of smooth muscle cells at abnormally

short lengths could underlie the pathology of asthma. Similar speculations can be extended to other smooth muscle related organ dysfunction where exaggerated shortening of smooth muscle is the root problem. Although the difference in the maximally shortened length (with different starting lengths) decreased at lighter loads, the difference did not disappear when extrapolated to a zero (external) load. In fact, the maximally shortened length at zero load was linearly related to the initial length of the muscle (i.e., the length at which the muscle was adapted) (Fig. 23). This raises a question of what determines that maximally shortened length under a zero load (minimum muscle length). According to the model presented in Fig. 29, under no load, a contractile unit will continue to shorten until the dense bodies meet. The final length of a contractile unit under a zero load therefore will be determined (at least partly) by the size of the dense bodies. The increase in the number of in-series contractile units (and therefore dense bodies) associated with adaptation of the muscle at a longer length therefore could explain the longer minimum muscle length.

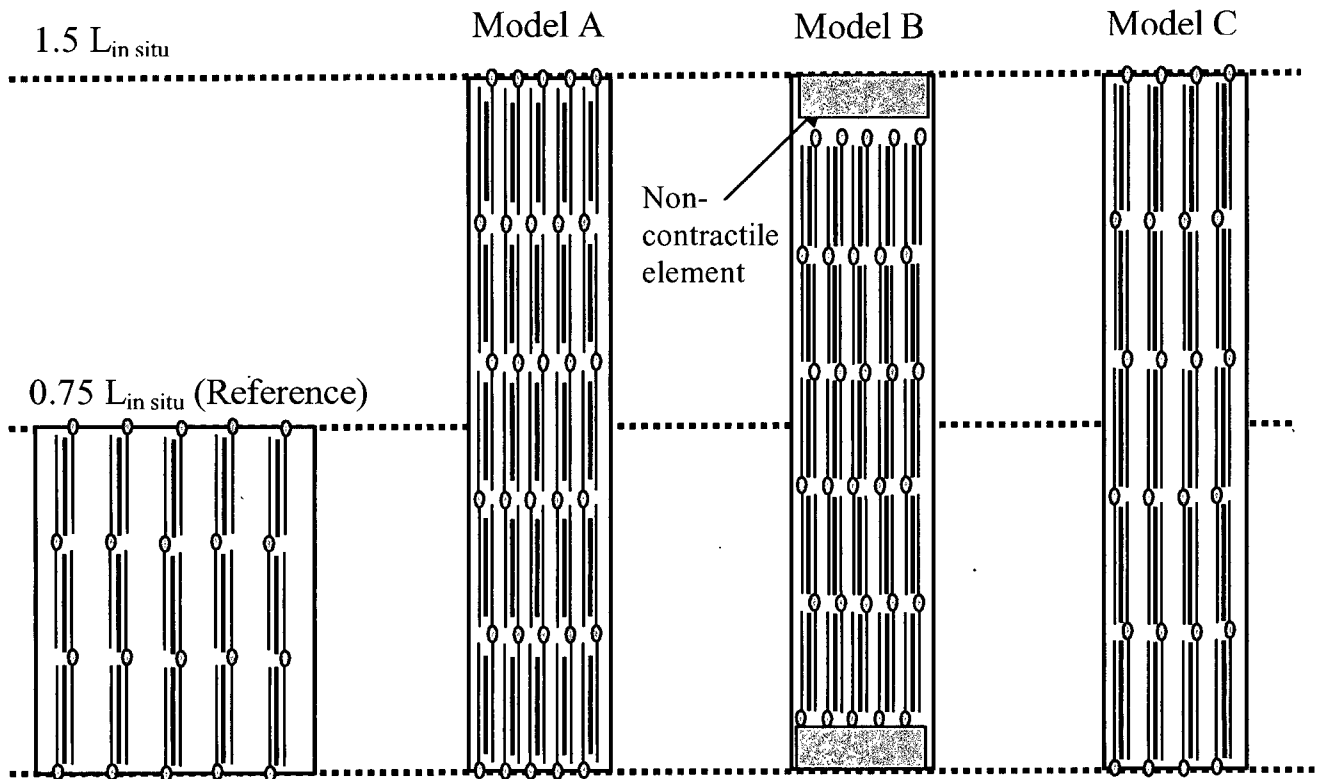


**Figure 30. Schematic representation of a trachealis cell and the intracellular arrangement of contractile units at different lengths.** Possible arrangement at  $0.75 L_{in\ situ}$  (left most rectangle, Reference), and the three possible rearrangements of the contractile units after the cell has been fully adapted at  $1.5 L_{in\ situ}$ . Assuming that the kinetics of actomyosin cross-bridge interaction is not affected by the contractile unit reconfiguration, all three models predict no change in isometric force with length doubling; all three models also predict an increase of 67% in shortening velocity, muscle power output, rate of ATP consumption, and myosin thick filament density with length doubling (consistent with observations made by Kuo et al, 2003). In all models (A, B, and C), the number of contractile units in series has increased by 67%. In **Model A**, the

increase in cell length is associated with the appearance of non-overlap zones between thick and thin filaments, and no change in the thick filament length. It is assumed that the thin filaments are longer than the thick filaments. In **Model B**, the increase in cell length is associated with the appearance of non-contractile elements (instead of non-overlap zones) in series with the contractile units, and no change in the thick filament length. Although the non-contractile elements are placed at the ends of the cell in the drawing (for sake of simplicity), in reality the non-contractile elements can be any where in the cell as long as they are serially attached to the contractile units. In **Model C**, the increase in cell length creates neither non-overlap zones nor non-contractile elements, instead, the thick filament length is increased by 20% and the number of contractile units in parallel decreased by 20%.

## Model Predictions

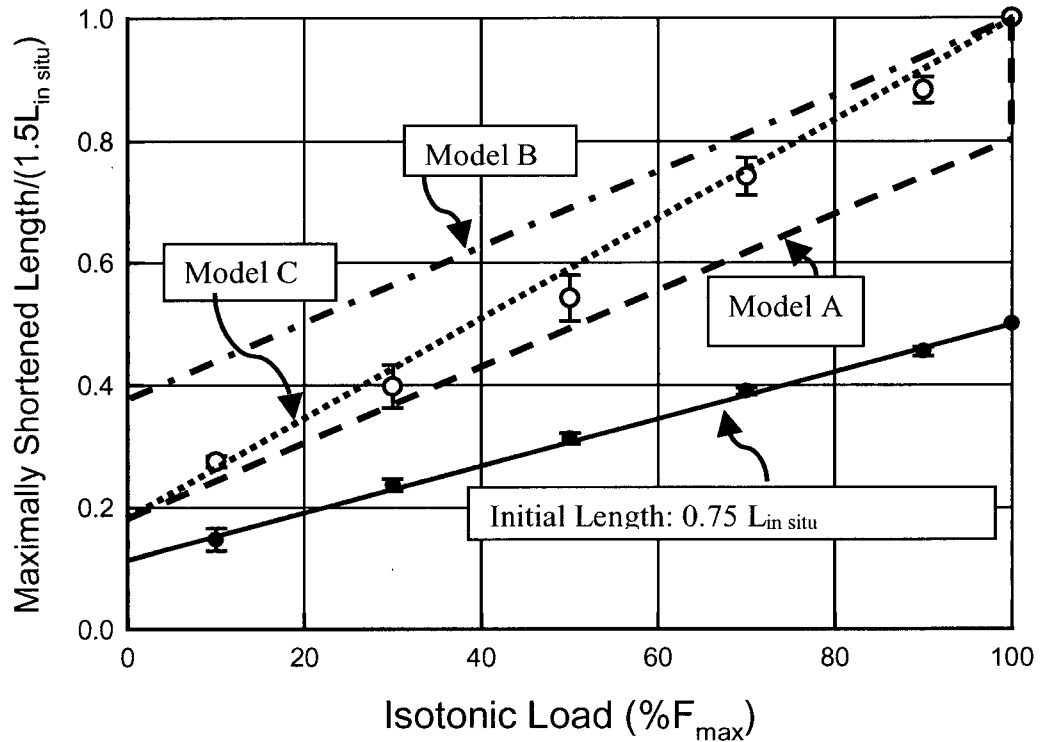


**Figure 31. Predictions by the models regarding the relationship between maximally shortened length and isotonic load.** The data points are redrawn from Fig. 22A. The model predictions are based on the linear regression line (solid) for the data collected at  $0.75 L_{in\ situ}$ . The maximally shortened length under zero-load is assumed proportional to the number of dense bodies in series plus any serially connected non-contractile elements.

## **CHAPTER 8. Conclusions and future directions**

The purpose of this thesis research was to elucidate the underlying mechanisms involved in ASM plasticity, specifically, to elucidate the ultrastructural changes responsible for the mechanical function of the muscle. The results presented in this dissertation bring us a step closer to the understanding of how ASM contractile machinery is organized and how it responds to the physiological demands imposed on the muscle.

The following conclusions are presented following the sequence of the hypotheses and specific aims proposed in Chapter 3.

### **8.1 Thick filament stability and factors affecting thick filament formation *in vivo***

In smooth muscle, myosin thick filaments have been shown to exist in abundance in the relaxed state when myosin light chain is not phosphorylated. Based on the results of this thesis research, it can be concluded that myosins exist in monomer-polymer equilibrium and that the resting intracellular calcium level is necessary for the stability and maintenance of filamentous myosins in the relaxed state. The effect of the resting intracellular calcium level on the thick filament stability appears to be independent of MLC phosphorylation (Chapter 5).

Morphological analysis of ASM under different conditions suggests that the muscle cells undergo active rearrangement of the contractile filaments upon activation and during

length adaptation. This plastic rearrangement is shown to be associated with polymerization/depolymerization of myosin filaments when the muscle is activated and adapted at different lengths (Chapter 5). Based on this finding, it can be speculated that during muscle activation, the increase of thick filament density observed in our first study is due to active polymerization that adds myosin molecules to existing filaments (i.e., elongation of thick filaments during the contractile activation) or creates new filaments. It can also be conjectured that after length adaptation, the number of thick filaments in series increases, which can then explain the observed increase in the thick filament density when the muscle is lengthened and adapted at a longer length. Although these speculations regarding structural changes agree with the functional data collected from our previous studies, complementary structural analysis is necessary to establish the differences in the thick filament length in the relaxed and activated muscles, as well as in the muscles adapted at a longer length.

## **8.2 Thin filament stability and factors affecting thin filament formation *in vivo***

In the present study, structural analysis of ASM after contractile activation and length adaptation showed that the phenomenon of plastic rearrangement of contractile units is also associated with polymerization/depolymerization of actin filaments (Chapter 6). At the same time, mechanical strain, which has been previously shown to have a relaxation-like effect on ASM by causing partial dissolution of the thick filaments, was shown to

have the opposite effect on thin filaments; it caused a slight but significant increase in the thin filaments density (Chapter 6).

Thin filaments are abundantly present in the ASM cellular cytosol and in this study it was found that the ratio of thin/thick filaments is ~28-30:1 in the relaxed state. Despite this large excess of thin filaments, during muscle activation, mechanical strain and after muscle adaptation at a longer length, actin filament density significantly increased. The exact need for actin polymerization under these conditions is not clear, but it can be assumed that the mechanical changes caused by actin polymerization/depolymerization are necessary for the normal function of the muscle. Whether this increase in the thin filament amount and the consequent mechanical changes are due to cytoskeletal remodelling or contractile apparatus remodelling, or both, is not known. More studies involving analysis of the different actin isoforms in ASM under different experimental conditions are needed to clarify this issue.

### **8.3 Contractile unit reorganization in ASM adapted to different lengths**

Based on morphological and functional data obtained from this study, the structure of a contractile unit in ASM is proposed to be composed of a myosin thick filament that spans end-to-end between two dense bodies with attached actin thin filaments. When the muscle is adapted to a different length, the data suggest that thick filament polymerization/depolymerization occurs and leads to a change in the number of

contractile units in series and in parallel that in turn maintains the optimal thin-thick filament overlapping. This structural reorganization leads to conservation of isometric force and preservation of linear load-shortening relationship over a large length range (Chapter 7). In this study, we also proposed a model for the intracellular rearrangement of contractile units after adaptation of ASM at a longer length ( $2x L_{in situ}$ ) that better fits our data. The model suggests that after length adaptation at twice the initial length, there is a 20% increase in the thick filament length and a 20% decrease in the number of contractile units in parallel. This model prediction has yet to be confirmed with more structural studies.

In summary, the results presented in this dissertation offer new insights into the basic mechanism of ASM contraction by showing that the contractile apparatus of airways smooth muscle is highly malleable, the malleability allows the muscle to adapt to changes in length by altering the number and arrangement of the contractile units within the ASM cell. This ability of the muscle to adapt to different lengths is likely to be involved in the pathophysiology of diseases such as asthma and emphysema, where excessive shortening of ASM could be due to adaptation to pathologically short lengths.

#### **8.4 Future directions**

As previously stated, complementary structural analysis of ASM is necessary to determine the average length of the thick filaments in the relaxed muscle. It is also

important to establish the differences in the thick filament length in the relaxed and activated muscles, as well as in the muscles adapted at a longer length. At the same time, the definite architecture and dimensions of an ASM contractile unit still need to be elucidated.

Our understanding of smooth muscle structure at nanometer resolution so far has mostly been derived from electron microscopic studies of two-dimensional cell cross-sections. Modeling of 3-D structure of a smooth muscle cell from random 2-D cell sections involves extrapolation of information and simplifying assumptions that often lead to uncertainties in the 3-D model. Three-dimensional reconstruction of longitudinal and transverse segments of an ASM cell from consecutive serial electron microscopic sections will provide insights of the intracellular organization of the contractile apparatus in this muscle. A thorough understanding of structural reorganization of smooth muscle under various conditions, such as those during contractile activation and adaptation to externally applied strain, will be greatly enhanced with the information provided by detailed 3-D model of the cell obtained under the corresponding conditions.

## BIBLIOGRAPHY

1. **Adler KB, Krill J, Alberghini TV, and Evans JN.** Effect of cytochalasin D on smooth muscle contraction. *Cell Motil* 3(5-6): 545-551, 1983.
2. **Amrani Y, Panettieri RA.** Airway smooth muscle: contraction and beyond. *Int J Biochem Cell Biol* 35(3): 272-6, 2003.
3. **An SS, Laudadio RE, Lai J, Rogers RA, and Fredberg JJ.** Stiffness changes in cultured airway smooth muscle cells. *Am J Physiol Cell Physiol* 283(3): C792-C801, 2002.
4. **Arner A and Hellstrand P.** Activation of contraction and ATPase activity in intact and chemically skinned smooth muscle of rat portal vein. Dependence on  $Ca^{2+}$  and muscle length. *Circ Res* 53: 695-702, 1983.
5. **Babu GJ, Warshaw DM, Periasamy M.** Smooth muscle myosin heavy chain isoforms and their role in muscle physiology. *Microsc Res Tech* 50(6): 532-40, 2000. Review.
6. **Bagby RM.** Organization of contractile/cytoskeletal elements. In: *Biochemistry of Smooth Muscle*, edited by Stephens NL. Boca Raton, FL: CRC, 1983, p. 1-84.
7. **Bárány M.** *Biochemistry of smooth muscle contraction*, edited by Bárány M. Academic Press, 1996.
8. **Blikstad I, Markey F, Carlsson L, Persson T, Lindberg U.** Selective assay of monomeric and filamentous actin in cell extracts, using inhibition of deoxyribonuclease I. *Cell* 15(3): 935-43, 1978.
9. **Carroll N, Elliot J, Morton A, and James A.** The structure of large and small airways in nonfatal and fatal asthma. *Am Rev Respir Dis* 147: 405-410, 1993.

10. **Chacko S, Rosenfeld A and Thomas G.** Calcium regulation of smooth muscle actomyosin. In: *Calcium and contractility*, edited by Gover AK and Daniel EE. Clifton, New Jersey: 1985, p. 175-190.
11. **Cipolla MJ, Gokina NI, Osol G.** Pressure-induced actin polymerization in vascular smooth muscle as a mechanism underlying myogenic behavior. *FASEB J* 16(1): 72-6, 2002.
12. **Cooke PH, and Fay FS.** Thick filaments in contracted and relaxed mammalian smooth muscle cells. *Exp Cell Res* 71: 265-272, 1972.
13. **Cooke PH, Kargacin G, Craig R, Fogarty K, Fay FS.** Molecular structure and organization of filaments in single, skinned smooth muscle cells. *Prog Clin Biol Res* 245:1-25, 1987.
14. **Craig R, and Megerman J.** Assembly of smooth muscle myosin into side-polar filaments. *J Cell Biol* 75: 990-996, 1977.
15. **Craig R, Smith R, and Kendrick-Jones J.** Light-chain phosphorylation controls the conformation of vertebrate non-muscle and smooth muscle myosin molecules. *Nature* 302: 436-439, 1983.
16. **Dillon PF, Aksoy MO, Driska SP and Murphy RA.** Myosin phosphorylation and the crossbridge cycle in arterial smooth muscle. *Science* 211: 495-497, 1981.
17. **Fabry B, Maksym GN, Butler JP, Glogauer M, Navajas D, and Fredberg JJ.** Scaling the Scaling the microrheology of living cells. *Physiol Rev* 87: 148102, 2001.
18. **Farkas GA and Roussos.** Diaphragm in emphysematous hamsters: sarcomere adaptability *J Appl Physiol* 54: 1635-1640, 1983.
19. **Fernandes DJ, Mitchell RW, Lakser O, Dowell M, Stewart AG, Solway J.** Do inflammatory mediators influence the contribution of airway smooth muscle

- contraction to airway hyperresponsiveness in asthma? *J Appl Physiol* 95(2): 844-53, 2003.
20. **Ferrari MB, Ribbeck K, Hagler DJ, Jr, and Spitzer NC.** A calcium signaling cascade essential for myosin thick filament assembly in *Xenopus* myocytes. *J Cell Biol* 141: 1349-1356, 1998.
21. **Filipe JA, and Nunes JP.** Functional importance of the actin cytoskeleton in contraction of bovine iris sphincter muscle. *Auton Autacoid Pharmacol* 22(3):155-159, 2002.
22. **Fish JE, Peterman VI, Cugell DW.** Effect of deep inspiration on airway conductance in subjects with allergic rhinitis and allergic asthma. *J Allergy Clin Immunol* 60(1): 41-6, 1977.
23. **Fredberg JJ.** Airway obstruction in asthma: does the response to a deep inspiration matter? *Respir Res.* 2(5): 273-5, 2001.
24. **Fredberg JJ, Inouye D, Miller B, Nathan M, Jafari S, Raboudi SH, Butler JP, Shore SA.** Airway smooth muscle, tidal stretches, and dynamically determined contractile states. *Am J Respir Crit Care Med* 156(6): 1752-9, 1997.
25. **Fredberg JJ, Inouye DS, Mijailovich SM, and Butler JP.** Perturbed equilibrium of myosin binding in airway smooth muscle and its implication in bronchospasm. *Am J Respir Crit Care Med* 159: 959-967, 1999.
26. **Ford LE, Seow CY, and Patrusевич VR.** Plasticity in smooth muscle, a hypothesis. *Can J Physiol Pharmacol*, 72(11): p.1320-4, 1994.
27. **Fultz ME, Li C, Geng W, and Wright GL.** Remodeling of the actin cytoskeleton in the contracting A7r5 smooth muscle cell. *J Muscle Res Cell Motil* 21(8): 775-787, 2000.

28. **Fultz ME, Wright GL.** Myosin remodelling in the contracting A7r5 smooth muscle cell. *Acta Physiol Scand* 177(2): 197-205, 2003.
29. **Gabella G.** Morphology of smooth muscle. In: *Cellular aspects of smooth muscle function*, edited by Kao CY and Carsten ME. Cambridge, UK: 1997, p. 1-47.
30. **Garamvölgyi N, Vizi ES, and Knoll J.** The regular occurrence of thick filaments in stretched mammalian smooth muscle. *J Ultrastruct Res* 34: 135-143, 1971.
31. **Garamvölgyi N, Vizi ES, and Knoll J.** The site and state of myosin in intestinal smooth muscle. *Philos Trans R Soc Lond B Biol Sci* 265: 219-222, 1973.
32. **Garfield RE and Somlyo AP.** Structure of smooth muscle. In: *Calcium and contractility*, edited by Gover AK and Daniel EE. Clifton, New Jersey: 1985, p. 1-36.
33. **Gerthoffer WT, and Gunst SJ.** Invited review: focal adhesion and small heat shock proteins in the regulation of actin remodeling and contractility in smooth muscle. *J Appl Physiol* 91(2):963-972, 2001.
34. **Gillis JM, Cao ML, and Godfraind-De Becker A.** Density of myosin filaments in the rat anococcygeus muscle, at rest and in contraction. II. *J Muscle Res Cell Motil* 9: 18-29, 1988.
35. **Godfraind-De Becker, A, and Gillis JM.** Analysis of the birefringence of the smooth muscle anococcygeus of the rat, at rest and in contraction. I. *J Muscle Res Cell Motil* 9: 9-17, 1988.
36. **Gordon AM, Huxley AF, and Julian FJ.** The variation in isometric tension with sarcomere length in vertebrate muscle fibres. *J Physiol* 184: 170-192, 1966.
37. **Guilford, W. H., and D. M. Warshaw.** The molecular mechanics of smooth muscle myosin. *Comp Biochem Physiol B Biochem Mol Biol.* 119(3): 451-458, 1998.

38. **Gunst SJ.** Contractile force of canine airway smooth muscle during cyclical length changes. *J Appl Physiol* 55(3): 759-69, 1983.
39. **Gunst SJ.** Effect of length history on contractile behavior of canine tracheal smooth muscle. *Am J Physiol* 250(1 Pt 1): p. C146-54, 1986.
40. **Gunst SJ, Meiss RA, Wu MF, Rowe M.** Mechanisms for the mechanical plasticity of tracheal smooth muscle. *Am J Physiol* 268(5 Pt 1): C1267-76, 1995.
41. **Gunst SJ and Tang DD.** The contractile apparatus and mechanical properties of airway smooth muscle. *Eur Respir J* 15(3): 600-16, 2000.
42. **Gunst SJ, Tang DD, Opazo Saez A.** Cytoskeletal remodelling of the airway smooth muscle cell: a mechanism for adaptation to mechanical forces in the lung. *Respir Physiol Neurobiol* 137(2-3): 151-68, 2003.
43. **Gunst SJ and Wu MF.** Plasticity in skeletal, cardiac and smooth muscle. Selected contribution: plasticity of airway smooth muscle stiffness and extensibility: role of length-adaptive mechanisms *J Appl Physiol* 90: 741-49, 2001.
44. **Halayko AJ, and Solway J.** Molecular mechanisms of phenotypic plasticity in smooth muscle cells. *J Appl Physiol* 90(1):358-368, 2001.
45. **Harris DE and Warshaw DM.** Length vs. active force relationship in single isolated smooth muscle cells. *Am J Physiol* 260(5 Pt 1): C1104-12, 1991.
46. **Hedges, JC, Dechert MA, Yamboliev IA, Martin JL, Hickey E, Weber LA, and Gerthoffer WT.** A role for p38 (MAPK)/HSP27 pathway in smooth muscle cell migration. *J Biol Chem* 274: 24211-24219, 1999.
47. **Herrera, A. M., K.-H. Kuo, and C. Y. Seow.** Influence of calcium on myosin thick filament formation in intact airway smooth muscle. *Am. J. Physiol* 282: C310-C316, 2002

48. **Herrera, A. M., E. C. Martinez, and C. Y. Seow.** Electron microscopic study of actin polymerization in airway smooth muscle. *Am. J. Physiol* 286(6): L1161-8, 2004.
49. **Hill AV.** The mechanics of active muscle. *Proceedings of the Royal Society of London. Series Biological Sciences (London)* 141: 104-117, 1953.
50. **Hirshman CA, Zhu D, Panettieri RA, and Emala CW.** Actin depolymerization via the beta-adrenoceptor in airway smooth muscle cells: a novel PKA-independent pathway. *Am J Physiol Cell Physiol* 281(5):C1468-C1476, 2001.
51. **Horowitz A, Trybus KM, Bowman DS, and Fay FS.** Antibodies probe for folded monomeric myosin in relaxed and contracted smooth muscle. *J Cell Biol* 126: 1195-1200, 1994.
52. **Huxley AF.** Cross-bridge action: present views, prospects, and unknowns. *J Biomech.* 33(10): 1189-95, 2000.
53. **Huxley AF, and Niedergerke R.** Structural changes in muscle during contraction. *Nature (London)* 173: 971-973, 1954.
54. **Ishii N and Takahashi K.** Length-tension relation of single smooth muscle cells isolated from the pedal retractor muscle of *Mytilus edulis*. *J Muscle Res Cell Motil* 3: 25-38, 1982.
55. **Jakubiec-Puka A, Carraro U.** Remodelling of the contractile apparatus of striated muscle stimulated electrically in a shortened position. *J Anat* 178:83-100, 1991.
56. **Jiang H, Rao K, Halayko AJ, Kepron W, Stephens NL.** Bronchial smooth muscle mechanics of a canine model of allergic airway hyperresponsiveness. *J Appl Physiol* 72(1): 39-45, 1992.

57. **Jones KA, Perkins WJ, Lorenz RR, Prakash YS, Sieck GC, and Warner DO.** F-actin stabilization increases tension cost during contraction of permeabilized airway smooth muscle in dogs. *J Physiol* 519: 527–538, 1999.
58. **Kannan MS, and Daniel EE.** Structural and functional study of control of canine tracheal smooth muscle. *Am J Physiol* 238(1): C27-33, 1980.
59. **Karaki H, Ozaki H, Hori M, Mitsui-Saito M, Amano K, Harada K, Miyamoto S, Nakazawa H, Won KJ, Sato K.** Calcium movements, distribution, and functions in smooth muscle. *Pharmacol Rev* 49: 157-230, 1997.
60. **Kamm KE and Stull JT.** Myosin phosphorylation, force and maximal shortening velocity in neurally stimulated tracheal smooth muscle. *Am J Physiol Cell Physiol* 249: 238-247, 1985.
61. **Kendrick-Jones J, Smith RC, Craig R, and Citi S.** Polymerization of vertebrate non-muscle and smooth muscle myosins. *J Mol Biol* 198: 241-252, 1987.
62. **Kenney RE, Hoar PE, and Kerrick WGL.** The relationship between ATPase activity, isometric force, and myosin light chain phosphorylation and thiophosphorylation in skinned smooth muscle fiber bundles from chicken gizzard. *J Biol Chem* 265: 8642–8649, 1990.
63. **King GG, Moore BJ, Seow CY, Pare PD.** Airway narrowing associated with inhibition of deep inspiration during methacholine inhalation in asthmatics. *Am J Respir Crit Care Med* 164(2): 216-8, 2001.
64. **King GG, Pare PD, Seow CY.** The mechanics of exaggerated airway narrowing in asthma: the role of smooth muscle. *Respir Physiol* 118(1):1-13, 1999. Review.
65. **Kuo KH, Herrera AM, Wang L, Pare PD, Ford LE, Stephens NL, Seow CY.** Structure-function correlation in airway smooth muscle adapted to different lengths. *Am J Physiol Cell Physiol* 285(2):C384-90, 2003.

66. **Kuo KH, Herrera AM, Seow CY.** Ultrastructure of airway smooth muscle. *Respir Physiol Neurobiol* 137(2-3): 197-208, 2003.
67. **Kuo KH, Wang L, Pare PD, Ford LE, Seow CY.** Myosin thick filament lability induced by mechanical strain in airway smooth muscle. *J Appl Physiol* 90(5): 1811-6, 2001.
68. **James AL, Paré PD, and Hogg JC.** The mechanics of airway narrowing in asthma. *Am Rev Respir Dis* 139: 242-246, 1989.
69. **Lambert RK, Pare PD, Seow CY.** Mathematical description of geometric and kinematic aspects of smooth muscle plasticity and some related morphometrics. *J Appl Physiol* 96(2): 469-76, 2004.
70. **Larsen, JK, Yamboliev IA, Weber LA, and Gerthoffer WT.** Phosphorylation of the 27-kDa heat shock protein via p38 MAP kinase and MAPKAP kinase in smooth muscle. *Am J Physiol Lung Cell Mol Physiol* 273: L930-L940, 1997.
71. **Lesh RE, Emala CW, Lee HT, Zhu D, Panettieri RA, and Hirshman CA.** Inhibition of geranylgeranylation blocks agonist-induced actin reorganization in human airway smooth muscle cells. *Am J Physiol Lung Cell Mol Physiol* 281(4): L824-L831, 2001.
72. **Loukianov E, Loukianova T, Periasamy M.** Myosin heavy chain isoforms in smooth muscle. *Comp Biochem Physiol B Biochem Mol Biol* 117(1): 13-8, 1997. Review.
73. **Loutzenhiser R, Leyten P, Saida K and Van Breemen C.** Calcium compartments and mobilization during contraction of smooth muscle. In: *Calcium and contractility*, edited by Gover AK and Daniel EE. Clifton, New Jersey: 1985, p. 61-92.

74. **Ma X, Cheng Z, Kong H, Wang Y, Unruh H, Stephens NL, Laviolette M.** Changes in biophysical and biochemical properties of single bronchial smooth muscle cells from asthmatic subjects. *Am J Physiol Lung Cell Mol Physiol* 283(6): L1181-9, 2002.
75. **Maass-Moreno R, Burdyga T, Mitchell RW, Seow CY, Ragozzino J, and Ford LE.** Simple freezing apparatus for resolving rapid metabolic events associated with smooth muscle activation. *J Appl Physiol* 90: 2453-2459, 2001.
76. **Malmberg P, Larsson K, Sundblad BM, Zhiping W.** Importance of the time interval between FEV1 measurements in a methacholine provocation test. *Eur Respir J* 6(5): 680-6, 1993.
77. **Martin AF, Bhatti S, Paul RJ.** C-terminal isoforms of the myosin heavy chain and smooth muscle function. *Comp Biochem Physiol B Biochem Mol Biol* 117(1): 3-11, 1997. Review.
78. **Matrougui K, Tanko LB, Loufrani L, Gorny D, Levy BI, Tedgui A, and Henrion D.** Involvement of Rho-kinase and the actin filament network in angiotensin II-induced contraction and extracellular signal-regulated kinase activity in intact rat mesenteric resistance arteries. *Arterioscler Thromb Vasc Biol* 21(8):1288-1293, 2001.
79. **Mauss S, Koch G, Kreue VAW, and Aktories K.** Inhibition of the contraction of the isolated longitudinal muscle of the guinea pig ileum by botulinum C2 toxin: evidence for a role of G/F-actin transition in smooth muscle contraction. *Naunyn-Schmiedebergs Arch Pharmacol* 340:345-351, 1989.
80. **Mehta D, Gunst SJ.** Actin polymerization stimulated by contractile activation regulates force development in canine tracheal smooth muscle. *J Physiol* 519 Pt 3:829-40, 1999.

81. **Meiss RA.** Mechanics of smooth muscle contraction. In: *Cellular aspects of smooth muscle function*, edited by Kao CY and Carsten ME. Cambridge, UK: 1997, p. 169-208.
82. **Miller JD and Carsten ME.** Calcium homeostasis in smooth muscle. In: *Cellular aspects of smooth muscle function*, edited by Kao CY and Carsten ME. Cambridge, UK: 1997, p. 48-97.
83. **Mitchell RW, Seow CY, Burdyga T, Maass-Moreno R, Pratusевич VR, Ragozzino J, and Ford LE.** Relationship between myosin phosphorylation and contractile capability of canine airway smooth muscle. *J Appl Physiol* 90: 2460-2465, 2001.
84. **Murphy RA, Walker JS, Strauss JD.** Myosin isoforms and functional diversity in vertebrate smooth muscle. *Comp Biochem Physiol B Biochem Mol Biol* 117(1): 51-60, 1997. Review.
85. **Naghshin J, Wang L, Pare PD, Seow CY.** Adaptation to chronic length change in explanted airway smooth muscle. *J Appl Physiol* 95(1): 448-53, 2003.
86. **Needham, DM, and Shoenberg CF.** Proteins of the contractile mechanism of mammalian smooth muscle and their possible location in the cell. *Proc R Soc Lond B Biol Sci* 148: 517-524, 1964.
87. **Obara K, and Yabu H.** Effect of cytochalasin B on intestinal smooth muscle cells. *Eur J Pharm* 255:139-147, 1994.
88. **Onishi H, and Wabakayashi T.** Electron microscopic studies of myosin molecules from chicken gizzard muscle. I. The formation of the intramolecular loop in the myosin tail. *J Biochem (Tokyo)* 92: 871-879, 1982.
89. **Onishi H, Wabakayashi T, Kamata T, and Watanabe S.** Electron microscopic studies of myosin molecules from chicken gizzard muscle. II. The effect of

- thiophosphorylation of the 20-kDa light chain on the ATP-induced change in the conformation of myosin monomers. *J Biochem (Tokyo)* 94: 1147-1154, 1983.
90. **Opazo Saez AM, Seow CY, Pare PD.** Peripheral airway smooth muscle mechanics in obstructive airways disease. *Am J Respir Crit Care Med* 161(3 Pt 1): 910-7, 2000.
91. **Persechini A, Kamm KE, and Stull JT.** Different phosphorylated forms of myosin in contracting tracheal smooth muscle. *J Biol Chem* 261: 6293-6299, 1986.
92. **Pfitzer G.** Invited review: regulation of myosin phosphorylation in smooth muscle. *J Appl Physiol* 91(1): 497-503. Review.
93. **Podlubnaya Z, Kulikova N, Dabrowska R.** The effect of Ca<sup>2+</sup> on the structure of synthetic filaments of smooth muscle myosin. *J Muscle Res Cell Motil* 20(5-6): 547-54, 1999.
94. **Pratusevich VR, Seow CY, and Ford LE.** Plasticity in canine airway smooth muscle. *J Gen Physiol* 105: 73-94, 1995.
95. **Qi D, Mitchell RW, Burdyga T, Ford LE, Kuo KH, Seow CY.** Myosin light chain phosphorylation facilitates in vivo myosin filament reassembly after mechanical perturbation. *Am J Physiol Cell Physiol* 282(6): C1298-305, 2002.
96. **Rembold CM and Murphy RA.** Muscle length, shortening, myoplasmic [Ca<sup>2+</sup>], and activation of arterial smooth muscle. *Circ Res* 66: 1354-1361, 1990.
97. **Rovner AS, Fagnant PM, Lowey S, Trybus KM.** The carboxyl-terminal isoforms of smooth muscle myosin heavy chain determine thick filament assembly properties. *J Cell Biol* 156(1): 113-23, 2002.

98. **Scichilone N, Permutt S, Togias A.** The lack of the bronchoprotective and not the bronchodilatory ability of deep inspiration is associated with airway hyperresponsiveness. *Am J Respir Crit Care Med* 163(2): 413-9, 2001.
99. **Seow CY.** Response of arterial smooth muscle to length perturbation. *J Appl Physiol* 89(5): 2065-72, 2000.
100. **Seow CY, Fredberg JJ.** Historical perspective on airway smooth muscle: the saga of a frustrated cell. *J Appl Physiol* 91(2): 938-52, 2001. Review.
101. **Seow CY, Pratusевич VR, and Ford LE.** Series-to-parallel transition in the filament lattice of airway smooth muscle. *J Appl Physiol* 89:869-876, 2000.
102. **Seow CY, Schellenberg RR, Pare PD.** Structural and functional changes in the airway smooth muscle of asthmatic subjects. *Am J Respir Crit Care Med* 158(5 Pt 3): S179-86, 1998. Review.
103. **Seow CY, Stephens NL.** Force-velocity curves for smooth muscle: analysis of internal factors reducing velocity. *Am J Physiol Cell Physiol* 251:C362-C368, 1986.
104. **Seow CY, Stephens NL.** Changes of tracheal smooth muscle stiffness during an isotonic contraction. *Am J Physiol* 256(2 Pt 1): C341-50, 1989.
105. **Shaw L, Ahmed S, Austin C, and Taggart MJ.** Inhibitors of actin filament polymerisation attenuate force but not global intracellular calcium in isolated pressurised resistance arteries. *J Vasc Res* 40(1): 1-10; discussion 10, 2003.
106. **Shen X, Wu MF, Tepper RS, Gunst SJ.** Mechanisms for the mechanical response of airway smooth muscle to length oscillation. *J Appl Physiol* 83(3): 731-8, 1997.

107. **Small JV and Sobieszek A.** Contractile and structural proteins of smooth muscle. In: *Biochemistry of Smooth Muscle*, edited by Stephens NL. Boca Raton, FL: CRC, 1983, p. 85-140.
108. **Smith PG, Roy C, Fisher S, Huang QQ, Brozovich F.** Selected contribution: mechanical strain increases force production and calcium sensitivity in cultured airway smooth muscle cells. *J Appl Physiol* 89(5): 2092-8, 2000.
109. **Smith PG, Roy C, Zhang YN, and Chauduri S.** Mechanical stress increases RhoA activation in airway smooth muscle cells. *Am J Respir Cell Mol Biol* 28(4):436-442, 2003.
110. **Somlyo AP.** Myosin isoforms in smooth muscle: how may they affect function and structure? *J Muscle Res Cell Motil.* 14(6): 557-63, 1993. Review.
111. **Somlyo AV, Butler TM, Bond M, and Somlyo AP.** Myosin filaments have non-phosphorylated light chains in relaxed smooth muscle. *Nature* 294: 567-569, 1981.
112. **Somlyo AP, Devine CE, Somlyo AV, and Rice RV.** Filament organization in vertebrate smooth muscle. *Philos Trans R Soc Lond B Biol Sci* 265: 223-229, 1973.
113. **Somlyo AP and Somlyo AV.** Smooth muscle: excitation-contraction coupling, contractile regulation and the cross-bridge cycle. *Alcoholism: Clin. Exp. Res.* 18: 138-143, 1994.
114. **Steinmetz MO, Goldie KN, Aebi U.** A correlative analysis of actin filament assembly, structure, and dynamics. *J Cell Biol* 138(3): 559-74, 1997.
115. **Stephens NL.** Airway smooth muscle. *Lung.* 179(6): 333-73, 2001. Review.
116. **Stephens NL, Kroeger E, and Mehta JA.** Force-velocity characteristics of respiratory airway smooth muscle. *J Appl physiol* 26(6): p.685-92, 1969.

117. **Stephens NL, Halayko AJ.** Airway smooth muscle contractile, regulatory and cytoskeletal protein expression in health and disease. *Comp Biochem Physiol B Biochem Mol Biol* 119(3): 415-24, 1998. Review.
118. **Stephens NL, Kagan ML, and Packer CS.** Time dependence of shortening velocity in tracheal smooth muscle. *Am J Physiol* 251:C435-C439, 1980.
119. **Stephens NL, Li W, Wang Y, Ma X.** The contractile apparatus of airway smooth muscle. Biophysics and biochemistry. *Am J Respir Crit Care Med* 158(5 Pt 3): S80-94, 1998.
120. **Stephens NL, Seow CY.** Mechanical properties of smooth muscle. *Prog Clin Biol Res* 327:409-33, 1990.
121. **Stephens NL, Seow CY, Halayko AJ, Jiang H.** The biophysics and biochemistry of smooth muscle contraction. *Can J Physiol Pharmacol* 70(4): 515-31, 1992.
122. **Stephens NL and Van Niekerk W.** Isometric and isotonic contractions in airway smooth muscle. *Can J Physiol Pharmacol* 55(4): p. 833-8, 1977.
123. **Stromer MH, Mayes MS, Bellin RM.** Use of actin isoform-specific antibodies to probe the domain structure in three smooth muscles. *Histochem Cell Biol* 118(4): 291-9, 2002.
124. **Symons MH, Mitchison TJ.** Control of actin polymerization in live and permeabilized fibroblasts. *J Cell Biol* 114(3): 503-13, 1991.
125. **Szymanski PT, Chacko TK, Rovner AS, Goyal RK.** Differences in contractile protein content and isoforms in phasic and tonic smooth muscles. *Am J Physiol* 275(3 Pt 1): C684-92, 1998.

126. **Tang DD, and Tan J.** Downregulation of profilin with antisense oligodeoxynucleotides inhibits force development during stimulation of smooth muscle. *Am J Physiol Heart Circ Physiol* 285(4): H1528-H1536, 2003.
127. **Trybus KM, Huiatt TW, and Lowey S.** A bent monomeric conformation of myosin from smooth muscle. *Proc Natl Acad Sci USA* 79: 6151-6155, 1982.
128. **Trybus KM, and Lowey S.** Conformational states of smooth muscle myosin: effects of light chain phosphorylation and ionic strength. *J Biol Chem* 259: 8564-8571, 1984.
129. **Tseng, S, Kim R, Kim T, Morgan KG, and Hai CM.** F-actin disruption attenuates agonist-induced  $[Ca^{2+}]$ , myosin phosphorylation, and force in smooth muscle. *Am J Physiol Cell Physiol* 272: C1960-C1967, 1997.
130. **Tsukita S, Tsukita S, Usukura J, and Ishikawa H.** Myosin filaments in smooth muscle cells of the guinea pig taenia coli: a freeze-substitution study. *Eur J Cell Biol* 28: 195-201, 1982.
131. **Uvelius B.** Isometric and isotonic length-tension relations and variations in cell length in longitudinal smooth muscle from rabbit urinary bladder. *Acta Physiol Scand* 97: 1-12, 1976.
132. **Wang L and Pare PD.** Deep inspiration and airway smooth muscle adaptation to length change. *Resp Physiol Neuro* 137: 169-78. 2003.
133. **Wang L, Pare PD, Seow CY.** Effects of length oscillation on the subsequent force development in swine tracheal smooth muscle. *J Appl Physiol* 88(6): 2246-50, 2000.
134. **Wang L, Pare PD, Seow CY.** Selected contribution: effect of chronic passive length change on airway smooth muscle length-tension relationship. *J Appl Physiol* 90(2): 734-40, 2001.

135. **Wang L, Pare PD, Seow CY.** Changes in force-velocity properties of trachealis due to oscillatory strains. *J Appl Physiol* 92(5): 1865-72, 2002.
136. **Watanabe, N, Kato T, Fujita A, Ishizaki T, and Narumiya S.** Cooperation between mDia1 and ROCK in Rho-induced actin reorganization. *Nat Cell Biol* 1: 136-143, 1999.
137. **Watanabe M, Takemori S, and Yagi N.** X-ray diffraction study on mammalian visceral smooth muscle in resting and activated states. *J Muscle Res Cell Motil* 14: 469-475, 1993.
138. **Wheatley JR, Pare PD, and Engel LA.** Reversibility of induced bronchoconstriction by deep inspiration in asthmatics and normal subjects. *Eur Respir J* 2:331-339, 1989.
139. **Williams PE and Goldspink G.** Changes in sarcomere length and physiological properties in immobilized muscle *J Anat* 127: 459-468, 1978.
140. **Wingard CJ, Browne AK, and Murphy RA.** Dependence of force on length at constant cross-bridge phosphorylation in the swine carotid media. *J Physiol* 488: 729-739, 1995.
141. **Word RA and Kamm KE.** Regulation of smooth muscle contraction by myosin phosphorylation. In: *Cellular aspects of smooth muscle function*, edited by Kao CY and Carsten ME. Cambridge, UK: 1997, p. 209-252.
142. **Xu JQ, Gillis JM, and Craig R.** Polymerization of myosin on activation of rat anococcygeus smooth muscle. *J Muscle Res Cell Motil* 18: 381-393, 1997.
143. **Yamboliev, IA, Wiesmann KM, Singer CA, Hedges JC, and Gerthoffer WT.** Phosphatidylinositol 3-kinases regulate ERK and p38 MAP kinases in canine colonic smooth muscle. *Am J Physiol Cell Physiol* 279: C352-C360, 2000.